POLITECNICO DI MILANO

Scuola di Ingegneria Industriale

Corso di Laurea in Ingegneria Energetica

“Benefits analysis of subsea multiphase pumps deployment in deepwater oilfields”

Anno accademico 2011/12

Relatore: Prof. Giovanni Lozza

Correlatore: Ing. Stefano Magi

Tesi di Laurea di:

Giorgio Sbriglia

768406

Dissertation developed in collaboration with:

Exploration&Production Division

ISTAC department

“Studere studere studere, post mortem quid valere?”

Anonymous

Abstract

In this dissertation a benefits analysis of subsea multiphase pumps deployment in deep water oilfields is performed. To this purpose, a deepwater oilfield, located in west Africa, was simulated using OLGA as field simulator. However, OLGA cannot predict the pump performances, nevertheless manufacturers provide simple performance curves for air-water mixtures, not suitable for hydrocarbon mixtures. Thus, a thermodynamic model was built in HYSYS for pump performances prediction. The model-predicted performances have been compared with those of an existing pump, then validated for an air-water mixture. Once validated the model, the analysis has been focused on the system performances assessment during six different production scenarios:

- Natural flow wells: hydrocarbon production is entrusted to the reservoir energy and none artificial lift is used to prompt production;
- Riser base located pump;
- Manifold located pump;
- Riser base gas lift;
- Riser base located pump coupled with riser base gas lift;
- Manifold located pump coupled with riser base gas lift.

Pump deployment and position strongly affect system performances, as well as pump performances depend on its location; therefore, a further analysis is performed to assess which is the pump location that best improves the system performances. The production strategies comparison has been carried out during several producing years, to take into account reservoir conditions decay. Each production strategy was analyzed during:

- Nominal conditions;
- Turndown I;
- Turndown II;
- Shutdown from nominal conditions;
- Shutdown from turndown I and II;
- Restart.

During each of these operating conditions, a sensibility analysis, respect to those variables (pump differential pressure and gas injection flow rate) which can definitely affect the analysis outcomes, has been carried out.

The analysis was structured on five sections:

- Flow stability and system operability analysis: this analysis is mainly focused on determining which is the system operational range and how each production strategy affects it. System operational range is mainly bounded by slugging flow condition and by wells choking;
- Oil recovery analysis: production strategies are simply compared by investigating their effect on the system oil production;
- Thermal analysis: the thermal analysis is performed by measuring the cool down times of each production strategy; the cool down time is the time the system takes, after a shutdown, to reach the hydrate formation temperature. Hydrates are one of main threats in subsea oil industry: they can occlude the pipe cross section and induce to catastrophic failures. Each production strategy has its own pressure and temperature profiles which greatly affects the cool down time;
- Power analysis: in this section, the power consumption of each production strategy is evaluated. The section is split into shaft and electrical power analysis. Such division underlines both the technology power requirements and the electrical losses occurring during the electrical transmission;
- Restart analysis: restart operation is quite threatening due to lower operating temperatures, which reduce the cool down time in case of unexpected shutdown; thus, restart is preferably performed as quickly as possible. Production strategies are compared measuring their warmup time, which is the time the system takes to reach the warmup temperature. The warmup temperature is the lowest temperature which, in case of shutdown, ensures a cool down time long enough to allow operators to preserve the line and avoid hydrate formation and deposition.

Sommario

La tesi ha come oggetto l'analisi dei benefici apportati dall'introduzione di una pompa multifase in sistemi di produzione di petrolio "deepwater". A tale scopo, si è simulato in ambiente OLGA un campo ad olio offshore sito in Africa occidentale. Tuttavia, OLGA non contiene nel suo codice un modello per simulare una pompa multifase e la rappresenta come una differenza di pressione tra due punti della pipeline. Poiché le pompe multifase sono una tecnologia emergente, non ci sono ancora software commerciali che simulino le performace di tali pompe al variare delle condizioni di lavoro. Generalmente, i produttori di tali pompe forniscono le curve di prestazione con miscele aria-acqua, non adatte quindi all'applicazione diretta a miscele idrocarburiche. Per tale ragione si è sviluppato un modello in ambiente HYSYS che permette di simulare il comportamento di pompe multifase volumetriche (in particolare a doppia vite) al variare delle condizioni di carico e della miscela aspirata. Il modello è stato confrontato con dati forniti da un'azienda produttrice di queste pompe per una miscela di aria e acqua ed in seguito validato.

Si è potuto così procedere con l'analisi del campo, confrontando sei strategie di produzione:

- Natural flow: pozzo senza nessun sistema per incrementare l'estrazione di petrolio;
- Pompa multifase posizionata "riser base";
- Pompa multifase posizionata "manifold";
- Gas lift "riser base";
- Pompa multifase posizionata "riser base" + Gas lift "riser base";
- Pompa multifase posizionata "manifold" + Gas lift "riser base";

L'introduzione della pompa e la sua posizione fortemente influenzano le performance del sistema e degli altri componenti, così come le perfomance della pompa dipendono dalla sua posizione nel sistema. Il confronto delle sei strategie di produzione è stato svolto in diversi anni di vita del pozzo per valutare come il sistema si comporti nei sei scenari al variare delle condizioni di giacimento. Ognuno degli scenari è stato analizzato in condizioni nominali, di turndown ("carico parziale"), di shutdown da condizioni nominali, di shutdown da due diverse condizioni di turndown e di avviamento per ognuno degli anni di vita analizzati.

Per ognuna di queste condizioni si è eseguita un'analisi di sensibilità rispetto ai parametri regolabili dagli operatori di piattaforma, come portata di gas lift e prevalenza della pompa. Entrando più nel dettaglio, l'analisi è stata suddivisa in cinque macro sezioni:

- Analisi di operabilità del sistema: in questa fase preliminare si è studiato quale sia il campo di funzionamento del sistema per ogni tecnologia utilizzata. Il limite di funzionamento è dato dalla condizione di "slug flow" (flusso a tappi) e di "choking", ovvero la chiusura delle valvole disposte a testa pozzo che comporta la parziale ostruzione del flusso di petrolio;

- Analisi di produttività di petrolio: l'impiego di sistemi di "artificial lift" è finalizzato all'aumento di produzione di olio. Si tratta dunque dell'attività core delle tecnologie analizzate;

- Analisi termica: per analisi termica s'intende la misura dei tempi di raffreddamento, a seguito di uno shutdown, dalla temperatura di funzionamento a quella di formazione di idrati. Gli idrati rappresentano un'enorme minaccia per i sistemi subsea, infatti essi possono portare all'occlusione della sezione di passaggio dei tubi, quindi a rotture catastrofiche del sistema di produzione. Pressione e temperatura di funzionamento del sistema fortemente influenzano il tempo di raffreddamento; conseguentemente, ogni tecnologia impiegata per stimolare il giacimento avrà un effetto diverso sul tempo di raffreddamento del sistema.

- Analisi di potenza: in questa parte si è analizzato quale sia la tecnologia più efficiente per il sistema analizzato. L'analisi è stata suddivisa in due fasi per tenere conto delle prestazioni della tecnologia utilizzata e della sua posizione nel sistema, la quale fortemente determina la potenza elettrica dispersa nella fase di trasmissione e conversione;

- Analisi di riavvio del sistema: la fase di riavvio del campo è particolarmente critica a causa delle basse temperature operative che, in caso di shutdown, possono portare velocemente alla formazione d'idrati. E' generalmente preferibile portare il sistema nelle condizioni nominali il più velocemente possibile. Si è quindi misurato il "warmup time" per ogni tecnologia impiegata, ovvero il tempo che il sistema necessita per portarsi a una temperatura che consenta agli operatori di avere un tempo sufficiente per prendere tutte quelle misure cautelari idonee a preservare il sistema sottomarino dalla formazione di solidi.

Index

List of figures

List of tables

List of graphs

1. Introduction

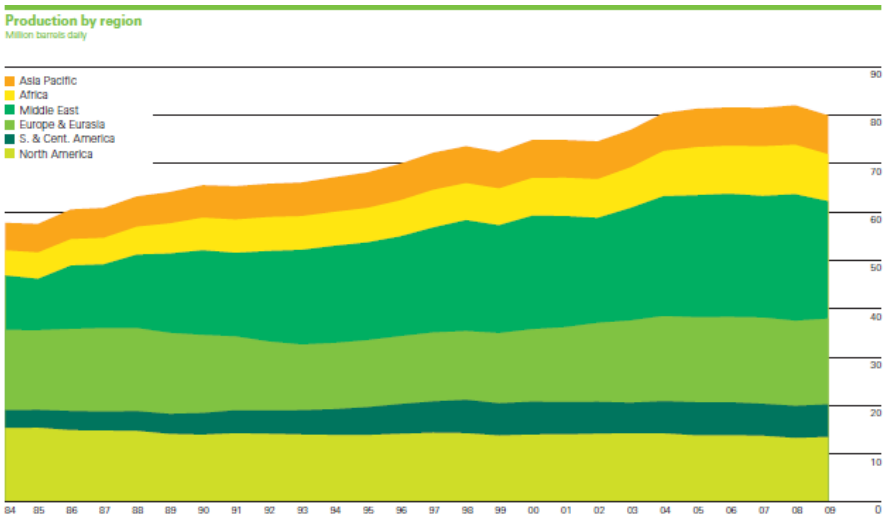

Fig.1: World oil production in MMbbl/d (BP).

World energy demand is keeping growing since 1970 and oil consumption, as main primary energy source, is growing as well. The overall oil production increased consequently and the global oil reserves were expected to decrease at the same rate. However, technological progress and price growth lead to the discovery and the exploitation of new oilfields, which were either unknown or considered too expensive to be exploited.

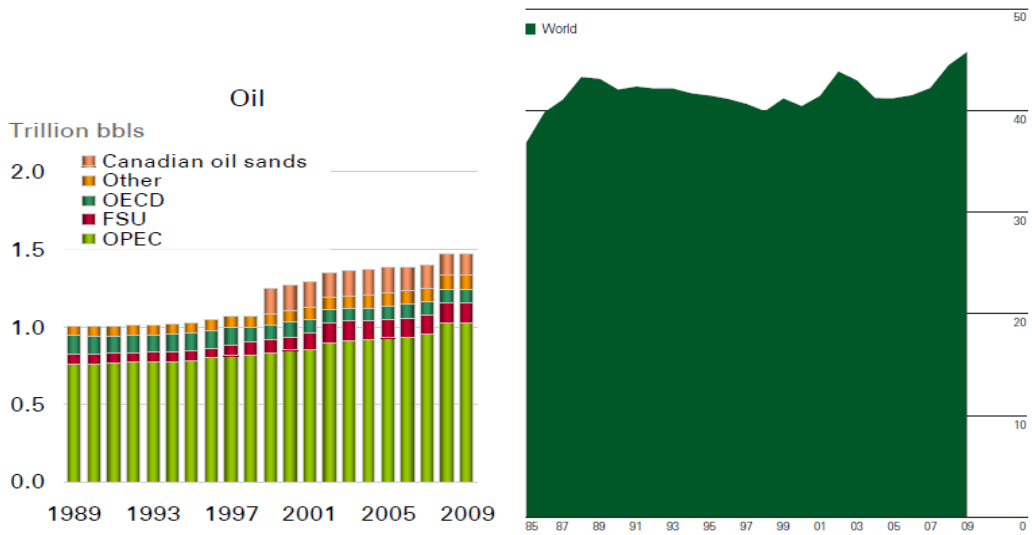

Fig.2: World oil reserves (left) and reserves/production ratio (right). (BP)

As a result, the ratio between oil production and reserves remained steady during time. Now “easyoil” age is ended and most of new oilfields have been discovered offshore, where there is a unexploited huge potential due to the remote and critical environment, the extreme distances to be covered and because monitoring

and maintenance are much more complex and expensive to be performed. Only overcoming these challenges the offshore industry has developed through years. The offshore oil and gas industry started in 1947, when Kerr-McGee completed the first successful offshore well in the Gulf of Mexico (GoM) in 4,6 m of water. The first subsea field was developed in the early 1970 by displacing wellhead and production equipment from topside to seabed, sealing most of the components in a waterproof chamber. Then, produced fluid was conveyed through pipeline to a nearby processing facility, either onshore either offshore located. Subsea systems refer to those systems which have a well and associated equipment below the water surface. System operating up to 200 m (in other words, those reachable by human divers) of water depth are referred as shallow water completions, while those beyond this depth are referred as deepwater ones. If the field is located deeper than 1500 m, it is considered a ultra-deepwater one. Thanks to technology improvements, such as remote control, subsea developments have moved towards deeper waters reaching 3,000 meters in Gulf of Mexico.

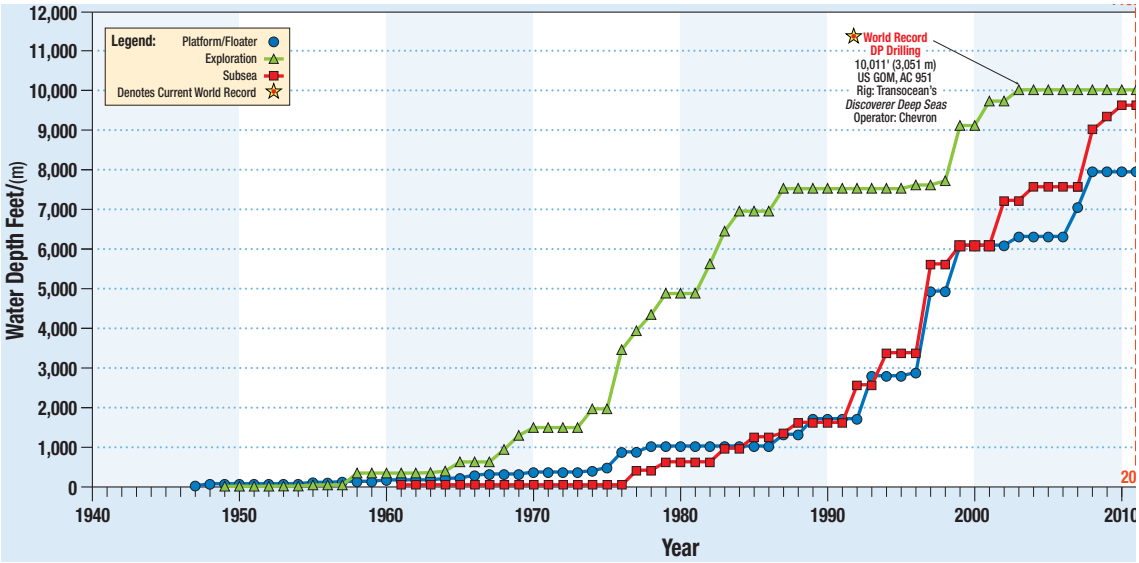

Fig.3: Subsea developments moving towards deeper developments.

2. Subsea production systems

Subsea oilfields usually are turbidite sandstone formations and show extraction problems because they are characterized by small difference between reservoir and wellhead pressures. Indeed, the reservoir is often close to the seabed, resulting in low reservoir-pressures, while wellhead pressure is usually high due to frictional losses across the pipeline and geodetic pressure difference across the riser.

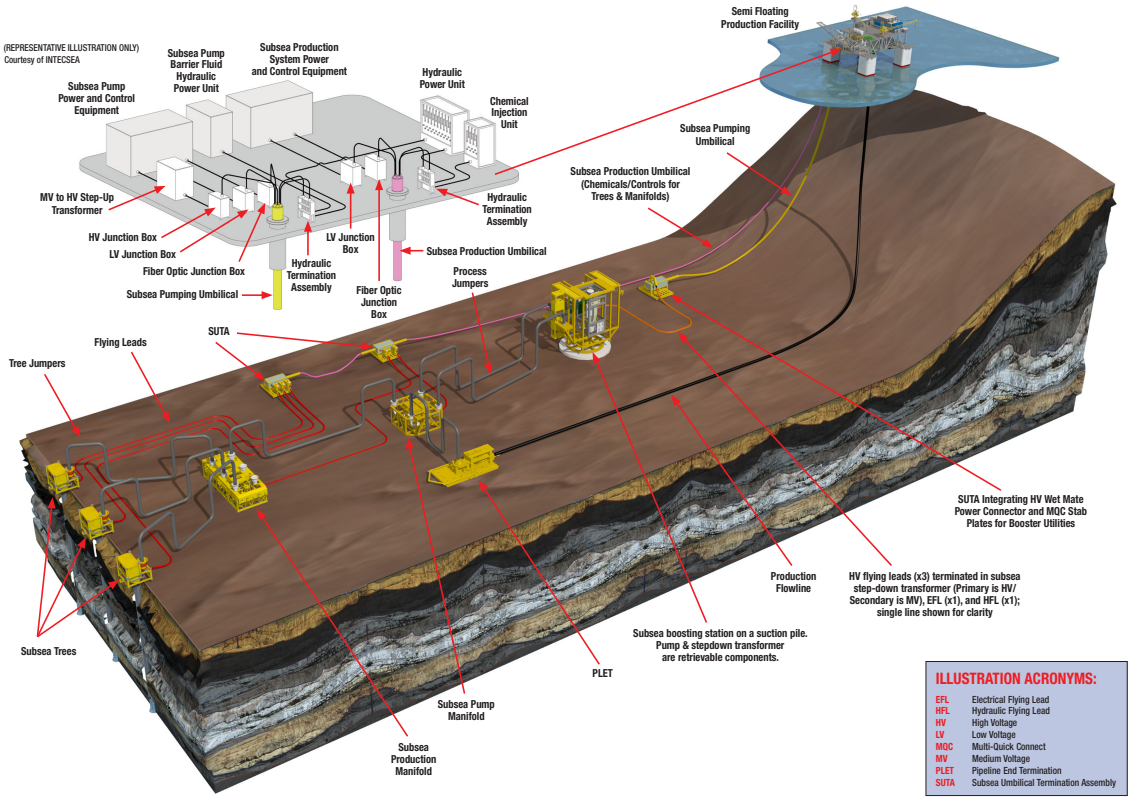

Fig.4: Subsea tieback system development.

A subsea production system can be made of a single satellite well or several wells linked to a manifold with a flowline conveying the fluid to a fixed platform, FPSO (Floating Production, Storage and Offloading), or onshore facility. When some reservoirs cannot be reached due to geometry and water depth, subsea production systems are used to extend existing platforms. Subsea production systems can be divided depending on whether the Xmas tree arrangement has been located:

- Dry tree systems, when the Xmas tree is topside located;
- Wet tree systems, when the Xmas tree is subsea located.

The main parts of a subsea production system usually are:

- Subsea completed wells;
- Seabed wellheads and Xmas trees;
- Subsea tie-in to flowline systems;
- Umbilicals;
- Riser;
- Subsea manifolds and jumpers;
- Subsea equipment and control facilities.

In the following chapters, each system component will be briefly described.

2.1. Subsea developments

2.1.1. Wet and dry tree systems

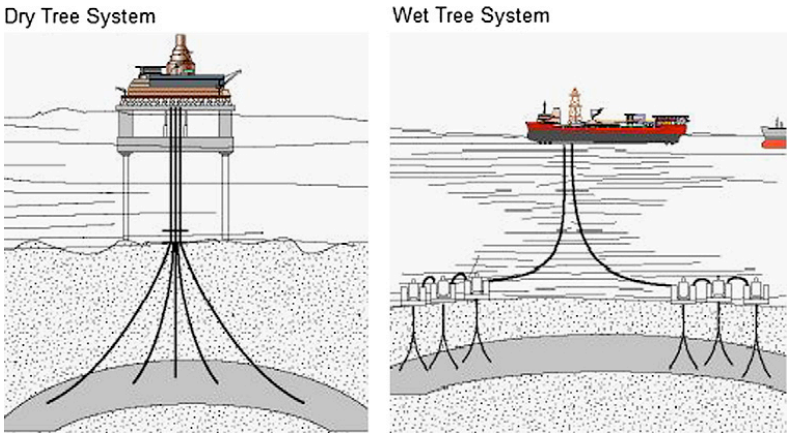

Fig.5: Dry tree and wet tree systems layout.

Subsea systems developments can be divided on whether the Xmas tree is located:

- Dry tree development, when the Xmas tree is located on a surface structure. They are preferred when a fixed platform, a tension leg platform (TLP) or SPAR is available, due to their reduced sensibility to the wave movement. Thanks to their accessibility, they reduce the maintenance costs and simplify the well control. A deepwater surface well architecture in the form of a wellhead platform (WHP or FDU) combined with either an FPSO or an FPU

are starting to establish as alternative solution to wet tree wells clusters development. This combination can eventually become an interesting technology in the Gulf of Mexico as the FPSO philosophy becomes progressively widespread. To date, existing (or actually planned) WHP systems are based on TLP concept.

- Wet tree development, when the Xmas tree is located on the seafloor. Its does not require a fixed host facility and is particularly appreciated for long subsea tieback applications. For its nature, it has lower CAPEX and higher OPEX than dry tree development. Two main layouts of wet tree development can be identified: subsea wells clusters and direct access wells. Wet tree development can be accomplished with three different types of riser, steel catenary, top tensioned and flexible risers.

To date, most of operators has felt more comfortable in dealing with wet tree developments for deepwater systems and considers dry tree ones more suitable for shallow water fields.

2.1.1.1. Wet tree developments: direct access wells

This development allows to directly perform workover and drilling activities from the production support, which is very useful in marginal field development.

2.1.1.2. Wet tree developments: wells clusters

This production solution is the most efficient and cost-effective one, either suitable for close located wells, either for remote ones, linked to an already existing infrastructure through a long distance subsea tie-back. The infrastructure is, in most of the cases, a FPSO unit.

2.1.2. Stand alone development

This solution is viable when reservoir size justifies the economic development of topside processing facilities, which is further verified for gas fields. Thus, the choice of whether developing a stand-alone or tie-back system is dictated by economic parameters (as discussed in paragraph 2.1.3). Stand alone developments are generally divided accordingly to the type of facility connected to the field.

2.1.2.1. Fixed platforms

These platforms best suite big reservoir and shallow (up to 520m) developments. Indeed, these platforms are built on steel legs anchored directly onto the seabed (thus shallow water applications), supporting a deck with space for drilling rigs, production facilities and crew apartments. These structures, due to their immobility, are designed for long term use, thus for big reservoir exploitation.

Various types of structure are used: steel jacket, concrete caisson, floating steel, and even floating concrete.

2.1.2.2. Compliant towers

The main component of these platforms is a narrow tower, supported by a foundation on the seafloor. This tower is more flexible than the fixed platform one. This flexibility allows to operate in much deeper waters, as they can sustain lateral deflections due to forces exerted by wind and sea. Petronius is actually the deepest compliant tower in world and is located in 531 m of water depth.

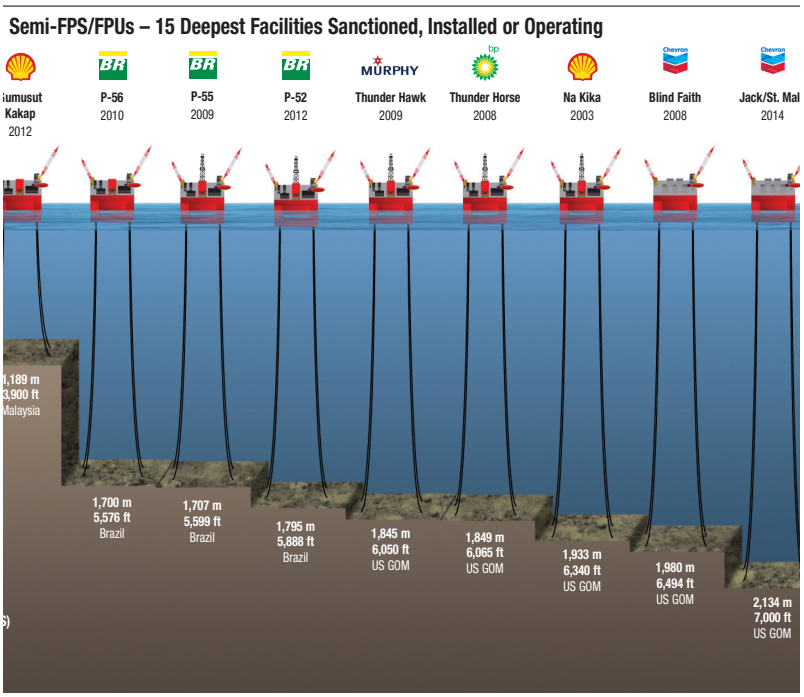

Fig.6: Deepest semi-submersible platforms in the world.

2.1.2.3. Semi-submersible platforms

Semi-submersible platforms are not supported by a foundation linked to seabed, whereas they are equipped with large hulls (column and pontoons), which allow the structure to float. Semi-submersibles were used in water depths up to 2500 m. They differ from tensioned-legs platforms in the mooring mechanism: they are generally anchored by combinations of chain, wire rope or polyester rope. Actually, the deepest platform is Independence Hub, which is located in 2415m of water depth.

2.1.2.4. Jack-up platforms

These platforms are suitable for small reservoirs in shallow waters. Indeed, thanks to their unique feature, they can be jacked up above the sea level by lowering their four legs. Once the field has been exploited, they can be moved to the next producing site. They can normally operate up to 120 m of water depth (some special designs allow to reach 170 m).

2.1.2.5. Floating production systems (FPS)

FPSs are large monohull structures, which are often derived from ship ones, equipped with processing facilities. There are different technical solutions such as FSOs, FSUs, and FPSOs. They often offer nice economic advantages, thanks to their similarities to ships in the building process.

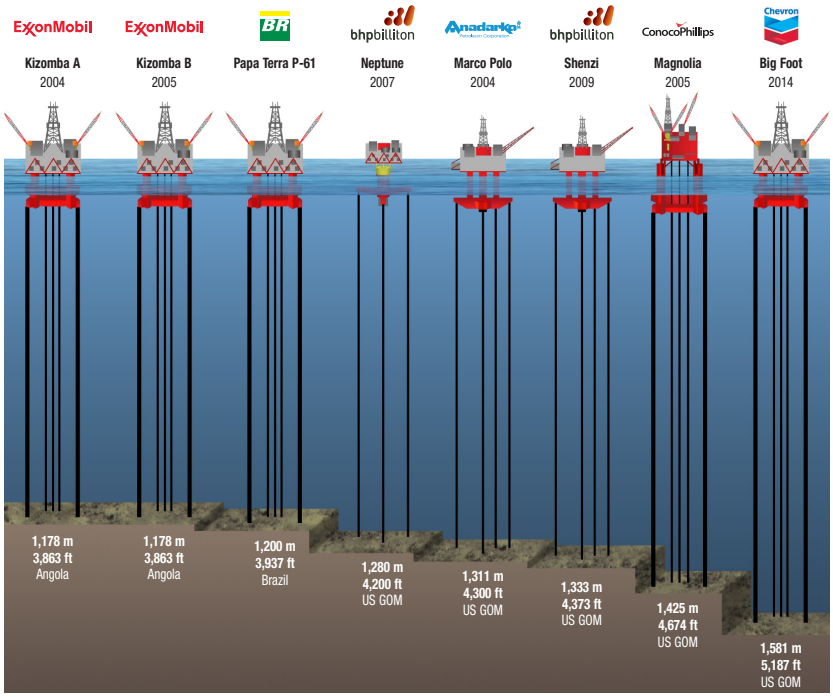

Fig.7: Deepest TLPs in the world.

2.1.2.6. Tension leg platforms (TLPs)

TLPs are floating structures, similar to semi-submersible platforms, tethered to the seabed in order to avoid vertical movements of the structure. The structure is tethered to seabed throughout four tension legs, each one corner located. The tension leg is made of tubular steel members, called tendons. The tendon system is highly tensioned due to excess of the platform hull buoyancy. TLPs are best suited for applications between 100m and 1500m of water depths.

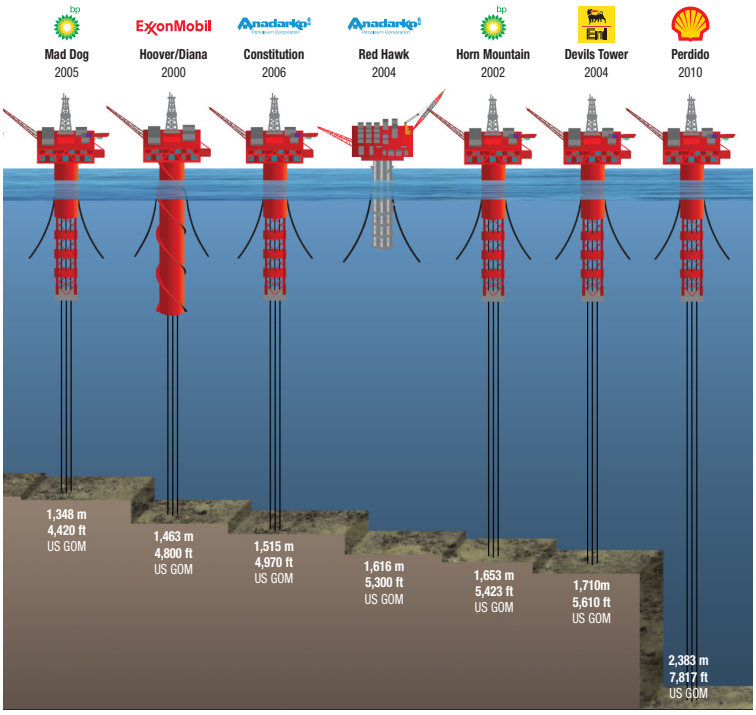

Fig.8: Deepest SPARs in the world.

2.1.2.7. Spar platforms

There are different types of spar used, classified by the platform hull:

- Cylindrical hull: This is the very first version of these floating platforms;
- Truss spar: in these platforms, the upper buoyant hull is connected to bottom stabilizer ballast through a midsection, composed of truss elements. This is, actually, the most widespread spar platform;
- Cell spar: cell spars, for example the Red Hawk, are built from multiple vertical cylinders.

Spars are similarly moored to the seabed as TLPs, but they do not have either tension legs either a tendon system. Spars are tethered to seabed through a conventional catenary mooring line. Shell Perdido is actually the deepest spar in the world and is located in Gulf of Mexico in 2383 m of water depth.

2.1.3. Subsea tieback development

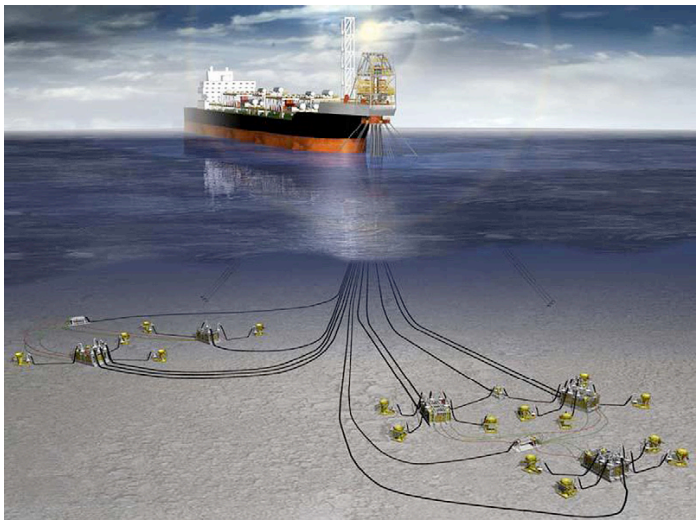

Fig.9: Subsea tie back to FPSO.

The exploitation of deepwater reservoirs has been feasible only when huge amount of hydrocarbons could be recovered, otherwise the capital cost investment for the establishment of these subsea systems could not be justified. As consequence of that, marginal oilfields have been often ignored. Recently, operators have found in tie-back developments the key solution to economically exploit these fields, by connecting them to an existing processing facility and saturating the spare processing capacity.

Subsea tiebacks are denoted by lower capital cost investments and by high technical complexity. This emerging solution is continuously spreading out and establishing all over oil&gas industry, reaching deeper and farther fields. Indeed, tieback economics is mainly governed by the following parameters:

- Distance from existing installation;
- Water depth;
- Recoverable volumes, reservoir size, and complexity;
- Potentially lower recovery rates from subsea tie-backs versus standalone development, due to limitations in the receiving facility's processing systems and to higher back pressure on wells (longer distance to be covered).

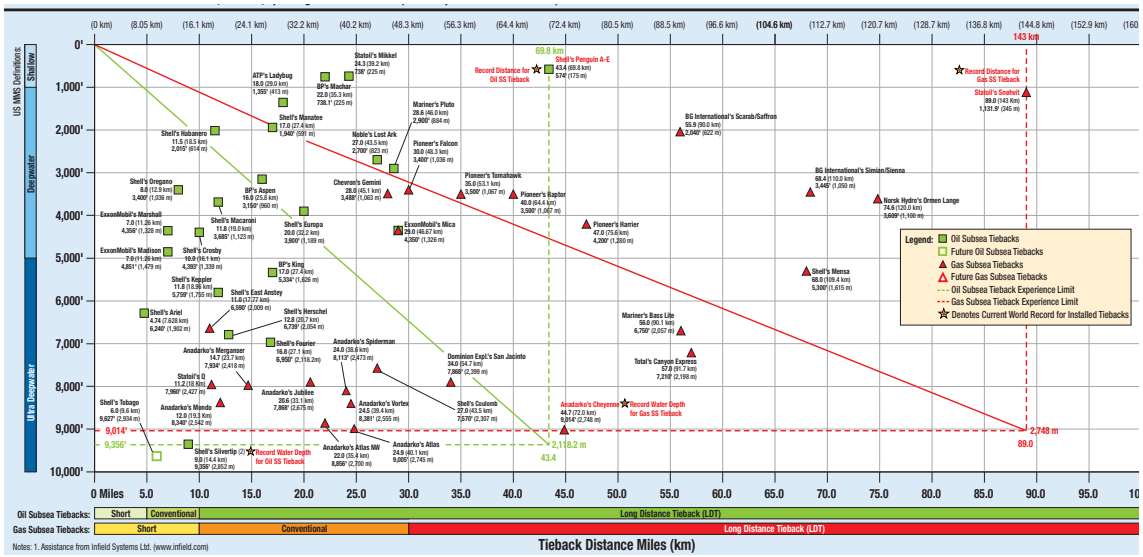

Fig.10: World record subsea Tiebacks

The former graph shows how tie-back length and water depth have increased during time, thank to strong improvement in the subsea technology and economics, making feasible the exploitation of marginal fields.

The marginal field can either be linked to a FPSO (Fig. 9), a fixed platform or to an onshore facility, generally throughout a dual flowline with an end-to-end loop, which are customarily built for subsea tie-backs and provide a full circuit for the pig, which can travel from the processing facility to the manifold then turn and come back to the facility.

The tieback development should deliver the conveyed fluid at temperatures above the solid formation ones (such as hydrate formation, cloud point and wax appearance temperatures). Concerning this issue, pipe insulation and heat retention strategies represent a key design feature. Indeed, solid formation (and consequent solid structures building up) can lead to pipe occlusion and catastrophic failures.

During the project development, it is essential to assess whether the reservoir energy can overwhelm the backpressure and lead the hydrocarbon to the processing facility with acceptable flow rates. To this purpose, multiphase subsea boosting offers many advantages (better discussed in the following chapters). Riser-base gas injection is another interesting solution to reduce back pressure by lightening the fluid column in the riser. A further advantage is to reduce slugging and to provide the possibility of depressurizing the line during a shutdown.

2.2. Subsea layouts

Depending on the field characteristics and specifications, different common layouts can be used to develop the subsea system. The well location layout is generally a trade-off between the need of space, for oil recovery maximization, against cost saving benefits due to well grouping in clusters. In the following paragraphs, four main subsea layouts are briefly exposed in following paragraphs and illustrated in the picture below.

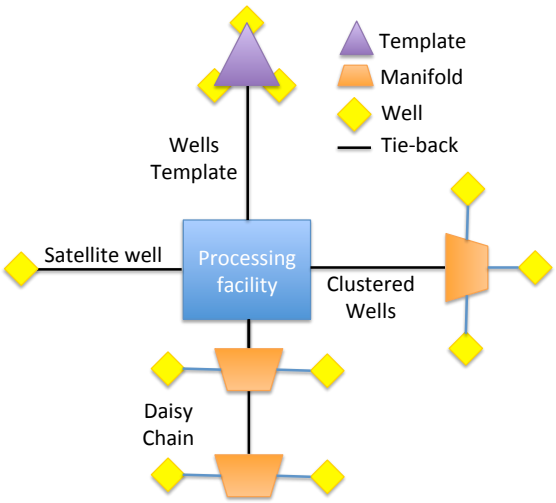

Fig.11: Subsea conceptual layouts.

2.2.1. Satellite well layout

A satellite well is a single subsea well. A satellite well layout means that each well is independently connected to the process facility. This solution is preferred when the distance between wells is high.

2.2.2. Clustered Satellite Wells

When distance between wells is small, it is convenient to collect all the reservoir produced fluid in a single flowline. Wells are connected by means of a manifold. This arrangement allows cost saving both for the flowlines and for the umbilicals.

2.2.3. Production Well Templates

While well clusters layout aims to connect many close wells, a well template is designed to closely locate a group of wells. Well templates are prefabricated steel structures which accommodate both well heads and manifold. They can support from two to twelve wells. The number of wells, a template could host, is simply limited by reservoir considerations and by template weight, which can be handled by the installation vessel. The choice of whether applying a cluster o template layout is simply a tradeoff between advantages and disadvantages.

Well template layout advantages and disadvantages compared to cluster layout	
Advantages	Disadvantages
• Wells are precisely spaced.	• Design and fabrication time may be longer due to greater complexity.
• Manifold piping and valves can be incorporated.	• There may be safety concerns related to simultaneous drilling and
• Piping and umbilical jumpers between the trees and manifolds prefabricated and tested prior to deployment offshore.	
• Piping and umbilical interfaces are less expensive than for clustered wells.	
• Installation time is reduced by modularizing much of the equipment.	
• Short flowline piping distances (compared to a cluster) reduce the problems associated with flow assurance (e.g., wax and hydrate formation).	

Tab.1: Wells template and wells cluster layouts comparison.

2.2.4. Daisy Chain

When there are one or more wells, which are far located by another group of wells, it is possible to connect both groups of wells through a single subsea flowline. This layout, which connects two or more well hubs with a single flowline, is called Daisy Chain. When this layout is used, it is possible to create a continuos loop, so that the flow line is piggable, leading to the following advantages:

- Round trip pigging;
- Possibility to redirect both production flows into a single flowline if the second is damaged;

Most of Daisy Chain configuration advantages can be summed up as follows:

- Similar to a single satellite well, cost is upfront: only when the installation is performed the cost is faced by the operator;
- Flowlines sharing may be possible;
- Wells position not fixed, which is especially important in low permeability oil fields;

- Potential damage from dropped objects is limited;
- Simultaneous production and drilling.

Disadvantages of Daisy Chain wells include:

- Subsea chokes possibly required on each well;
- Relocation of the drilling rig vessel in order to reach another well.

2.3. Subsea Processing

Subsea processing refers to those physical or chemical treatments subsea performed to improve the system flow assurance and performance. Subsea processes include:

- Subsea boosting;
- Subsea separation;
- Solids management;
- Heat exchange;
- Gas treatment;
- Chemical injection.

Most of the times, subsea processing is required in order to exploit the field (chemical injection to avoid hydrate formation or gas injection to mitigate severe slugging), but often it simply provides some advantages. For instance, the deployment of a subsea multiphase pump allows to increase the oil production or to extend the field life.

3. Subsea Components

Hereafter, a brief description of main subsea components will be carried out. The description includes the following subsea equipment:

- Wellhead;
- Subsea Xmas tree;
- Jumper;
- Manifold;
- Subsea valve;
- Pipeline end termination (PLET);
- Subsea pipeline;
- Riser;
- Distribution system;
- Umbilical.

3.1. Wellhead

Wellhead is the pressure-containing component at the surface of an oil well. It supports casing strings and the subsea tree after completion; its function is mainly to operate as pressure-containing anchoring point on the seabed for the drilling and completion operations. It can be located on the offshore platform or onshore (surface wellhead); if it is located on the seabed, it is called subsea wellhead.

3.1.1. Subsea wellhead

A subsea wellhead is made of the following components:

- Wellhead housing: it is the main pressure-containing component of the subsea well head. It supports and seals the casing hangers and shifts external loads to the conductor housing;
- Conductor housing: it accommodates most of the wellhead equipment (mainly pipes);
- Casing hangers: they provide support to the casing strings.

- Annulus seals: they simply seal one environment from another, especially for isolating the geological formation;
- Guide base: it is a structure for guiding equipment into the wellhead. There are different kinds of subsea wellhead guide bases, depending on the subsea system conceptual layout. For instance, a Template-Mounted Guide Base (TMGB) is required if production well template layout is used. Single-Well or Cluster Production Guide Base (SWPGB) is suitable for both cluster and single-well configurations.

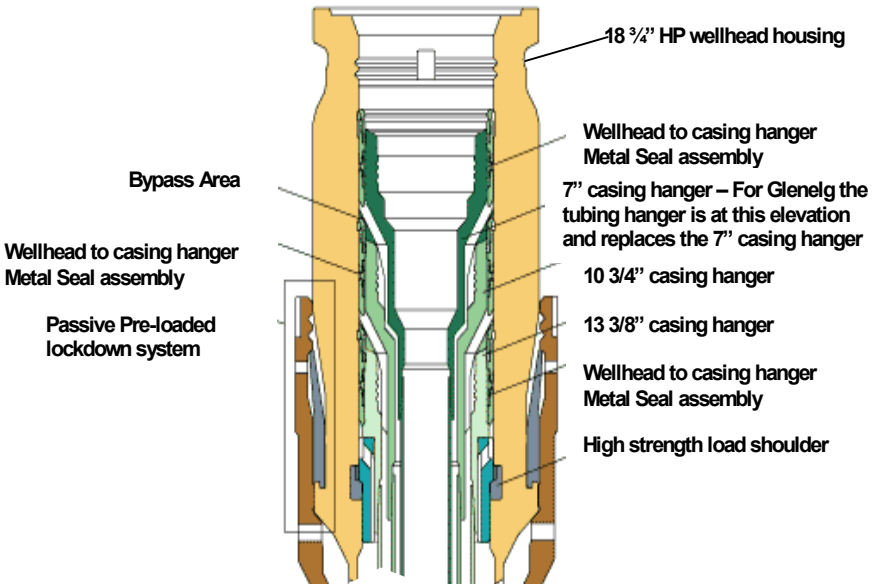

Fig.12: Wellhead cross section.

3.2. Subsea Tree

A subsea Xmas tree is an assembly of valves and spools (whose geometry resembles a Christmas tree and for such reason is called Christmas tree, Cross tree, X-tree, or just tree), used to control the flow rate of the well. They are also used for other auxiliary functions, such as:

- Chemical injection;
- Water/gas injection;
- Well intervention;
- Pressure relief means;
- Monitoring.

Subsea Xmas trees are classified on their orientation layout: they can be either vertical either horizontal trees.

3.2.1. Vertical Xmas tree

Vertical Xmas trees (VXTs) have vertical aligned master valves located above the tubing hanger. VXTs are definitely widespread thank to their lower cost (five to seven times lower than horizontal ones) and to their versatility. Indeed, they can be also deployed after well completion.

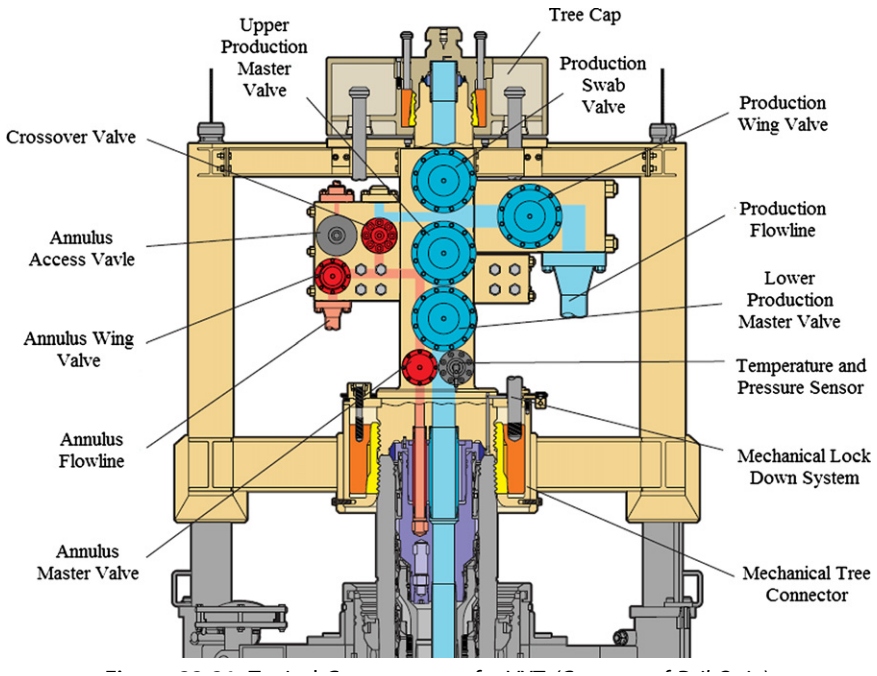

Fig.13:Vertical Xmas tree conceptual layout

The former picture illustrates the essential components of a VXT. As can be noticed, master valves are vertically aligned, as the production swab valve is. Another advantage of the vertical Xmas tree is that it can be retrieved without having to recover the downhole completion.

3.2.2. Horizontal Xmas Tree

Horizontal Xmas trees (HXTs) have found many applications in subsea fields, undermining VXTs supremacy. Indeed, they are lighter and more suitable for wells requiring frequent work-over. They allow simple well intervention thank to their valves disposal and electrical submersible pumps downhole deployment, thanks to the absence of the swab valves.

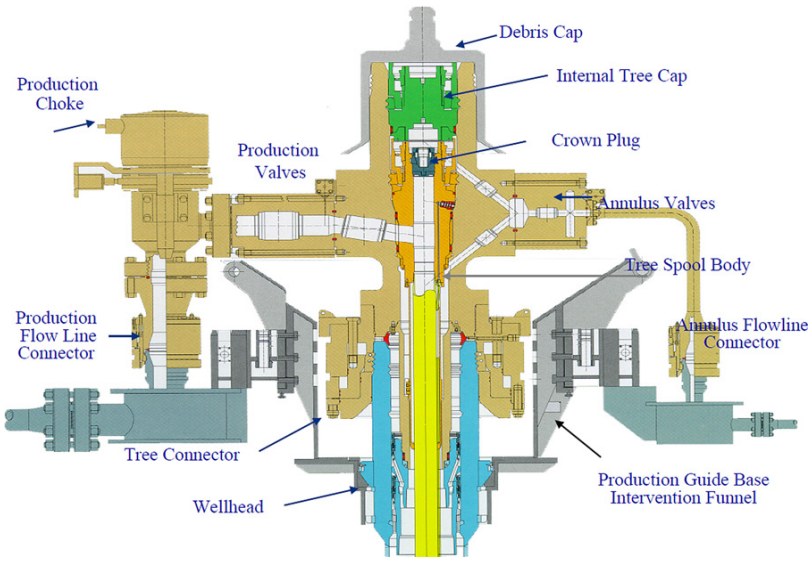

Fig.14: Horizontal Xmas tree conceptual layout.

Another difference between VXTs and HXTs is the tubing hanger location. While in VXTs the tubing hanger is located on the wellhead, in HVTs it is installed on the tree itself. Thus, it is absolutely necessary HXTs to be installed before the well completion, otherwise VXTs should be deployed.

3.3. Jumpers

Subsea jumpers are used to link two different subsea components, such as a manifold or a PLET, and allow the transported fluid to flow from one to another component. Their shape is aimed to accommodate thermal expansion during transient conditions.

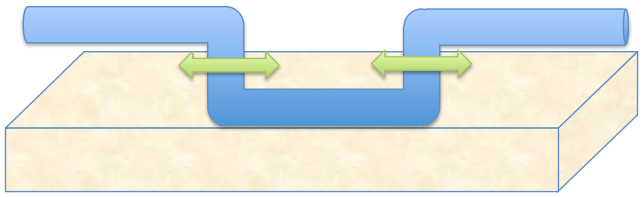

Fig.15: Jumper conceptual layout.

There are two different kinds of subsea jumpers:

- Rigid jumpers;
- Flexible jumpers;

Flexible jumpers are generally preferred to rigid ones, thanks to their geometrical versatility.

3.3.1. Rigid Jumpers

A rigid jumper is mainly made of a steel pipe and mechanical connections at each end for components linkage. The jumper is required to resist to the combined effect of internal pressure, external bending, torsion, tensile, thermal, and installation loads.

Rigid jumpers may have different configurations, such as "M" shaped or "U" shaped. The "M" shape also can be divided in categories depending on the connection configurations; indeed, it can be linked through bends or through elbow (see paragraph 3.3.3).

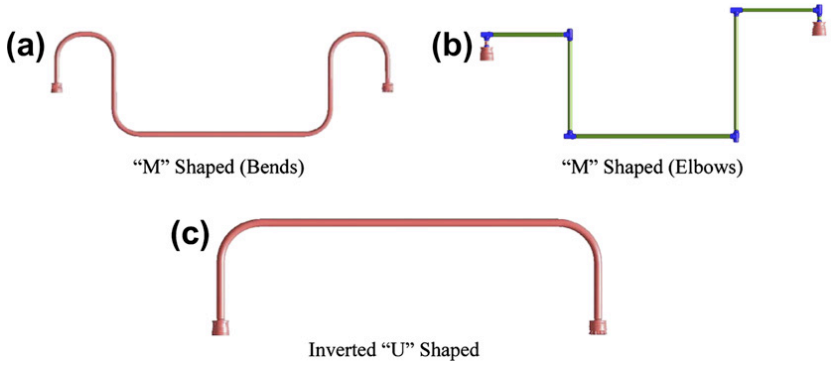

Fig.16: Common jumpers shapes.

The main concern on rigid jumpers is the installation procedure. Once the components to be connected are permanently deployed, their distance is measured or calculated. Then the connecting jumper is tailored on the measured length and equipped with coupling hubs on the ends. Once the jumper has been manufactured, it is delivered to the required location. Afterwards, the jumper is lowered and linked with the other two components and tested.

Measurements are absolutely critical for jumpers deployment, indeed if they are not precisely performed or if the components location changed from the previous one, new jumpers may need to be fabricated. Jumper design should take into account the changes in dimensions occurring when the component is lowered below the sea level. Indeed, thermal expansion and shape deformation, due to a load reduction induced buoyancy forces, definitely affect the jumper geometry.

3.3.2. Flexible Jumpers

Flexible jumpers are made of two connectors and a flexible pipe. The flexible connector is a layered set of concentric pipes which provide the physical properties required to face the flexible jumper requirements:

- Flexibility;
- H_2S and corrosion resistance;

- High-temperature resistance;
- Suitability for dynamic service and strong thermal dilatations;
- Fatigue resistance;
- High resistance to collapse;
- Low U-value.

The flexible pipe is generally composed of many layers which can move when the pipe is flexed, in order to improve the fatigue resistance. Layers have three main goals:

- Mechanical resistance;
- Thermal insulation;
- Corrosion resistance.

Fig.17: Flexible jumpers layers.

The main advantage of flexible jumpers is their simplified procedure during the length specification and installation. Indeed, length specification is not required to be so accurate as in the rigid jumper case. As long as the flexible jumper is longer than the distance between the two components to be connected, the installation can be successfully completed.

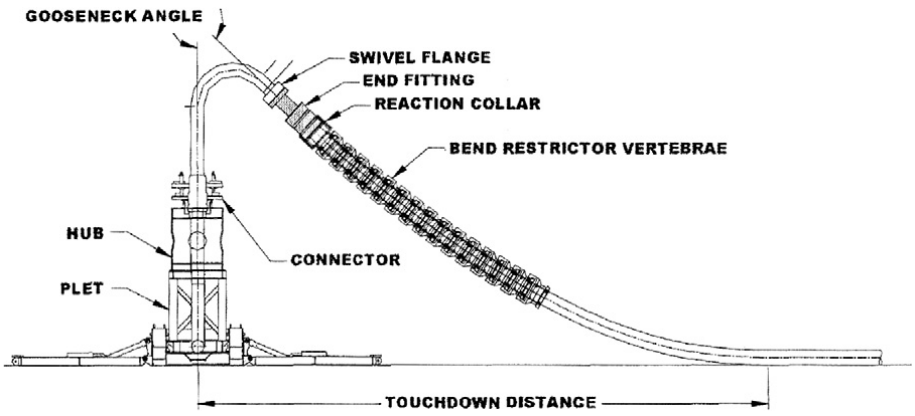

Fig.18: Flexible jumper and PLET connection.

3.3.3. Tie-in systems

A tie-in system allows to connect the jumper to a manifold or to a PLET. Tie-in systems used to be mainly horizontal, since subsea development were carried out in shallow waters with the auxiliary help of divers. Since subsea engineering has moved towards deeper waters, the development of vertical tie-in systems guided by control remote units has occurred. Actual horizontal tie-in systems need ROVs (Remote Operator Vehicles) auxiliary help to be installed in deep water oilfields.

3.3.3.1. Vertical tie-in systems

Vertical jumpers are often rigid "U-inverted" shaped jumpers. At both ends of the jumper a downward oriented connector is equipped, which is thought to fit the other components vertical hubs. Vertical connections are installed directly onto the receiving hub during tie-in, as shown in the following picture.

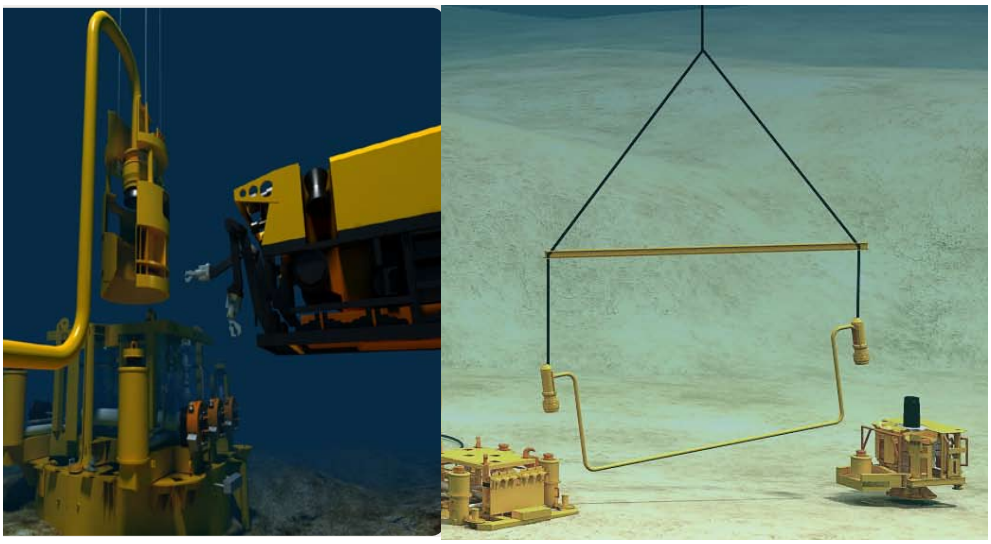

Fig.19: Vertical tie-in connection end (left) and deployment(right).

3.3.3.2. Horizontal tie-in systems

Most of the horizontal connection systems are based on mechanically fastened flange joints. Horizontal tie-in systems offer some interesting advantages against the vertical ones:

- Low possibility of being hooked by anchors or fisheries thanks to the lower geometrical profile;
- Longer tie-in life;
- Simple seal substitution;
- Low weather dependency;

- Simpler and smaller connector.

Horizontal tie-in systems require a complex installation procedure. Indeed, the installation process can be divided in four steps at least:

- The jumper is lowered from sea level just above the receiving hub (a);
- The jumper stab is aligned with and pushed in receptacle stab (b);
- The protection cap is removed from the jumper termination head (c);
- The jumper termination head is stroked inside the receiving hub (d).

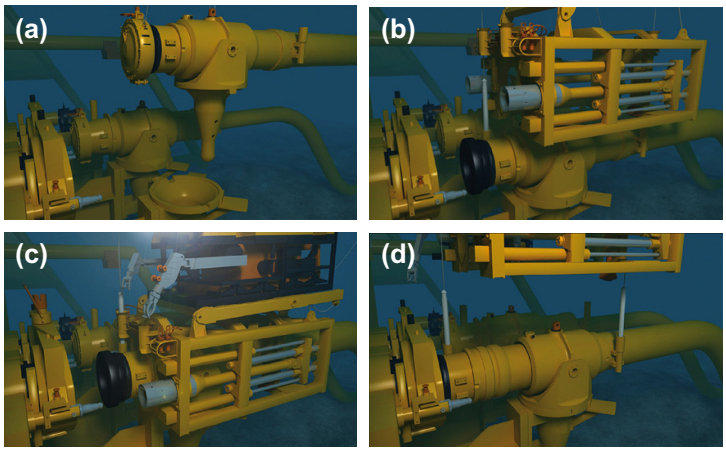

Fig.20: Horizontal tie-in connection procedure.

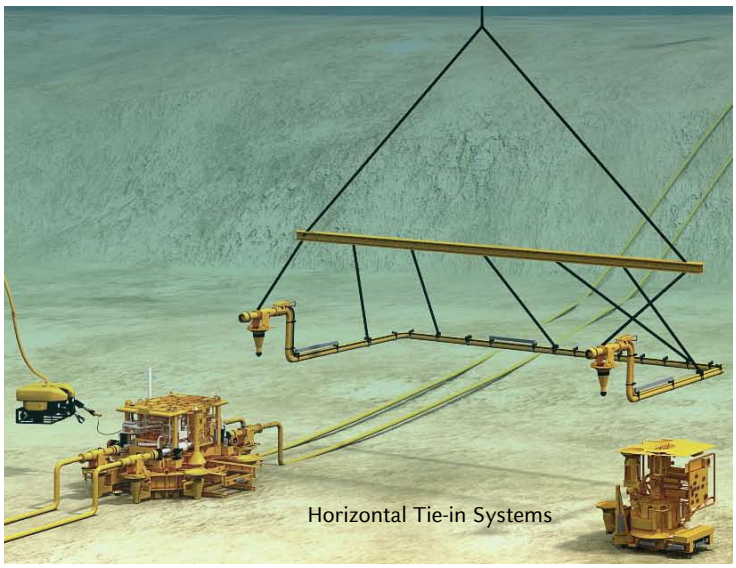

Fig.21: Horizontal tie-in deployment

3.4. Subsea Manifolds

Manifolds are assembly of piping and valves used to either mix or split the stream. They are also used for chemical, gas and water injection and for fluid flow monitoring. They allow to link more wells and convey the fluid through one single pipeline and riser. The linkage to other equipment is performed throughout jumper connection.

Fig.22: Subsea GE Manifold.

The subsea manifold system is equipped with a foundation, which provides structural support and anchors the system to seabed.

There are different types of subsea manifold system, depending on the application:

- Production manifolds, for flow and well control;
- Gas injection manifolds, for gas injection into the riser base to lighten the riser column, thus increase production and stabilize the flow;
- Gas lift manifolds, for gas injection at bottom hole to lighten the tubing column and increase production and stabilize the flow;
- Water injection manifolds, for supplying water to reservoir and support reservoir pressure;
- Choke or kill manifolds, for controlling well operations.

3.5. Subsea Valves

Subsea valves can be either gate or ball type. The formers have always been widespread, thanks to reliability they have shown till nowadays. They are used in subsea blowout prevention (BOP) stacks, trees, and manifolds. Ball valves, instead, were initially used in the downstream gas industry as gas pipeline valves. Thanks to operational and cost advantages compared to gate valves, they have succeeded as subsea valves. Historically, gate valves used to suit best liquid applications, while ball ones have been used in gas ones since 1960s.

Subsea manifold valves are mounted within the piping system to control the fluid production and injection and are usually hydraulically activated. They are characterized by longer activation times and usually are set in the retrievable manifold frames or modules.

3.6. Pipeline Ends and In-Line Structures

A pipeline end manifold (PLEM) is a subsea structure set at the end of a pipeline and it is also referred as pipeline end termination (PLET). It connects a rigid pipeline to other subsea equipment, throughout a jumper. A PLET is usually made of the following components:

- Structural frame, which supports the piping and components;
- Foundation (mudmat), which distributes the loads to the seabed and provides further support beside the structural frame;
- Installation system, which is hinged to the structural frame, to minimize torsion-related rotation during PLET deployment;
- A sliding support which accommodates reasonable thermal expansion of the flowline during transient operation.

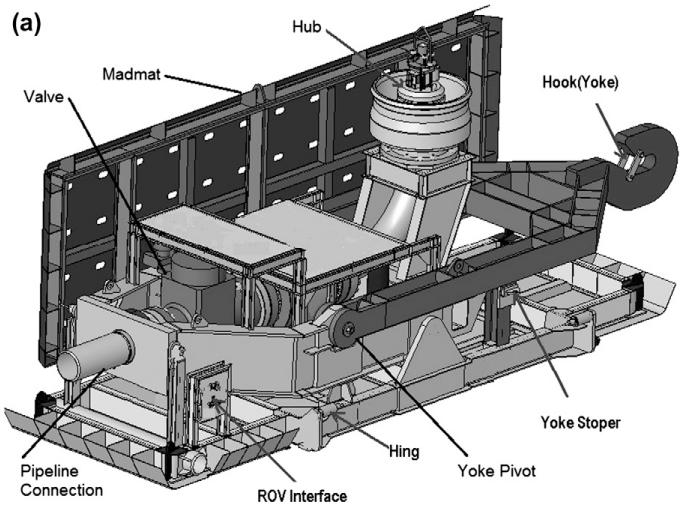

Fig.23: PLET's main components.

In subsea fields, there is a strong difference between the conveyed fluid and the environment temperatures, therefore during transient operational conditions the flowlines are affected by wide temperature oscillations, which means strong thermal expansions. If both ends are blocked and not allowed to move, snaking (lateral displacement) or upheaval buckling (vertical displacement) can occur due to excessive flowline elongation.

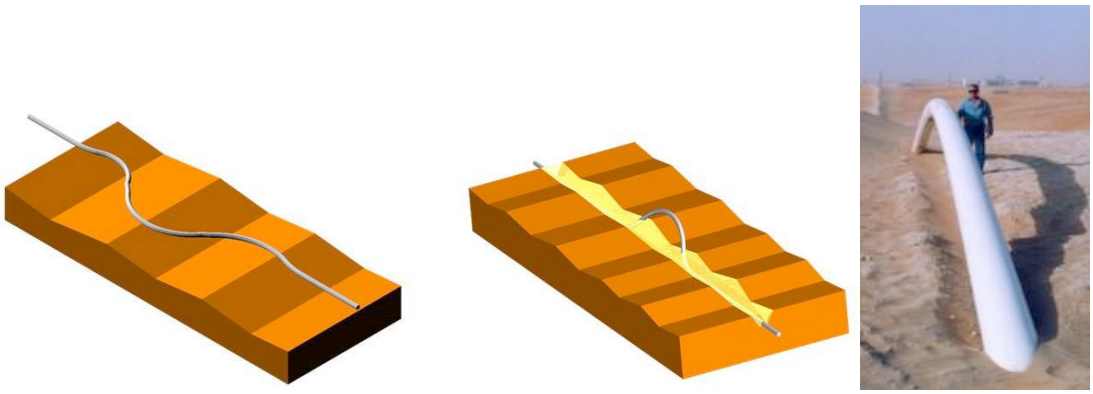

Fig.24: Pipeline elongation deformations: Snaking (left) and Upheaval Buckling (right).

3.7. Subsea pipelines

Subsea flowlines are definitely a key component in subsea systems. Indeed, they have outstanding physical properties to face:

- High pressure fluids;
- High corrosion environment;
- High insulation requirements.

As production moves towards deeper fields, subsea pipelines have to convey higher pressure fluid and insulate it from the cooler environment. Moving towards deeper waters means having higher fluid pressures and temperatures, which lead to pipe dilatation which generates compressive forces. Flowlines can be either flexible either rigid and they can be either single either bundled lines. Bundled flowlines consist in more lines packed together in a carrier pipe.

3.8. Production Risers

The production riser is a pipe which connects the flowline on the seabed to the processing facility. Depending on the associated processing facility, different types of risers can be deployed: they vary in shape and in materials. First classification can be made on whether the production riser is rigid or flexible. Also hybrid risers exist, they are almost a combination of these two types of riser.

Flexible risers are probably the most widespread production risers. Their main advantage is lower installation cost and their suitability for floating vessels. They may be deployed in a variety of configurations, depending on the water depth and environment. For deeper installations Steel Catenary Risers (SCRs) are generally preferred to flexible ones. Indeed, in many deepwater projects in the Gulf of Mexico and Brazil are now employing SCRs for both export and import risers. The choice of the riser type depends also on whether the production system development is wet tree or dry tree; flexible risers and import SCRs are more suitable for wet tree developments, while top tensioned risers for dry tree ones.

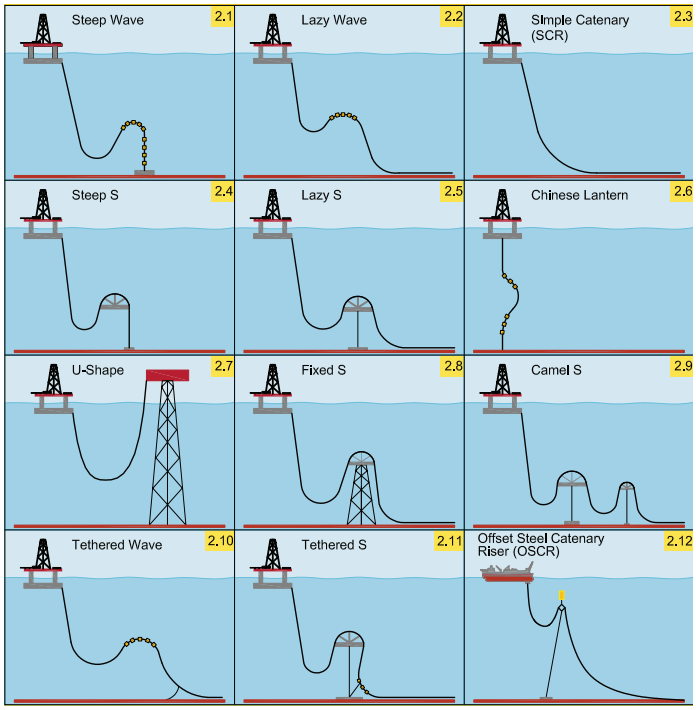

Fig.25: Free hanging riser systems

3.8.1. Steel Catenary Risers (SCRs)

A simple SCR is a free-hanging riser with no intermediate buoys or floating devices. They allow small relative rotations between the floating facility and the seabed flowline. They are the most widespread type of riser for deepwater applications. Their simple shape is the one which less affects and hampers the liquid accumulation at riser base, which is the main cause of terrain slugging. However, simple catenary shape cannot be used for deeper developments, due to the higher free hanging load caused by the integration of their weight over the water depth. In these cases an offset steel catenary riser layout is chosen; Each section (before and after the buoyancy tank) supports its own free-hanging load, thus deeper field can be reached.

3.8.2. Top Tensioned Risers (TTRs)

Top tensioned risers (TTRs) were designed to suit shallow-water developments, although design modifications have been carried out in order to face deepwater requirements. TTRs are simply arrays of straight cylinders which connect the seabed to a floating platform. They are fixed to the processing facility by means of a tensioner system. They do not allow relative rotation respect to the facility, thus they are suitable only for tensioned legs platforms or SPARs. This feature makes them ideal for dry tree developments. They allow direct access to well and are generally suitable for no tie-back applications.

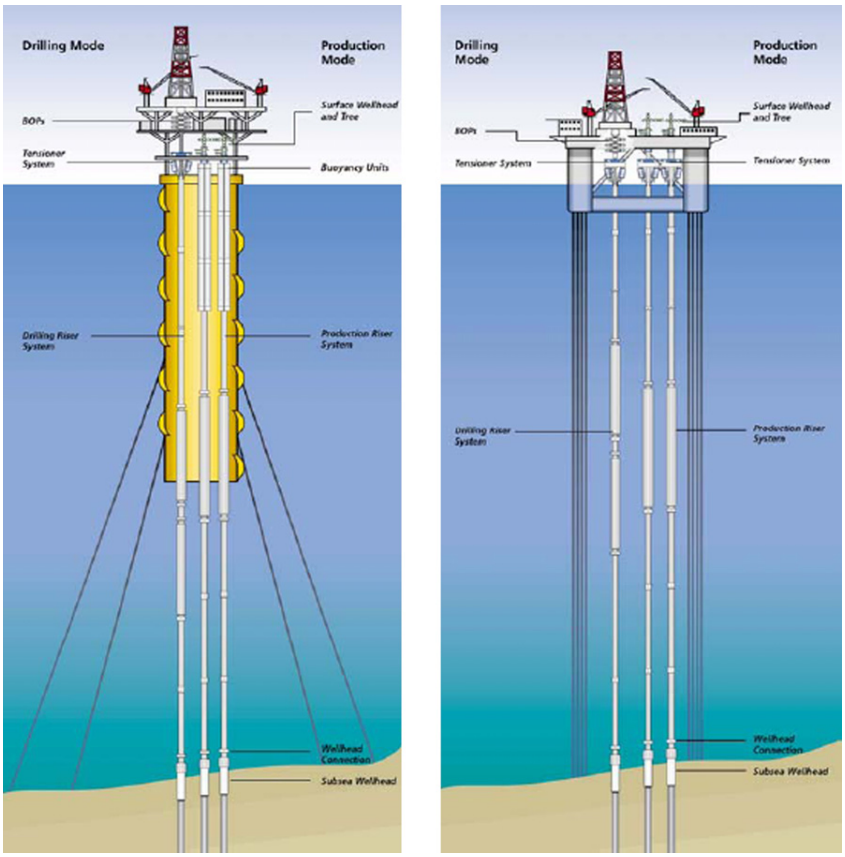

Fig.26: Top tensioned risers deployed in both SPARs and TLPs.

TTRs are composed of cylindrical pipes, known as joints, which can be made of steel, titanium, aluminum, or composites. The tensioning system and the array-style design allows the riser to move axially or stroke, relative to the platform. For deepwater applications, TTRs are also equipped with buoyancy systems which allow to reduce the load on the tensioners.

3.8.3. Flexible Risers

Flexible risers are an excellent solutions for both shallow and deep water developments. They best suit wet-tree developments, especially when a FPSO is used as processing facility. Indeed, they allow broad relative oscillations between the facility and the subsea system. Furthermore, they can be deployed in a variety of layouts.

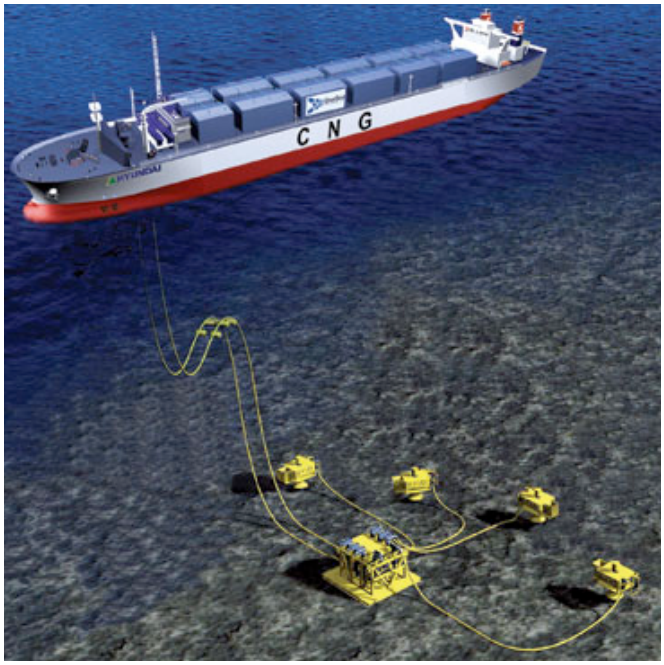

Fig.27: Flexible riser connected to a FPSO.

The key feature of flexible risers is their layered-sheath structure, where each layer is able to freely move respect to the others, when the riser is changing its shape. Generally flexible risers are composed of:

- An internal fluid containment barrier;
- A pressure armor, generally made of carbon steel;
- A carbon steel tensile armor for resisting tensile loading;
- A series of insulating layers for heat retention (generally made of poly propylene);
- A series of anti-friction tapes, which wound the armor layers;
- An external sheath for protecting the riser from environment effects.

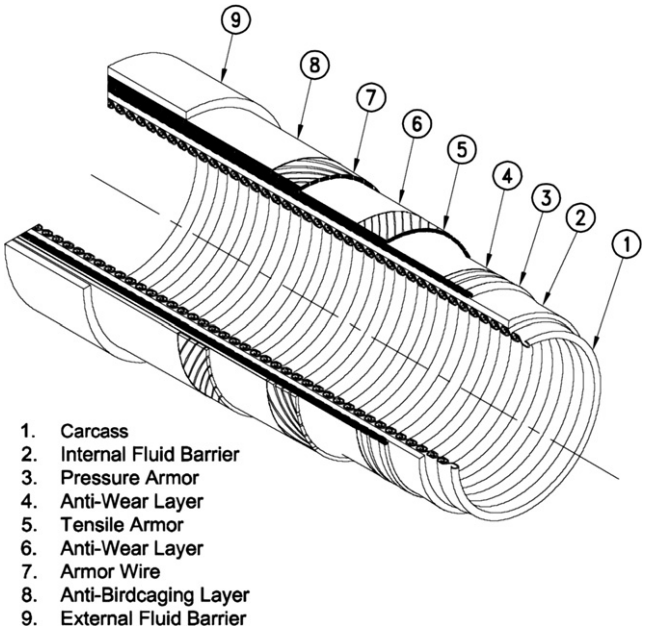

Fig.28: Flexible riser layers.

3.8.4. Hybrid Riser

TTRs are feasible only for TLPs or SPARs, thus their application is really restricted. However, adding to the top end of TTRs a flexible jumper it is possible, for instance, to couple a TTRs and a FPSO. When this solution is chosen, the riser system is referred as hybrid riser. The principal purpose of this riser is accommodating relative motion between the floating vessel and the subsea system. The rigid section of the riser is generally tensioned by a floating buoy.

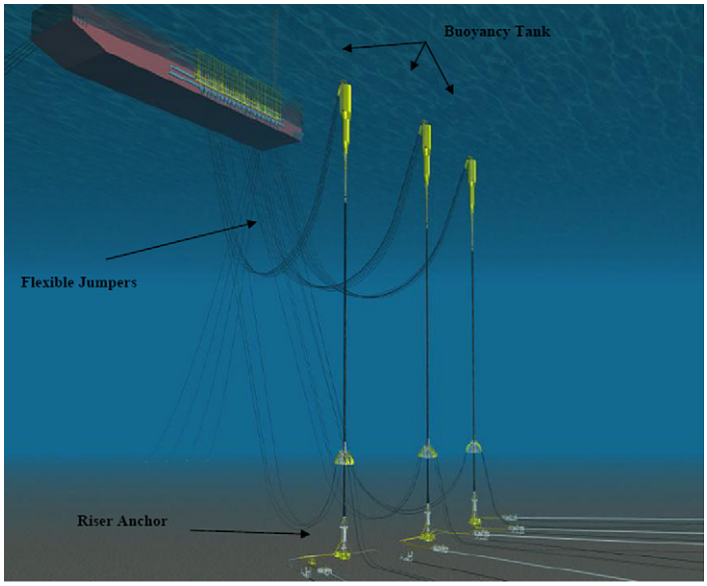

Fig.29: Hybrid riser connected to a FPSO.

3.9. Subsea Distribution system

A subsea distribution system (SDS) provides auxiliary functions to the producing system, with main concern on the transportation and delivery of electrical power, chemicals and control.

Power, control fluid and chemicals are delivered to the subsea system throughout the umbilical. The umbilical is connected to the umbilical termination assembly (UTA) which is linked to the subsea distribution assembly (SDA) or subsea distribution unit (SDU) via flying leads. The SDU has in charge to deliver power and hydraulics to trees and the manifold. On the seabed, power and fluids are respectively delivered via electrical and hydraulics flying leads (EFL and HFL).

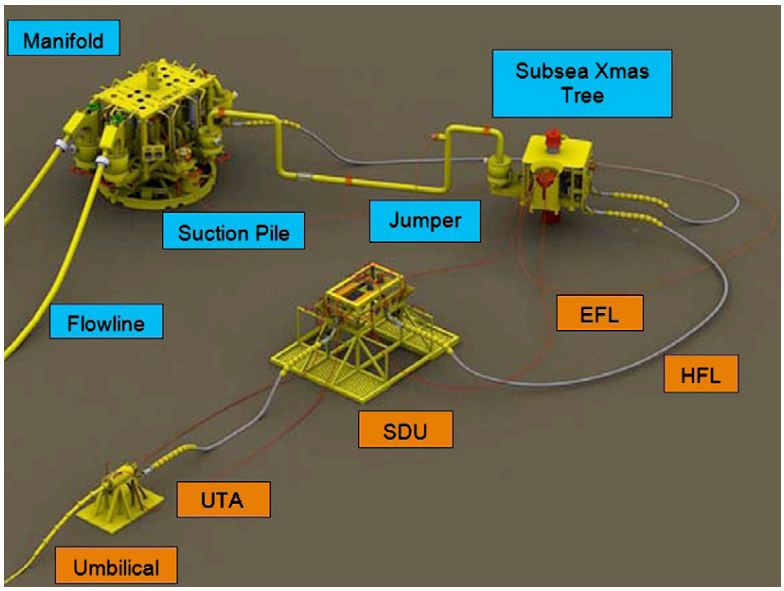

Fig.30: Subsea distribution system.

3.10. Umbilical Systems

An umbilical is an assembly of tubing, piping, and/or electrical conductors in an armored cylindrical sheath, connecting the topside facility with the subsea equipment. It conveys control fluid and/or electrical current necessary to control the functions of the subsea production system. Sometimes umbilical and flow line can be combined together creating an integrated production umbilical (IPU). Umbilical length, thus, is determined by the tieback length, while the diameter commonly ranges up to 25,4 cm.

Fig.31: Umbilical, umbilical layers and cables.

Umbilical main challenges are water depth and tieback length. In deepwater developments, the main challenge is concerning the steel tube design: indeed the tube is under high pressure and subjected to high tensile load, due to the hang-off load of the umbilical itself. In deeper applications lazy wave buoyancy modules are used to free the upstream part from the downstream hang-off load.

4. Flow Assurance principles

The term flow assurance was firstly casted by Petrobras in 1990s and refers to the set of topics related to the proper transportation of the produced fluid to the processing facility. These topics are:

- Hydraulics;
- Thermodynamic;
- Chemistry;

Fig.32: Asphaltene deposited layer on the internal wall of a pipeline.

Flow assurance importance is continuously increasing, as oilfields are moving in deeper waters and tieback lengths are increasing. Thus, flow assurance has become a critical part of both system designing and managing. It mostly concerns on avoiding solid deposition and accumulation. Most threatening solids are:

- Hydrates;
- Waxes;
- Asphaltenes.

There are typically two strategies for pipe occlusion avoidance:

- Prevention strategy: flow assurance mostly concerns on avoiding the formation of solids by maintaing the system far from the solid formation conditions, which are thermodynamically determined by pressure and temperature. Most efforts are, for instance, focused on hindering heat loss along the pipe. Another important solution to avoid hydrate formation is chemical injection. Chemicals

are used when the system has to run in thermodynamic conditions favorable to solid formation; chemicals can either change the solid existence envelope (thermodynamic inhibitors) either hamper and block solid growth (kinetic inhibitors);

- Remediation strategy: solid are allowed to form and deposit, although periodic removal is performed by means of pigging.

Flow assurance is required to determine the optimum flowline pipe size based on reservoir well fluid test results for the required flow rate and pressure. As the pipe size increases, the arrival pressure increases, while temperature decreases. Then, the fluid may not reach the destination and hydrate, wax, and asphaltene may be formed in the flowline. If the pipe size is too small, the arrival pressure may be too low and temperature too high, thus a thick wall pipe may be required and a large thermal expansion is expected.

In conclusion it is possible to sum up three main flow assurance issues as it follows:

- System (hydraulic) deliverability: Pressure drop versus production (pipeline size and pressure boosting) and slugging avoidance;
- Thermal behavior: temperature distribution and temperature changes during transient operating conditions;
- Solids and chemistry inhibitors.

Fig.33: Deposited Wax layer.

4.1. Flow assurance process

The flow assurance analysis is an integrated process from the beginning of front-end engineering and design (FEED) to the system operating conditions management. This process can be divided in the following steps:

- Fluid characterization and flow property assessments;
- Steady-state hydraulic and thermal performance analyses;
- Transient flow hydraulic and thermal performance analyses;
- System design and operating philosophy for flow assurance issues.

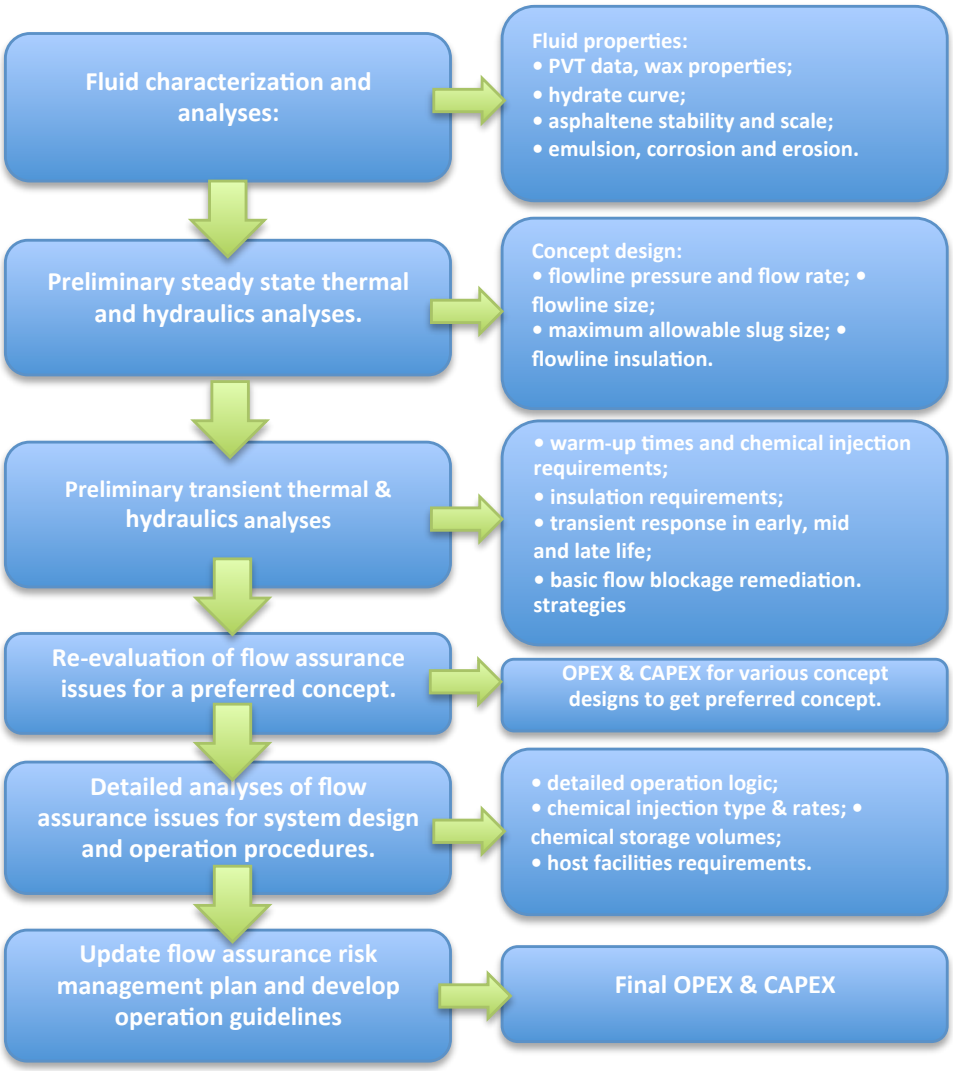

Tab.2: Flow assurance study: conceptual procedure.

4.1.1. Fluid characterization

The reliability of a flow assurance study is completely based on the wellbore sample analysis which allows to determine the fluid properties, such as phase composition, GOR (gas/oil ratio) and bubble point. The fluid characterization process generally concludes with a PVT report, which allows to perform the steady state hydraulic and thermal analysis.

4.1.2. Steady state hydraulic and thermal analysis

This analysis is completely carried out by process simulator such as OLGA and HYSYS. In this step, pipe diameters and insulation thickness are chosen in order to achieve the following goals:

- Reach the processing facility at an acceptable pressure even with the maximum flow rate;
- Avoid the fluid from entering into the hydrate formation region in any point of the flowline;
- Avoid the fluid arrival temperature at the processing facility from exceeding upper limits, set by the topside process equipment.

4.1.3. Transient conditions analysis

This analysis investigates the system behavior during transient operational conditions and is focused mainly on:

- Assessing the hydraulic flow conditions (i.e. severe slugging check out);
- Investigating the system thermal behavior and developing a hydrate-formation prevention strategy.

There are eight different transient operating conditions:

- Start-up;
- Shutdown;
- Blowdown;
- Warm-up;
- Turn down;
- Pigging/slugging.

4.1.3.1. Startup

During a startup, hydrate inhibitors are always required to be injected at wellhead. If reservoir temperature is low and the start-up rate is moderate, hydrate inhibitors are required at bottomhole too. Chemical injection must be performed until the coldest part of the system reaches the warm-up temperature. This temperature ensures, in case of emergency shutdown, a cool down time long enough to allow operators to handle the problem and inject chemicals where required. The start-up procedure can be performed with cold flowlines (cold startup) or with warm flowlines (warm startup). Generally cold startup requires more chemicals to be injected for longer periods.

4.1.3.2. Shutdown

During a shutdown, the flowline naturally cools down due to heat losses towards the environment. It is important to assess whether the system cool down time is longer or shorter than the no-touch time. Indeed, the during no-touch time, no actions are taken by the operators and the system should not enter in the hydrate-forming region during this period. Afterwards, jumpers are flushed with methanol and the line can be either blown-down and displaced with dead oil either restarted.

4.1.3.3. Blowdown

This procedure foresees the evacuation of the produced fluid from the riser and the its displacement with gas. Blowdown is performed to depressurize the line and to reduce the hydrate forming temperature. Until the blowdown procedure is completed the flowline must be preserved throughout the injection of hydrate inhibitors. For such reason it is useful to know the blowdown duration, which determines the period of time inhibitors need to be injected. Furthermore, blowdown operation cannot be performed too fast, otherwise the system would cool down for Joule-Thompson effect and it would further expose the most threatened parts.

4.1.3.4. Warm-up

During a warm-up procedure, the flowline is recirculated with warm dead oil. This is performed to warm up the line before a start-up: once the line has reached the warm-up temperature, production can be restarted and the produced fluid can travel along the tie-back. The warm-up is performed to:

- Reduce the amount of methanol required to be injected during a start-up;
- Reach faster the a shutdown safe temperature, which avoid the system from entering in the hydrate-forming region too quickly;
- Increase the cool down time, because even the pipe surrounding soil has been heated.

Warm-up simulations aim to determine the warm-up time, this is the period during which dead-oil must be recirculated in the line.

4.1.3.5. Riser cool down

Generally riser base cools down faster than the rest of line. This is due to gas accumulation and a different pipe insulation layout. Thus, riser cool down time is generally assessed during shut-down simulations and modifications can be applied to the previous design in case of unacceptable low cool down times.

4.2. Hydrates

Main efforts in flow assurance are made to avoid hydrate formation, which actually represents the main challenge due to its detrimental effects. Gas hydrates are crystalline, cage-like structures of water molecules similar to ice and for such reason hydrates are often referred as clathrates, which mean “cages” in ancient Latin. Such cages trap in them selves gas molecules of light hydrocarbons (methane, ethane, propane isobutane, normal butane) and even other molecules such as nitrogen, carbon dioxide, and hydrogen sulfide. Although even several heavy hydrocarbons, such as benzene, cyclopentane, cyclohexane, methylcyclopentane, methylcyclohexane, isopentane and dimethylbutane, can form hydrates under appropriate thermodynamic conditions.

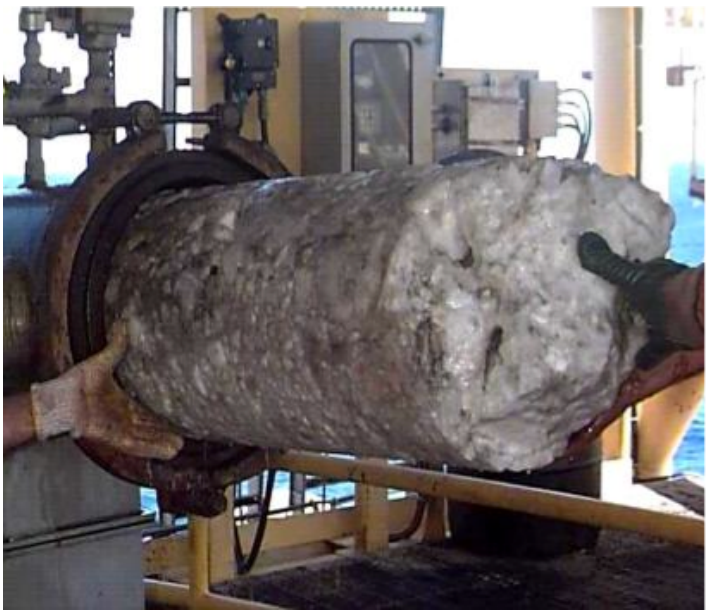

Fig.34: Hydrate plug.

Hydrates are likely to occur when light hydrocarbons are in presence of water at thermodynamically favorable pressure and temperature (high pressure and low temperatures). Such conditions are caused by heat loss along the flowline, or

after a choke where the fluid can be cooled down by Joule-Thompson effect. Although the main threaten to flow assurance is during transient operating conditions, for instance during shutdown operation when the fluid residence time is infinite. An opportune hydrate analysis should study and acquire the following informations:

- Hydrate structure;
- Operating pressure and temperature;
- Water composition and water cut;
- Residence time of fluids;
- Slugging, liquid hold-up;
- Joule-Thomson behavior;
- Other production chemicals in system;
- Topside fluid processing;
- Sub cooling.

4.2.1. Hydrates structures

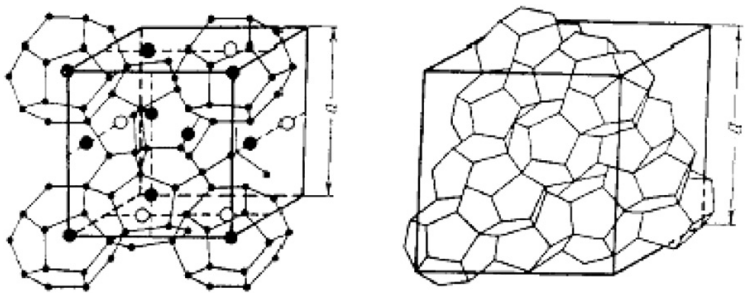

Fig.35: Hydrate crystal structures: type I (left) type II (right).

Von Stackelberg and Muller 1954 studied hydrates structure by performing X-ray diffraction analysis and discovered that two main types of hydrate structures occur in oil&gas production systems, depending on the size and on the concentration of guest molecules:

- Structure-I (or Type-I);
- Structure-II (or Type-II).

Former hydrate family has 46 water molecules for 8 cavities, 2 of which are spherical and 6 oblate, while the latter has 136 water molecules per 32 spherical cavities. Lighter hydrocarbons are more likely to form structure I hydrates, while heavy hydrocarbons can enter only large cavities and form structure II hydrates. The table below shows the hydrate structure each hydrocarbon can form.

Component	Structure I	Structure II
C1	X	X
C2	X	X
C3		X
nC4		X
iC4		X
CO2	X	X
N_2	X	X
H_2S	X	X
O_2	X	X
Ar	X	X
Dimethylpropane		X
Cyclopropane		X
Cyclohexane		X
C_6H_6		X

Tab.3: Hydrate host molecules.

In 1987 Ripmeester et al. discovered a third type of hydrate structure, known as H. Such structure is composed of 34 water molecules per 6 cavities, which can host both small and large guest molecules, although, it requires heavy hydrocarbon molecules to exist. Hydrates structure does not influence the time and the velocity of the hydrate crystallization process.

4.2.2. Hydrate preventing strategies

4.2.2.1. Chemical Injection

Hammersmith in 1934 firstly recognized that hydrate formation could occur above the water freezing temperature and decrease or even block the oil production in a short period of time. Remediation strategy is the least preferred solution, because is time consuming and expensive and, most of all, very risky: indeed, hydrate formation can lead even to catastrophic failures. It is common used to avoid and prevent hydrate formation through two main strategies:

- Thermodynamic prevention;
- Agglomerating prevention.

The first solution inhibits the very formation of the hydrate structure, while the latter slows down and limits the crystal growth avoiding plug formation. Thermodynamic prevention strategy can be pursued by:

- Reducing the water content in the stream;
- Operating at temperatures higher than hydrate-formation temperature by heat retention and generation;
- Operating at pressures lower than hydrate-formation one for a fixed temperature;
- Adding chemical inhibitors which shift the hydrate equilibrium envelope towards lower temperatures and higher pressures. Common inhibitors used are salts, methanol, and glycols. Such inhibitors require high injection rates, therefore regenerating units are required in order to recover the inhibitor itself.

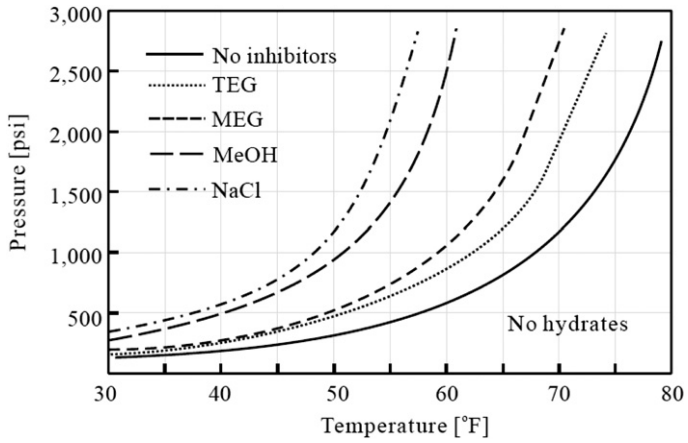

Fig.36: Effect of salt and inhibitors on hydrate forming envelope.

Agglomerating prevention strategy is pursued through adding low-dosage inhibitors which do not shift the hydrate formation envelope, but avoid the formation of hydrate plugs. There are mainly two types of low dosage inhibitors:

- Anti-agglomerates (AAs);
- Kinetic hydrate inhibitors (KHIs).

AAs are surface active molecules which react with hydrates and disperse them into fine particles: when the AA molecule and the hydrate crystal come in touch, the resulting particle is hydrophobic and repels further water molecules. The hydrate-oil mixture is carried as slurry to the processing facilities without any failure. AAs success is limited by the water content, indeed if the water cut is too high, the oil phase saturates and AAs are not able anymore to disperse the

hydrate crystals. Oppositely, kinetic hydrate inhibitors do not fear water content and act in a completely different way: they slow down crystallization process by delaying nucleation for an interval of time known as “hold time” or “induction time”. The main parameter affecting KHIs performances is the subcooling factor, which strongly reduces the hold time. Induction times can vary from few hours to several weeks, depending on the subcooling, which is usually lower than 12°C. If a higher subcooling is required, kinetic inhibitors may be combined with methanol which shifts the hydrate formation envelope towards lower temperature, thus decreasing the subcooling. KHIs are best suited for systems with low subcooling and operate under generally steady state conditions. Indeed, they cannot be effective during long shutdown conditions, because of their own time-dependent nature. They prefer heavy hydrocarbons, which produce structure-II hydrates, which are more susceptible to KHIs action. They are quite sensible to water conditions, as they become less soluble with water temperature and salt content. Thanks to reduced injection rate, KHIs have been successfully applied in field for about 13 years even in combination with thermodynamic inhibitors.

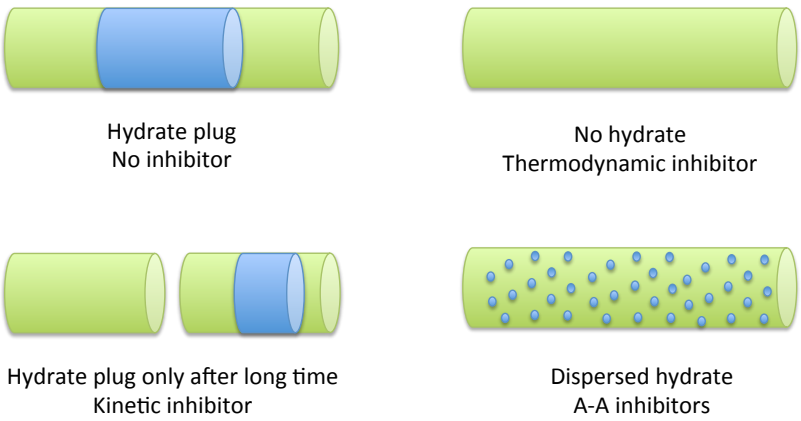

Fig.37: Hydrate distribution for each inhibitor type.

4.2.2.2. Water removal

Hydrate structure is mainly composed by water, thus it is reasonable to remove water in order to avoid hydrate structures formation. This is commonly performed in export pipelines. Dehydration can be performed by means of subsea separation systems, which, apart from separating water from the main stream, also lightens the fluid and:

- Eases the fluid lift up across the riser;
- Prompts hydrocarbon production by decreasing the backpressure on the well.

Subsea separators are located close to Xmas trees on the seabed, they are generally composed of the following major components:

- A separator, which splits water;
- A pump, which provides the pressure boost for water injection;
- A water well, which allows the water injection in the reservoir.

These systems generally do not separate all the free water in the stream and do not provide complete protection from hydrate formation; furthermore, their main weakness is generally reliability, thus a second hydrate prevention strategy should be developed.

4.2.2.3. Active heating

Active heating is both a prevention and a remediation strategy against hydrates. There are two different main techniques for active heating:

- Electric heating; this technique can be performed by dissipating electrical energy either directly in the pipe, which is used as conductor, (direct heating) either indirectly. Electrical heating has been successfully applied to different fields such as: Nakika, Serrano, Oregano, and Habanero in the Gulf of Mexico, and Asgard, Huldra, and Sliepner in the North Sea;
- Hot fluid recirculation; Hot fluid can circulate either in a pipe annulus either in auxiliary pipe close to the production one. Generally hot water is used as recirculating fluid. Examples of such heating techniques are Statoil Asgard and Gullfaks South, Conoco Britannia, and BP King.

4.3. Multiphase Hydraulics

Multiphase flow is continuously gaining importance in the oil&gas industry thanks to the economic advantages that multiphase transport offers, such as the use of one single pipeline instead of two. However, multiphase flow is really a complex topic, where there are many active variables which often cannot be effectively reduced. For instance, in an upward pipe vapor phase advances at higher velocity than the liquid one due to buoyancy forces. Thus two velocities exist and this affects all the mixture behavior and flow patterns. Before performing a deeper study on slugging, an overview on multiphase flow patterns is preliminary developed.

There are mainly three different types of flow patterns:

- Homogenous phase distribution;
- Separated phases in co-current flow;
- Separated phases in intermittent flow.

4.3.1. Multiphase flow patterns

The multiphase flow pattern depends on the equilibrium of body forces and surface forces: body forces tend to separate the two phases, while surface forces mix phases up. Body forces are those which act on a control volume, as gravitational fields or centrifugal forces, while shear stresses and surface tension are examples of surface forces.

Homogeneous flow occurs when turbulence forces are able to mix the two phases up, overwhelming body ones and when there is a dominating phase and a dispersed one, which is pneumatically transported. If the dominating phase is liquid, bubble flow is observed: higher flow velocity, turbulence and smaller bubbles lead to homogenous mixture. Turbulence and surface tension, acting on small bubbles, tend to create a relatively uniform distribution of bubbles. If the dominating phase is gas, liquid droplets are pneumatically transported; this flow pattern is very unsteady: as soon as the local velocity decreases, the droplets coalesce and fall on the pipe surface.

Separated-phases flow usually occurs when turbulence forces are weak and unable to mix the flow; here body forces dominate and separate the two phases. Buoyancy forces can create stratified flow at low GVF; if velocity is increased, wavy flow is observed. At high GVF, homogeneous flow changes into annular flow when flow velocity is reduced and droplets collapse on the pipe surface,

since high shear stresses distribute the liquid in form of a thin layer over the entire circumference of the pipe wall.

When neither body forces neither surface forces are able to dominate, the flow pattern changes along the pipe length. Bubbles coalesce creating larger gas accumulations ("plugs"). The effect grows when decreasing mixture velocity. In upward flow through a vertical pipe the gas plugs move faster than the liquid due to buoyancy. There is thus a "slip" between the liquid and gas phase. Slug flow occurs when in wavy flow the gas Reynold number is increased and the pressure oscillating effect is enhanced until the wave hight reaches the pipe upper wall creating gas chamber inside a liquid medium.

The following graph shows different flow patterns for an air/water mixture in a horizontal pipe.

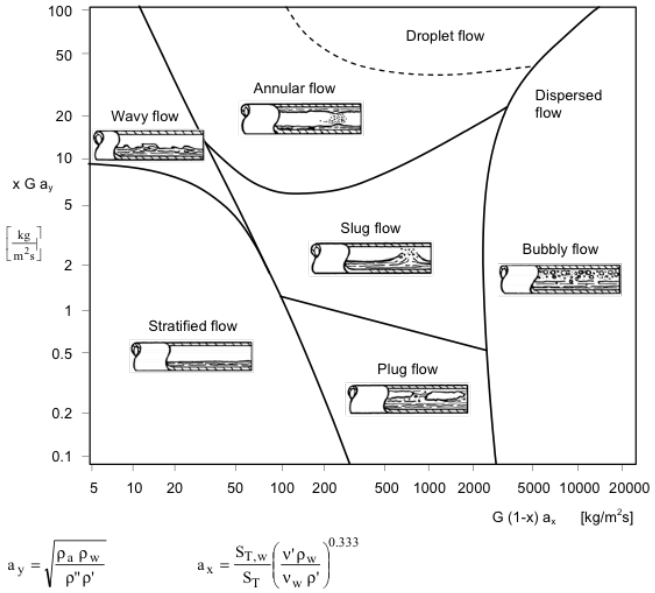

Fig.38: Flow patterns in horizontal pipes.

4.4. Slugging

Slugging is the most feared and threatening flow pattern which can occur in multiphase transportation, especially for the topside equipment. On onshore facilities large slug-catcher can be installed, although this not economically feasible in an offshore one. Most negative effects of slugging are:

- High kinetic forces on topside fittings and vessels;
- Pressure cycling;
- Control instability;
- Inadequate phase separation.

Indeed afterwards a liquid slug, there is always a bubble of compressed gas. The gas compression occurs along the riser, where the gas is moved up by buoyancy forces but it is blocked by the afterwards liquid slug. Thus, the bubble has to lift up the liquid slug pushing it upward. During this process gas must exert a pressure, on the liquid-gas interface, higher than the liquid one.

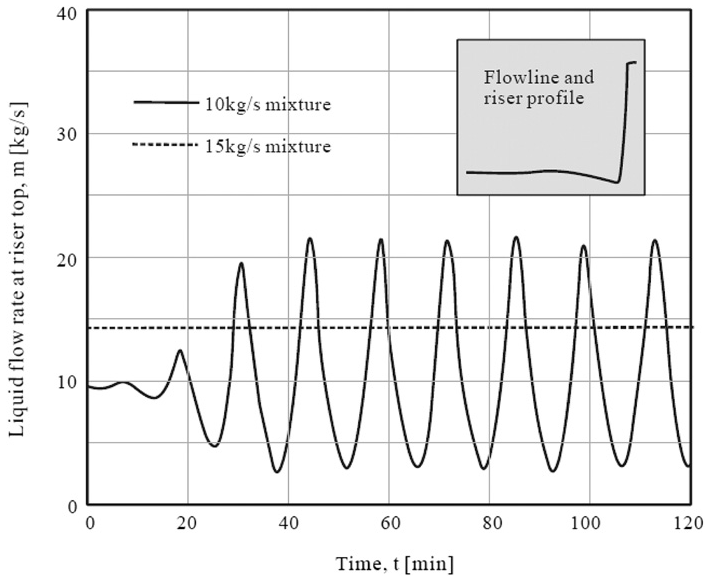

Fig.39: Flow stability at riser base.

Slugging is generally affected by the flowline geometry and by fluid flow rate. For instance, deploying a horizontal pipe afterwards the riser reduces severe slugging, while having a negative slope before riser base increases it. If the slope is positive, generally severe slugging does not occur. The deployment of a choke before the processing facility also smooths the slugs intensity.

Slugs can be classified depending on the causes which generate them:

- Hydrodynamic slugs: formed from the stratified flow regime due to instability of waves at high gas Reynolds numbers.
- Terrain-induced slugs: occurs at low flow rates, liquid can accumulate in lower parts of the system due to buoyancy forces.
- Operationally induced surges: they occur during the transition from one operational condition to another; for instance, during a start-up.

4.4.1. Hydrodynamic slugging

This is the main slugging cause when operating in steady state at high flow rates. At high gas Reynolds numbers, the gas turbulent flow exerts an oscillating pressure on the liquid surface, generating small waves. Then gas pushes further the wave, which starts to grow, triggered by Kevin-Helmoltz wave instability law, until reaches the upper part of the pipe. Once the slug is created, gas, which has a higher velocity than liquid, accelerates the liquid slug, which captures further liquid. During this process, some gas is captured by the slug creating a turbulent flow inside the slug its self. This turbulent flow is liable for most of the pressure losses occurring in slug flow.

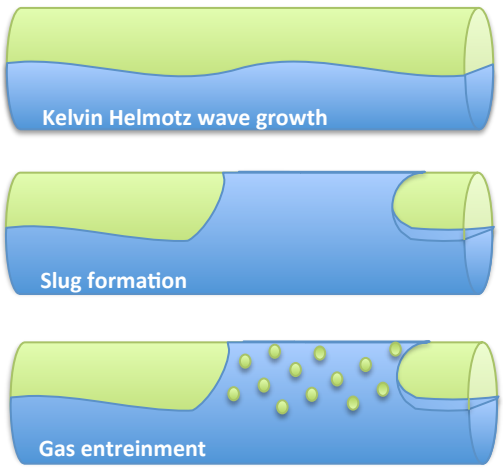

Fig.40: Slug formation process.

Then, the evolution of slug pattern is very sensitive to the pipe geometry. Small oscillations in height can lead to wide amplifications of the slugging phenomena. Thus, peaks and troughs, which can cause relatively small inclination changes such as 1 degree, may have a very significant effect on the slugs size and on the pressure drop too. This is very important because just few pipelines have really a steady inclination, while more often the pipe follows the soil bathymetry, which is commonly wavy. The following picture shows the pipe profile effect on the slug flow pattern.

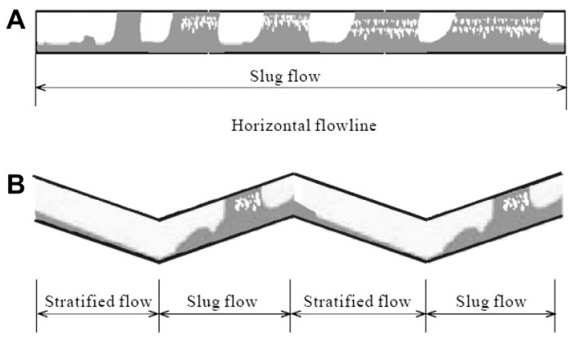

Fig.41: Effect of pipeline topography to flow pattern

4.4.2. Terrain slugging

Terrain slugging is often the main cause of severe slugging. Indeed, the strength which terrain slugging can reach is generally higher than the one reachable by hydrodynamic and transient slugging. This is due to the very nature of the physical process which underlies terrain slugging.

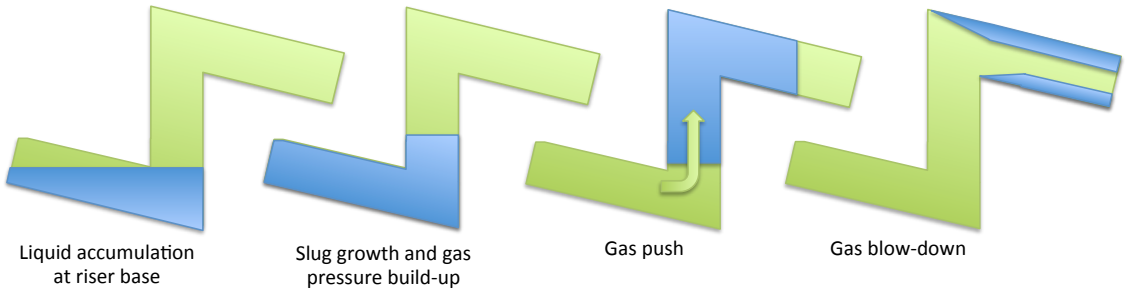

Fig.42: Formation of Riser Slugging

In case of low flow rates, liquid has not enough kinetic energy to climb up the riser, so it accumulates at riser base blocking even the gas from flowing. Pressure builds up until overwhelms the liquid hydrostatic head, then the liquid slug is able to climb up the riser.

4.4.3. Transient slugging

This type of slugging generally occurs when the system is operating in a different condition from the one it was designed for. For instance, when flow rate is decreased, the pipe diameter is over-dimensioned for the actual flow rate; another example is during a start-up, when some tubings may be filled with liquid and the system could work intermittently.

5. Multiphase pumps for subsea duties

5.1. Introduction to artificial lift methods

In order to enhance the oil flow rate, it is possible to decrease the bottomhole pressure (BHP) on formation; this practice is called artificial lift and is necessary when the reservoir energy is not sufficient to produce the required flow rate.

It can be achieved by deploying a pump, which supplies the required head, or by gas lift. The last one requires the injection of gas generally downhole (or riser base), which reduces the density in the tubing (or across the riser) and, thus, the bottom hole pressure. The choice of the most appropriate lift method is performed by economic factors, as the initial cost, the operating cost, the enhanced flow rate and the quality (then price) of the produced fluids. The costs vary broadly across the industry, according to field conditions:

- Reservoir depth;
- Pressure;
- Fluids;
- Distance of well from main platform;
- Environmental impact.

Conventionally, the best artificial lift method is considered to be the system which provides the highest net present value for the project life. Good data are required for a complete present-value analysis, and these data are not always broadly available.

In subsea applications, artificial lift is widely used in shallow waters, while in deepwaters is not widespread yet. However, such challenging fields will surely benefit the artificial lift advantages which will help to maintain production over the years and achieve economic objectives. In off-shore fields both ESP and gas lift have shown to be reliable and mature technologies. ESP are suitable only for low GVF fields or must be downhole located to prevent the pump from operating under gassy conditions. In most cases, GL is preferred over ESP, as less equipment is put at risk (in the case of equipment getting stuck in the hole). For the foregoing reason, Gas lift has proved to be the most reliable artificial lift method and has become the most widespread solution in the offshore environment to date; however, as operators progressively move into deeper waters, GL applications become more problematic due to higher operating pressures, which strongly reduces gas lift economic benefits. Indeed, as compressor duty increases, energy and equipment costs surge. Operators are

looking for more attractive solutions and other emerging technologies, such as subsea multiphase boosting and subsea gas/liquid separation.

5.2. Gas lift

Gas lift is an artificial lift method, which enhances production by lightening the fluid column through the injection of high-pressure gas; for this reason, gas lift is suitable only for oilfields. On the other hand, if the oilfield does not contain any gas at all, gas lift cannot be performed. Gas lift can be injected either continuously either intermittently. The latter solution presents many disadvantages, such as slug-induced flow and the detrimental effect on the reservoir permeability, and is the last preferred. Hereafter, gas lift will be considered only in continuous flow.

Gas lift benefits can be summed up as follows:

- It improves oil recovery;
- Reliable and mature technology;
- It reduces slugging;
- Simple and flexible artificial method;

While main disadvantages are:

- Not suitable for small platforms, due to wide footprint required for compressors
- Definitely threatening for flow assurance issues in deepwater fields.

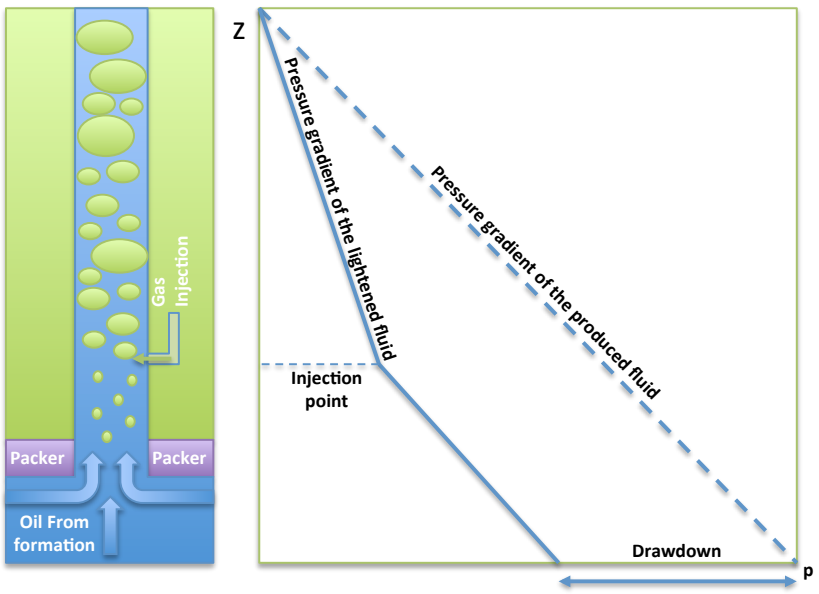

Fig.43: Gas lift effect on tubing pressure distribution.

The choice of injection pressure is one of the main concerns on designing the gas lift system. Indeed, it affects both field productivity both energy requirements, during the separation process (heat required) and during the compression one (power required). Injection pressure increases both recovered oil and compressor required power. Thus, the selected pressure is generally a trade-off between the two complementary benefits. The "*condicio sine qua non*" in choosing the injection pressure, is to have a gas pressure higher than the actual pressure in the tubing, at the injection point height. Indeed, actual pressure increases with tubing depth and gas will flow inside the tubing only if its pressure is higher than the tubing one. Furthermore, the actual pressure is influenced by downstream conditions and has a broad volatility range. Thus the gas injection pressure must be higher than the any possible actual pressure in the tubing. Therefore, gas is generally compressed at much higher pressure than the minimum required one; Furthermore, as the reservoir moves deeper, as injection pressure increases, as compression power surges. This is the main limit of gas lift in deepwater oilfields.

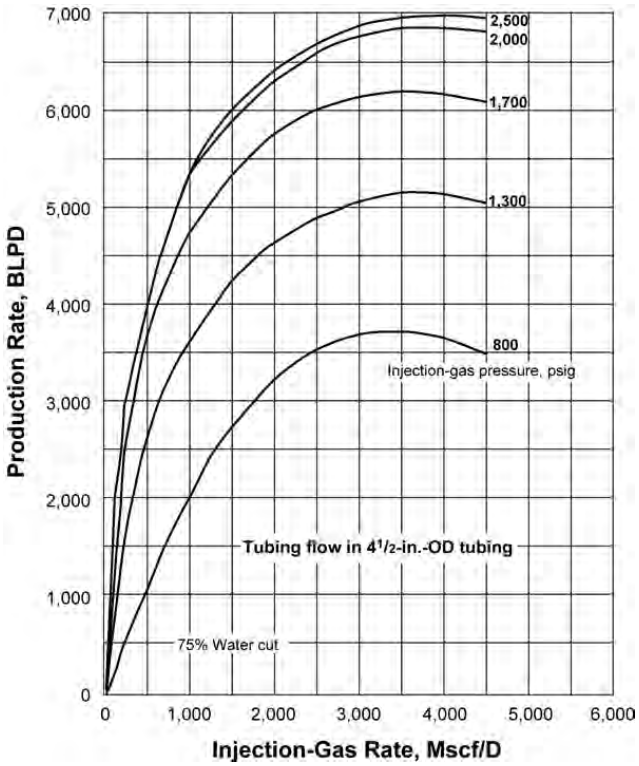

Fig.44: Well production against gas injection flow rate and pressure.

5.3. Introduction to Multiphase boosting

Multiphase boosters are machines which provide pressure boost to multiphase multicomponent fluid: gas, oil and water are the most common fluids elaborated in these machines. They can either be considered multiphase pumps either wet compressors depending on the phase fractions; indeed there is no clear limit between these nomenclatures. In the following text, it will be referred to multiphase pumps when the machine is designed to convey liquid in presence of gas and to wet compressors when the machine is designed to convey gas in presence of gas. However, multiphase pumps are required to work at very high gas volume fraction conditions even at 100% GVF for short periods of time.

Running in multiphase conditions permits to avoid the installation of a platform for gas/liquid separation and allows to deploy one single multiphase pipe, bringing the following advantages:

- Longer subsea tiebacks;
- Production increment, by reducing the flowing wellhead pressure. Indeed, the backpressure is sharply reduced by adding a pressure boost to the multiphase flow;
- Reduce CAPEX (capital expenditures) on topside equipments and pipelines. Moreover, it can reduce slugging activities, allowing to minimize upset equipment for slug handling;
- Environmentally friendly: small amount of gas are uneconomic to be exploited, therefore gas flaring is the most cost-effective solution. Indeed, gas facilities are capital intensive investments. MPPs allow longer tie-backs, then gas can be sent to central host facility where is properly handled to be sold;

Multiphase pumps have proven to be a mature technology and many installations have been successfully carried out worldwide. The following map shows the locations of pump deployment projects, specifying the current state of development (February, 2012).

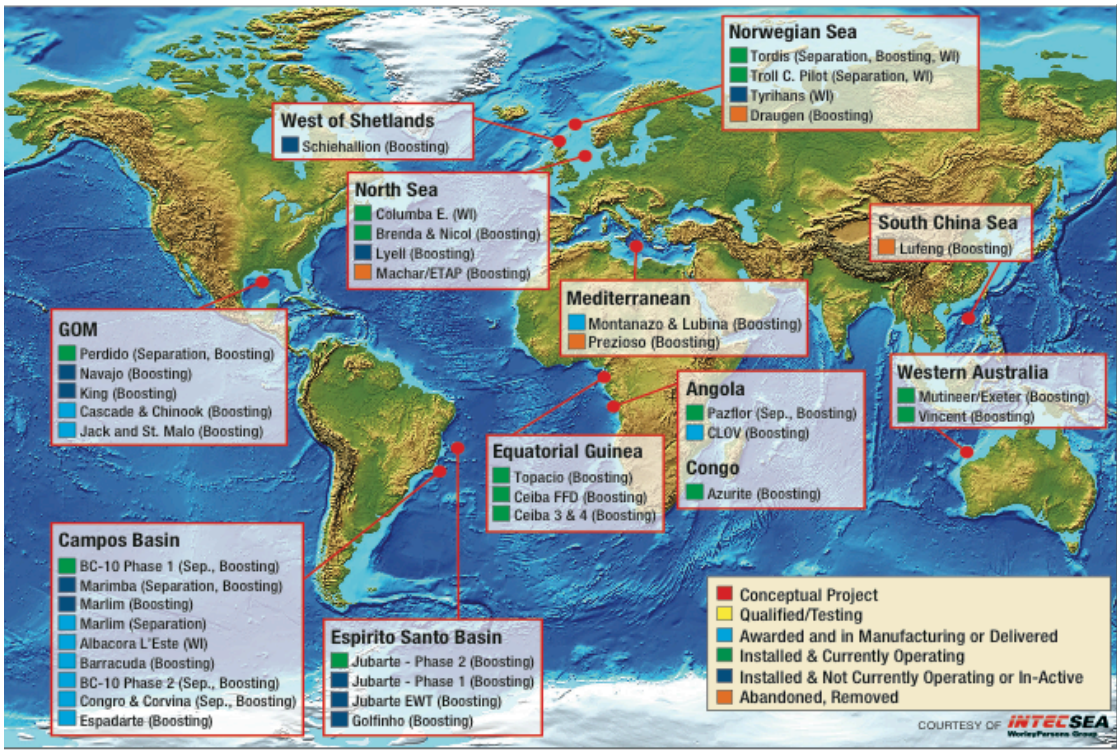

Fig.45: Worldwide locations for subsea pumping, water injection and separation systems.

5.3.1. Multiphase pump auxiliary components

A multiphase booster requires the following auxiliary components:

- An electric motor or a turbine;
- A subsea transformer;
- An electric power connector;
- The flow mixer for inlet flow conditioning;
- An electronic control unit;
- An environmental lip seal system.

Indeed the pump can be run by an electric motor or by a turbine connected directly to the pump. A control unit is always required for management tasks. The flow mixer helps to mix the different phases at the pump inlet, simplifying the pump duty.

5.4. Multiphase Pumping compared to conventional separation, pumping and compression

As explained previously, one of the actual challenge is to improve the well life and the ultimate recovery. Mack Shippen and Dr. Stuart Scott (Shippen & Scott, 2002) have performed an effective comparison between conventional single-phase technology and multiphase one.

In conventional production operations liquid and gas are separated on sea surface, then respectively pumped and compressed in different flow lines.

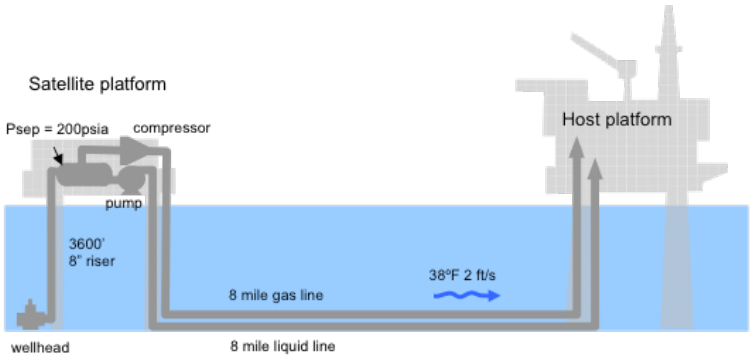

Fig.46: Conventional separation, pumping and compression conceptual layout.

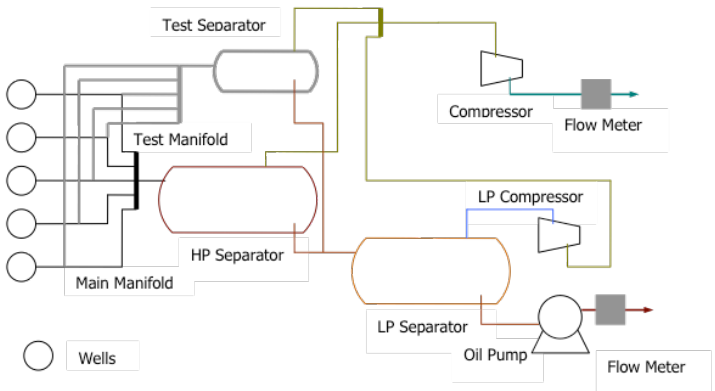

Fig.47: Conventional separation, pumping and compression process layout.

However, for long tiebacks one unique multiphase flow line is preferred rather than two, allowing a strong reduction in equipment cost.

A multiphase regime adds further backpressure to the flowline, raising the wellhead pressure from 7-14 bar (conventional development) to 70-140 bar, therefore a multiphase pump is required, which could even eliminate the need for the off-shore structure.

Moreover, such a steady high backpressure has a direct impact on production decline behavior, acting to reduce ultimate recovery (Martin & Scott, 2002).

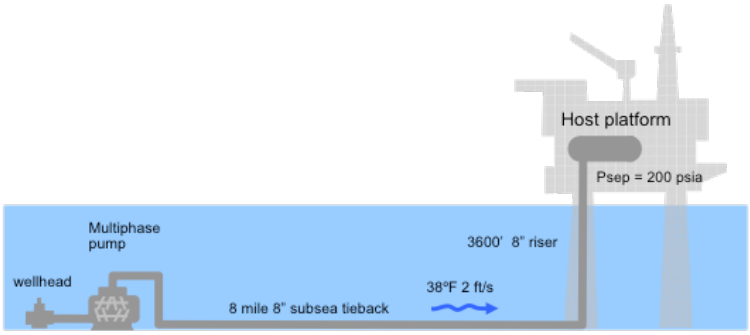

Fig.48: Multiphase boosting conceptual layout

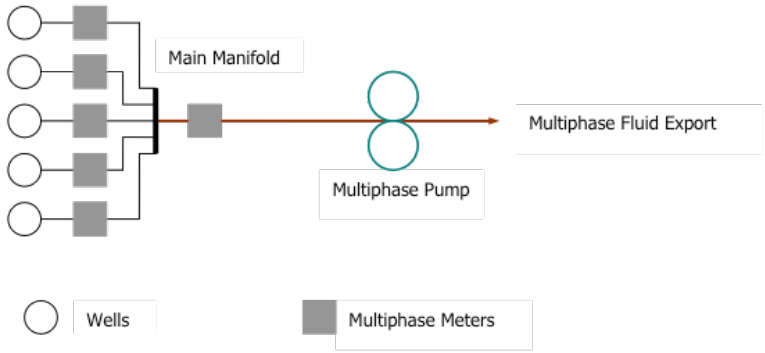

Fig.49: Multiphase boosting process layout.

The pump can be located either at the topside facility, at riser base, at wellhead or downhole. Despite from the first solution, all the other configurations are submerged. What changes from one another is the pressure profile: closer the the pump is to the wellbore, higher the volumetric flow will be. Indeed, backpressure can be seen as a waste of reservoir energy.

By means of lowering the wellhead pressure it is possible to achieve higher production rates, as shown in the picture below:

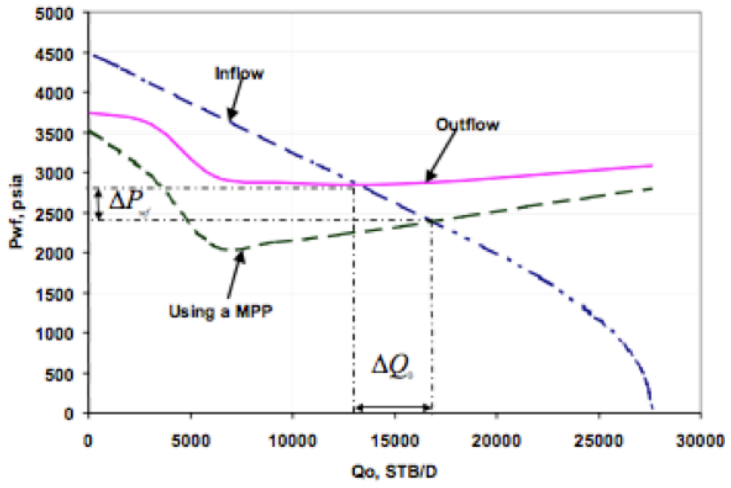

Fig.50: Effect of pump deployment on system flow matching

Therefore the deployment of pressure-supplier devices is very important in order to improve the well productivity. In the pictures below different pressure profiles have been plotted. The first one concerns a subsea field naturally flowing, the difference between the reservoir pressure and the wellhead pressure is quite small. The backpressure on the wellhead is mainly given by frictional losses along the pipe length and by the geodetic loss across the riser.

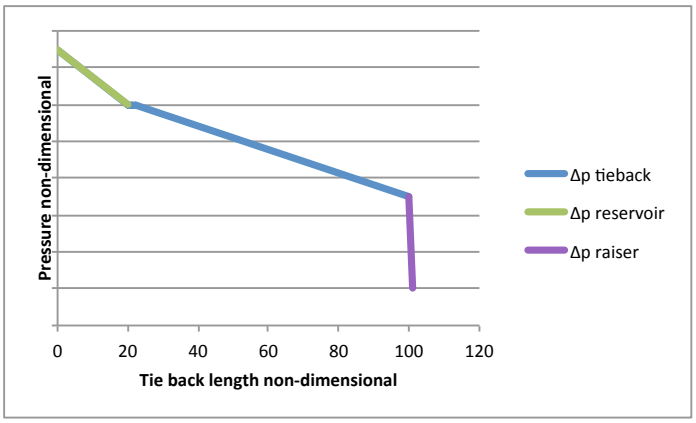

Fig.51: Pressure profile of natural flow system.

The second graph represents the pressure profile for a subsea rig with multiphase subsea booster. The difference between the reservoir pressure and the wellhead pressure is sensibly higher than the first case.

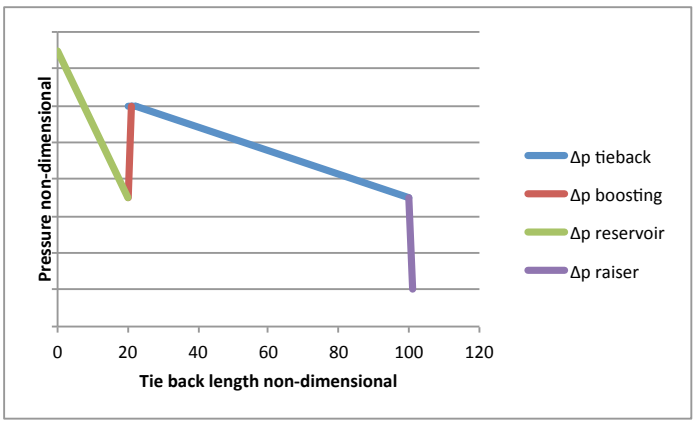

Fig.52: Pressure profile of subsea multiphase boosting system.

The third pressure profile concerns a conventional rig with a satellite platform required to separate and boost respectively gas and oil. The boosting benefits can be still appreciated, but the unfortunate pumping system position is liable for weakening them down.

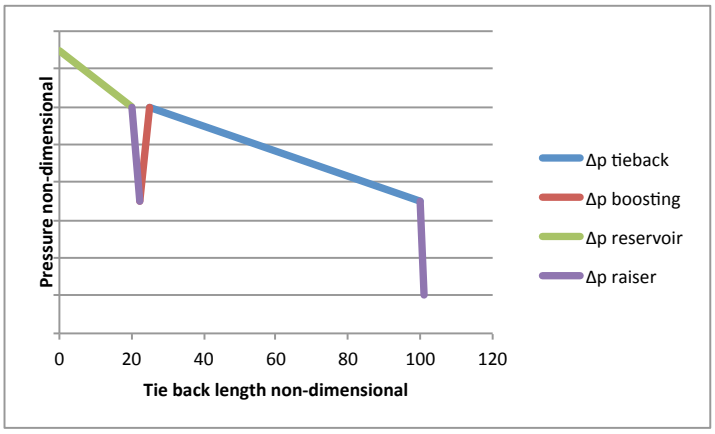

Fig.53: Pressure profile of conventional separation system.

The second solution appears to be the most effective one, despite the multiphase pumping is less efficient than a centrifugal one and than a compressor thanks to the displacement of the pump on the seabed.

5.5. Multiphase pump requirements for subsea applications

There are many types of multiphase pumps used in onshore applications, but just some have been deployed on the seabed. This is due to the subsea critical environment which transforms any weakness into a limitation, any failure into a huge economic loss.

Therefore, multiphase boosters for subsea applications must be reliable, thus they must be built with a minimum number of components, following the empiric rule "what is missing can't break down". Secondly, they must face and tolerate harsh erosive environment due to the sand presence. Another important feature is the pump weight: in case of failure a heavy pump requires a heavy vessel to be retrieved and replaced, which can need time to move and reach the failure location. Instead, a light pump can be substituted or repaired by a lighter ship, which allows easier and cheaper operations. Reducing the weight reduces downtime during mobilization, installation vessel cost and operational risks.

For these reasons, no planned maintenance is foreseen during the pump life and intervention is adopted only upon failure. Mitigation strategies are always welcome, as placement of all critical components, subject to possible failures (wear, fatigue), in a single easily retrievable cartridge.

Last but not least, the suction conditions are really variable and unsteady: gas volume fraction may vary from 0 to 100% during the reservoir life, as well as the fluid viscosity may have wide fluctuations. The pump must be able to handle all these alterations and manage them down.

Requirements
Sand Resistant
Able to handle high GVF
Tolerant to viscosity changes
Reliable and simple
Light

Tab.4: Subsea multiphase pump requirements.

5.6. Pump locations

Multiphase pump location in subsea fields is cause of very hard disputes, indeed there are many different and possible solutions, each one with different advantages and disadvantages. Therefore, the optimal pump location depends on the field characteristics, such as gas content and tieback length and on operator priorities. The main recognized locations for subsea applications are:

- Bottom hole;
- Wellhead;
- Riser base;

In high gassy well applications, bottom hole and wellhead locations are surely preferred due to higher pressure and lower gas content. Bottom hole would be better than wellhead, although in case of failure it would be more expensive to retrieve and replace the pump module. Riser base is recommended when the field has a lower gas content and the tie back length is high. Indeed, the umbilical system, which provides power to the pump, would be shorter than other solutions, thus cheaper.

The following picture illustrates the possible pump locations along the subsea system (green dots). Furthermore, umbilical path is shown in yellow; the continuous line stands for the common and minimum path, while the dashed one states for the optional route necessary to connect the pump when it is bottom hole or wellhead located.

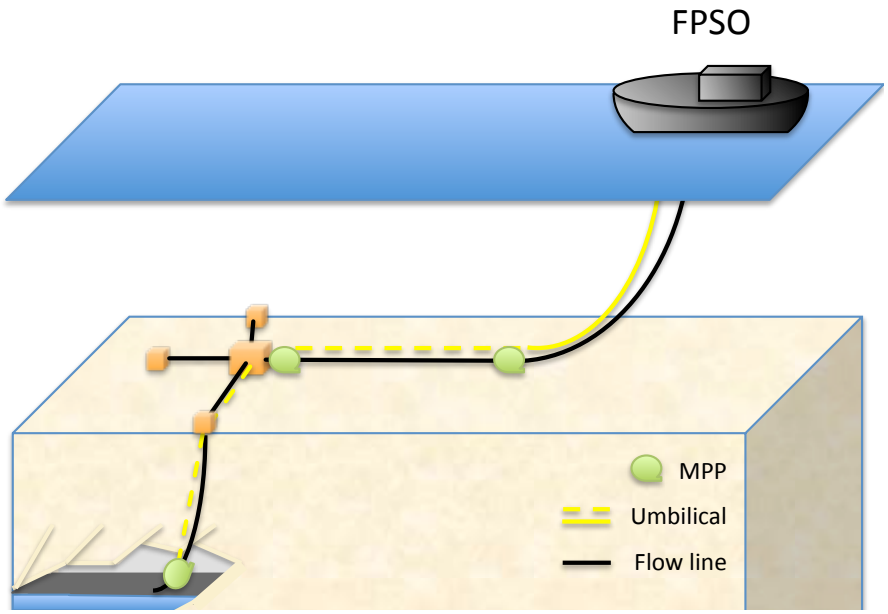

Fig.54: Common pump locations and umbilical paths.

5.7. Types of Pumps

Multiphase pumps can be either displacement either rotodynamic pumps. The former provides a flow rate which ideally does not depend on the differential pressure, indeed the only possible decline is due to a drop in volumetric efficiency. The differential pressure is determined by the difference between the discharge-environment pressure and the suction-environment pressure, or by the inbuilt volume ratio of the displacement pump. Picture below shows characteristic profile of a displacement pump.

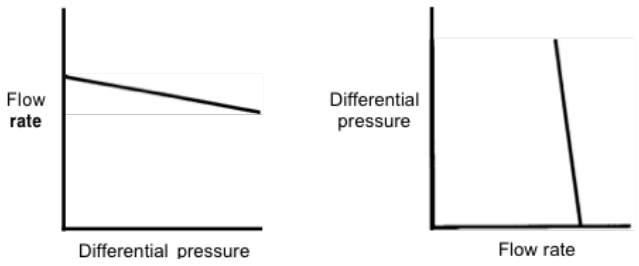

Fig.55: Volumetric pumps characteristic curves

The latter type of pump provides the required pressure by increasing the kinetic energy of the fluid, by means of impeller rotation, then converting it into pressure in a diffuser. Because the only energy exchange occurs in the impeller, in form of kinetic energy, and the pressure boost depends on the fluid density. Head and pressure characteristics are reported below.

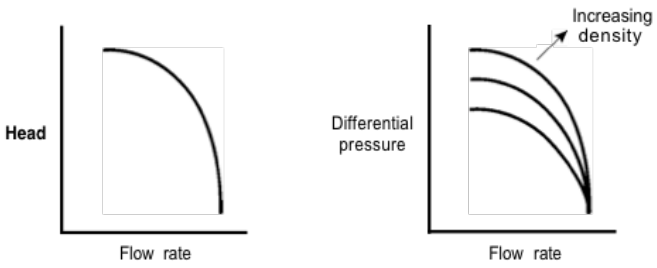

Fig.56: Dynamic pumps characteristic curves

This dissertation will consider only those multiphase pumps used for subsea duties. Main candidates for such purpose are:

- Helico-Axial;
- Twin screw;
- Progressing cavity;
- Hybrid.

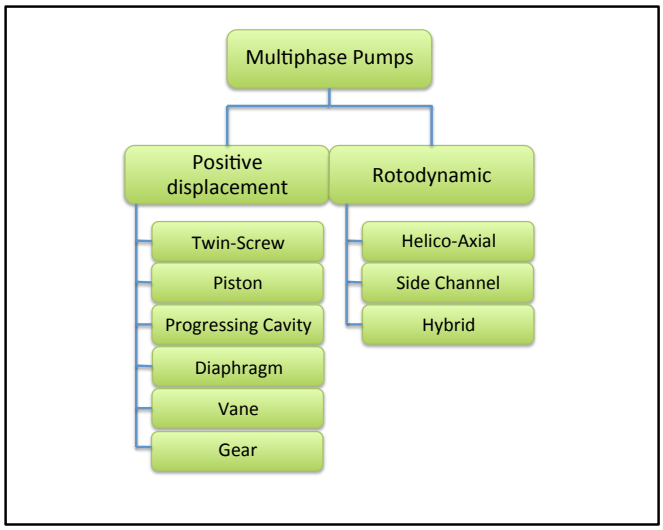

Fig.57: Multiphase pumps classification.

5.8. Rotodynamic pumps: Working principle

When multiphase flow occurs inside the machine, the working fluid has average properties between the liquid and gas phases. Ideally, the required Head would be:

$$H = \frac{(1-GVF)(p_2 - p_1) + GVF\,p_1 Ln\left(\frac{p_2}{p_1}\right)}{\rho_M}$$

where

$$\rho_M = GVF\,\rho_g + (1-GVF)\rho_l$$

GVF= gas volume ratio

p = absolute pressure

ρ = *density*

It has been shown that the similarity laws are respected even in multiphase flow conditions: the volumetric flow is proportional to rotational speed and head to speed squared.

$$\left(\frac{Q}{N \cdot D^3}\right)_1 = \left(\frac{Q}{N \cdot D^3}\right)_2$$

$$\left(\frac{gH}{D^2 \cdot N^2}\right)_1 = \left(\frac{gH}{D^2 \cdot N^2}\right)_2$$

However the process is very far from being ideal; indeed, the pressure gradient inside the impeller tends to separate the two phases, the liquid lies on the pressure side of the blades, while gas stands on the suction side of the blade. When phases are separated, the pressure rise is limited by the gas density, because the outlet velocity c_2 at the impeller tip radius is the same for both phases, while the density is different. The liquid kinetic energy cannot be converted in the diffuser if the two phases are separated. In addition, both phases have different velocity vectors, which generates shock losses in the diffuser or volute. Finally, due to the presence of the pressure field from inlet to outlet, gas bubbles travel to suction side pushed by buoyancy forces, resulting in a decreased volumetric efficiency.

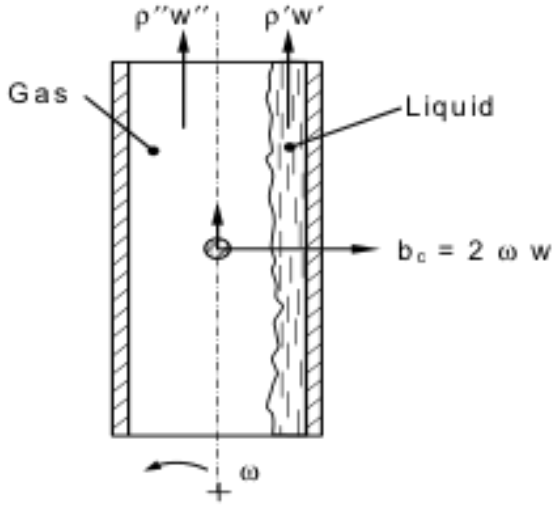

$$\Delta p = \frac{\rho_g}{2}\left(u_2^2 - u_1^2 + w_1^2 - w_2^2\right) - \rho_g g z$$

Fig.58: Phase separation in a rotating channel or an impeller with radial blades.

The phase distribution depends on many variables among which:

- Blade forces, caused by the flow around the blades;
- Centrifugal forces. Experience shows that the circumferential velocity imparted by an impeller to the fluid increases with the ratio of outlet to inlet radius;
- Coriolis forces;

- Velocity distribution at the impeller inlet;
- Boundary layers;
- Annular seal leakages;
- Interaction between impeller and stator during recirculation;
- Density difference between liquid and gas phases.

This complex forces equilibrium determines secondary flows which are essential in determining the pump performances. The Rossby number R_0 is a measure of these phenomena:

$$R_0 = \frac{\omega^2 \times r}{\omega \times w}$$

Where

ω = rotational velocity
r = radius
w = relative velocity

Indeed, if we consider a centrifugal impeller, the Rossby number shows the deviation of the fluid from the ideal path. If the Rossby number is higher than one, the centrifugal forces dominate and the fluid moves towards the suction face of the blades; instead, if R_0 is smaller than one, Coriolis forces dominate and the fluid moves towards the blade pressure face.

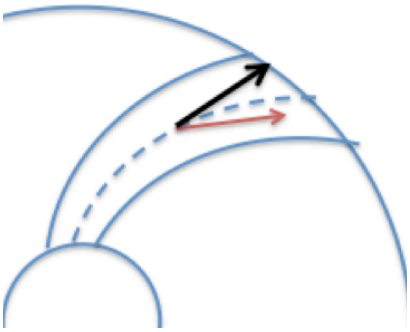

Fig.59: Fluid path in a rotating impeller: black arrow $R_0 > 1$; red arrow $R_0 < 1$.

In the same way, a Rossby number for axial impellers can be defined:

$$R_{0,ax} = \frac{U^2 / r}{\omega \times w_u}$$

Usually, in multiphase pumps $R_{0,ax}$ is equal to 0,5, therefore the centrifugal forces are weak and liquid is forced towards the hub while gas is trapped near the outer radius. This is absolutely non intuitive. When the gas bubbles occupy a wide area of the blade face, the head developed by the pump drops sharply and the flow stops.

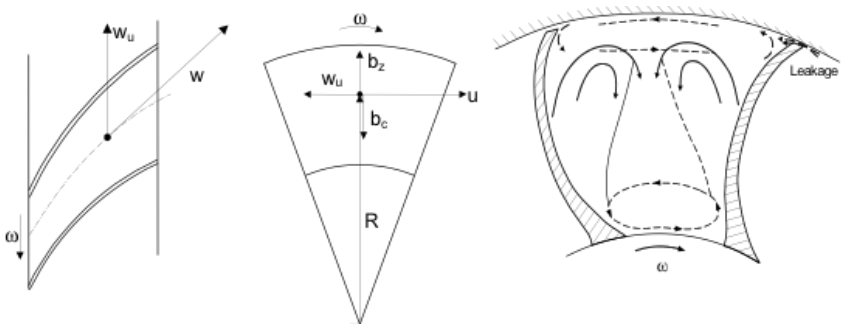

Fig.60: Accelerations acting on a fluid element in axial flow and secondary flow in an axial impeller (right).

5.8.1. Elico-Axial Rotodynamic Boosters

Multistage "helico-axial" pumps were specifically designed for oil, natural gas and water boosting, with sand and high gas volume fractions; differently from all other multiphase pumps, they were not adapted from similar pumps operating in single-phase conditions. As can be understood from their own definition, these machines provide kinetic energy to the stream which flows within alternatively in axial and helical direction (referred to the machine rotation axis). Indeed, the flow enters almost with axial direction, then is accelerated by the impeller in both axial and radial directions, gaining either kinetic either pressure energy. In these conditions, body forces, centrifugal forces and pressure gradients may prevail on surface forces, leading to phase separation which strongly limits the pressure rise as if there was only gas phase with its low density (see previous section). Therefore, the stream is mainly accelerated in axial direction and kinetic energy is converted in pressure by means of the stator. Because of this unstable force balance, the pressure is increased slowly in many stages, achieving good efficiencies.

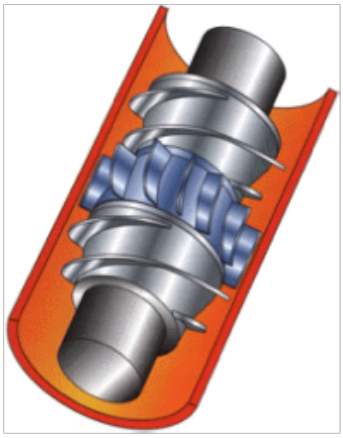

Fig.61: Helico-axial pump.

Unique design practices are used to build these pumps: in order to reduce centrifugal effects, the rotor tip diameter and hub diameter ratio is lower than in all other pumps and further decreases along the pump axis while the diffuser diameter ratio increases from inlet to outlet to match the impeller inlet of the subsequent stage. This special shaping of the rotor and stator hubs and blades limits the undesirable effects of phase separation, which strongly reduces the pressure rise.

5.8.1.1. Operational Conditions

Because their working conditions depend on the inlet fluid properties, helico-axial pumps have two unique features:

- Self adaptability to flow change: as dynamic machines, helico-axial pumps develop a constant head for a determined rotational speed and the overall pressure rise depends on the fluid density. If the actual gas flow rate suddenly increases, the outlet pressure remains steady, whereas the pressure boost decreases. Therefore, the inlet pressure increases and gas density with it, thus the pressure difference increases again. As can be noticed by the foregoing analysis, the helico-axial pump is able to self regulate respect to acceptable variations of the inlet conditions.

- Equivalent “gas locking”. Even if pure “gas locking” has never been observed in helico-axial pumps, the presence of gas pocket in the flow stream can lead the pump to steep reduction in differential pressure. This can be avoided by providing an auxiliary tank (buffer tank) placed upstream to the pump inlet. Such tank helps to smooth the oscillations of the inlet conditions, which occur in transient flow regimes; thus, it increases the pump life, by reducing the load variation on the pump shaft, due to liquid slugging. Indeed, changes in suction conditions mean a sudden change in required shaft power. Bratu (Bratu & Petrole, 1997) shown as the presence of a buffer tank can smooth down sudden oscillations in transient flow.

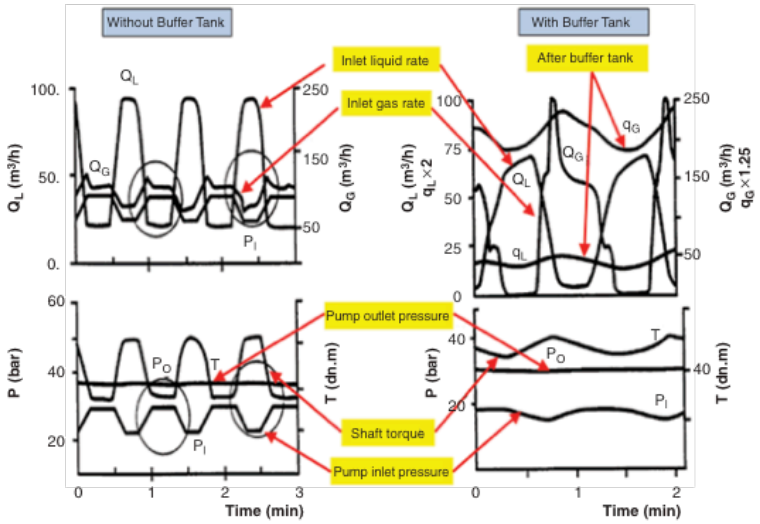

Fig.62: Buffer tank effect on shaft torque.

In order to protect the buffer tank from wide kinetic energy oscillations during slugging operation, fluid enters throughout a pipe with different perforations on the radial surface, called "slug breaker". Then the stream is split thanks to gravitational forces. Both gas and oil phases are sucked into a second holed pipe which is connected to the pump suction. Liquid is driven by gravitational force into the perforations and by the ejector effect generated by the gas stream flowing inside the pipe. The ejector effect increases with the gas flow rate. Liquid enters in those holes below the liquid level and gas into those above. For this very reason liquid level regulates the GVF of the outlet stream: when a liquid slug enters the tank the liquid level raises exposing more holes to liquid phase and less to the gas one. In the same way, a gas slug decreases the liquid level exposing more holes to the gas phase. The ability of the buffer tank to smooth the GVF oscillations down is given by the cylinder base surface S, indeed: $V_{slug} = S x \Delta z$. For constant slug volume, increasing the cylinder base area, the level oscillations tend to zero.

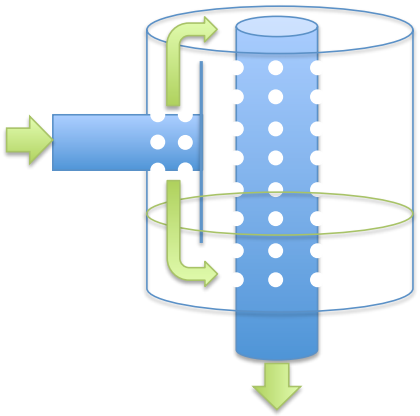

Fig.63: Buffer tank conceptual layout.

5.8.1.1.1. Sand Content

These machines are very suitable for high sand content, thanks to the absence of tight clearances. Indeed the fluid flows in wide hydraulic channels, minimizing the wear effect per volume of conveyed fluid, even if hard coating material are always required for machine life time maximization. Good practice design should avoid deposition and accumulation, by ensuring high fluid velocities in each channel.

5.8.1.1.2. Viscosity

These pumps are very susceptible to inlet fluid viscosity: at high rotational velocities, the fluid is strongly accelerated and high frictional losses occur in the boundary layer of the rotor hydraulic channel. A dynamic viscosity increment leads to higher increments in frictional losses. Therefore, it is practice to avoid the placement of these machines in heavy-oil fields.

5.8.1.1.3. Stability limits

Because a compressible fluid flows within the pump, operating condition points are limited by the machine stability, as occuring in compressors. Indeed, power, pressures and flow fluctuations occur at very low volumetric flow rate. In these conditions, low frequency and high intensity vibrations arise. The last operational point at which the machine is able to operate stably is known as surging limit.

5.8.1.1.4. Pump's Characteristic

In the following graphs, pump's characteristic is reported for different rotational speed and suction conditions. In both graphs, the higher operating boundary is given by the surge limit, while the lower one is given by the choke line. The first graph is built up at constant suction conditions, varying the pump rotational speed. Lines at constant speed are plotted and show sharper steepness at higher value of pump speed itself. Such behavior occurs because, at higher rotational velocities, pressure increases quicker thanks to lower GVF and higher gas densities. Similarity laws cannot be applied for such graph due to compressible effects of gas phase.

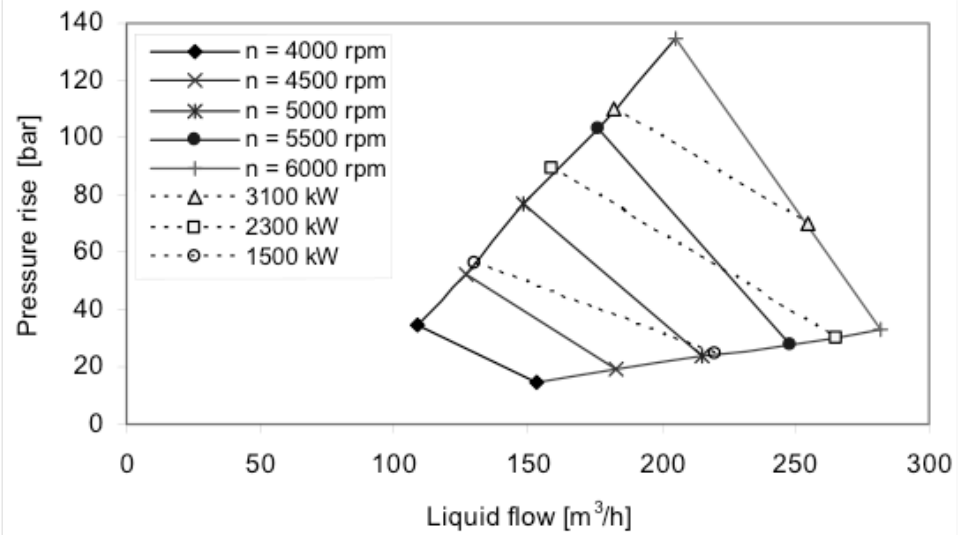

Fig.64:Rotodynamic pump characteristic at constant GVF and pressure.

The next graph shows previous pump's characteristic at constant speed, for different suction conditions, thus GVFs. As previously stated, pressure raise is compromised at high gas volume fractions and the allowable operation range narrows because stages are not designed to operate at low compression conditions.

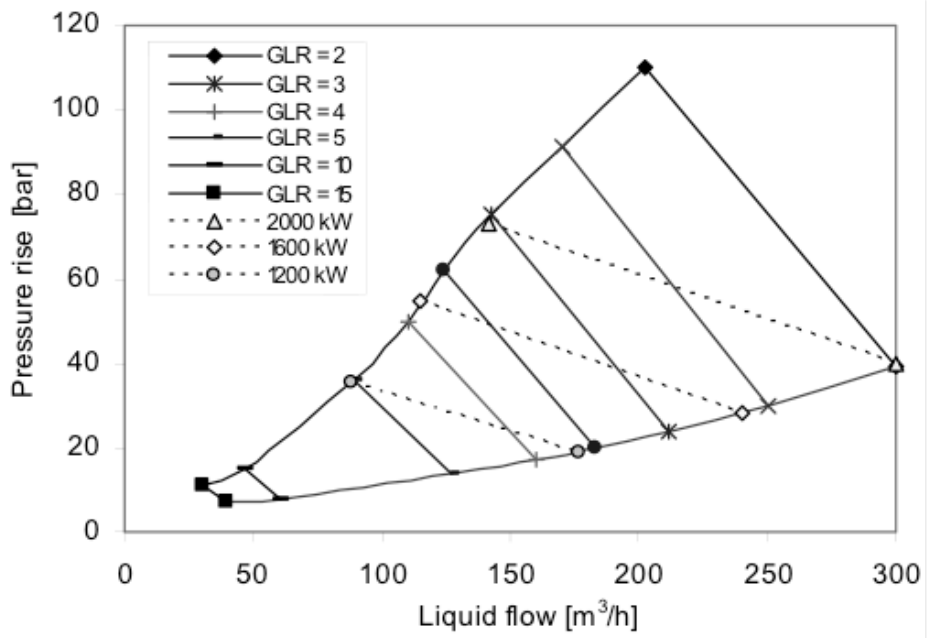

Fig.65: Rotodynamic pump characteristic at constant GVF and pressure.

5.8.1.1.5. System and pump characteristics integration

In single-phase flow, for given pump in given hydraulic circuit only one operational condition exists. In two-phase flow, this not true; indeed for given system and pump, infinite operational points exist, each one defined by a unique gas volume fraction which heavily affects frictional losses.

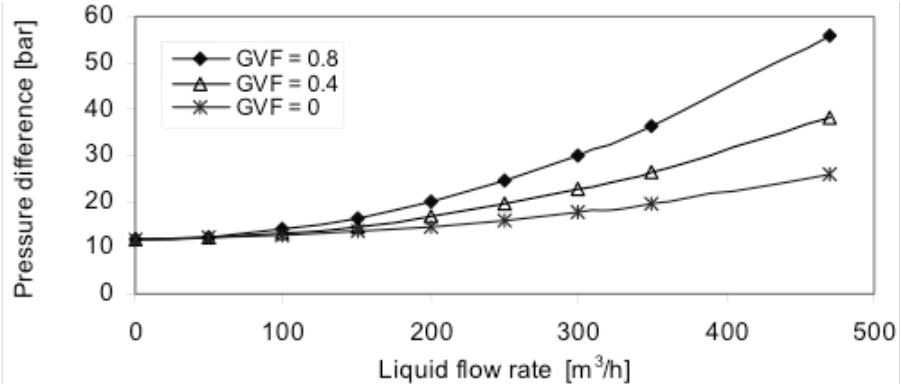

Fig.66: System characteristic curves for different vapor fractions.

In multiphase pipelines, the pump location greatly affects the pump performance itself. Indeed, closer will the pump be to downhole, higher will be the suction pressure, thus lower the GVF. The pump will work providing less head, but higher flow rate, increasing the oil production.

5.8.1.1.6. Brief History

Helico-axial pumps have been the first type of multiphase pump deployed in subsea applications in the Poseidon project, run by Total, Statoil and IFP in 1988. Thanks to their simplicity, they found a wide number of suitable applications, reaching 11 installations in different fields and becoming the most widespread multiphase pump for subsea duties.

5.8.2. Centrifugal Boosters

These pumps are derived from single phase cousins. They are referred either as radial, or multivane pumps. Due to their nature, fluid is accelerated mainly in radial direction, thus it is prone to phase separation. Once vapor phase is separated from liquid one, the pressure energy given to the stream is strongly limited by gas low density. For such reason they are quite sensible to gas content and are more suitable for down hole applications, where suction pressures are higher and gas content lower. In order to reduce phase separation, the impeller is provided of enlarged balance holes which smooth the pressure field and generate turbulence which mixes up both phases. Below has been reported pump's characteristic for a single stage double suction. As can be noticed, pump performance strongly deteriorates with gas content higher than 2%.

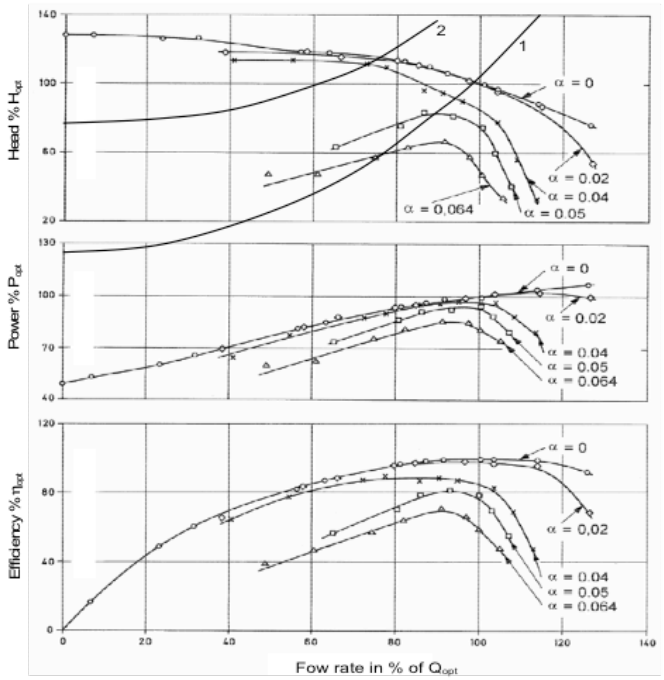

Fig.67: Influence of air content on the characteristics of a single-stage pump with inlet pressure of 2,5 bar.

5.8.3. Hybrid Boosters

In some multiphase applications, helico-axial pumps may not be able to provide the pressure boost required to overwhelm the friction losses in long tiebacks. Indeed either axial pumps either axial compressors are well known to require a higher number of stages than centrifugal ones to provide the same pressure increase and centrifugal machines are well known not to be suitable for multiphase conditions with high suction GVF. Hybrid pumps benefit the advantages of both technologies and overcome the disadvantages. Indeed, the fluid is initially compressed in helico-axial stages in order to reduce the GVF, then is compressed in centrifugal stages which provide the required pressure boost. The picture below shows the stage distribution for a centrifugal, an hybrid pump and a helico-axial pump (from right to left); centrifugal and helico-axial stages are respectively grey and blue colored. The main disadvantage is the coupling its self: the axial and centrifugal machines have different optimum rotational speeds, thus they are coupled on the same shaft rotating at an average velocity; Neither centrifugal stages neither helico-axial ones are able to perform at their best. The first hybrid multiphase pump was developed in 2008 to fit Pazflor oilfield requirements by Framo. Pazflor is characterized by low reservoir pressure, then high GVF. The most attractive technical solution appeared to be subsea separation and liquid boosting. The pump should able to ensure high pressure boost (105 bar) up to 15% of GVF, during nominal operation, and up to 40% during unexpected and temporary operating conditions.

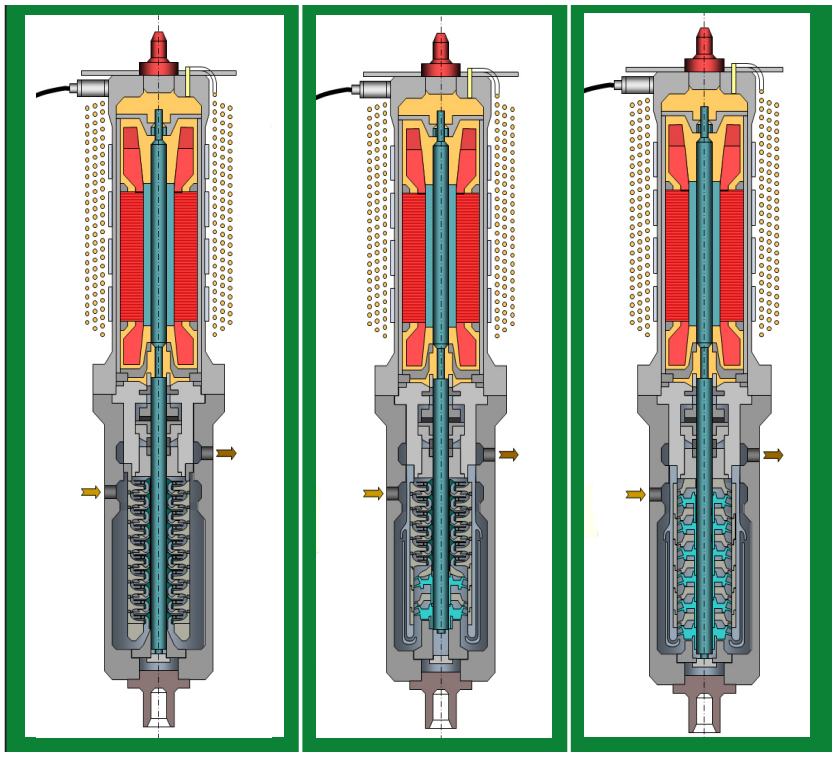

Fig.68: Cross sections of a centrifugal, an hybrid and a helico-axial pump (from right to left).

5.9. Volumetric Multiphase Boosters

Screw boosters are displacement machines in which meshed screws rotate in opposite sense. The fluid is conveyed axially from one side of the pump to the other, where it leaves the machine at discharge pressure. In all other rotary pumps, liquid somehow travels circumferentially: thanks to their unique axial flow pattern and low internal velocities screw pumps have interesting advantages in many applications. The machine is composed by enclosing chambers, which are formed by the intermeshing spindles and the surrounding liner or housing. These chambers are at different pressures, therefore the fluid is compressed gradually from suction to discharge.

There are different types of screw pumps, usually they are divided by number of rotors and the latter is divided into timed and untimed categories.

There are two main types of multiple-rotors screw pumps:

- Multiple-screw single ended pump;
- Twin-screw double ended pump;

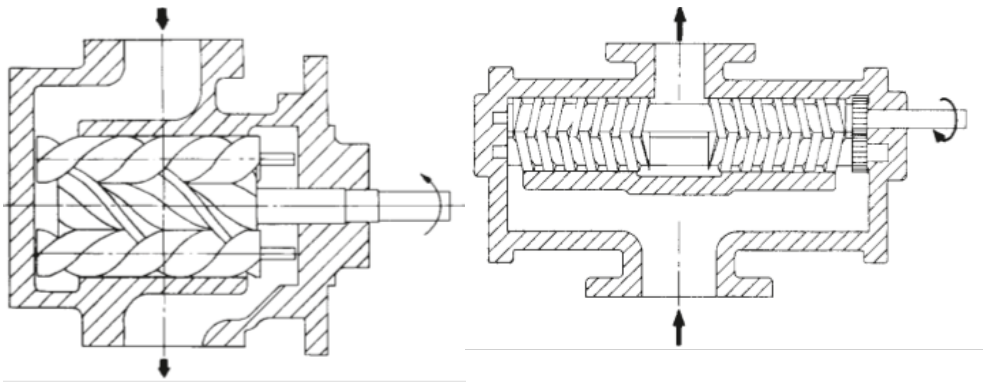

Fig.69: Multiple screw pump (left) and twin-screw pump (right).

The multiple-screw single ended pump is not used for subsea application for wear problems: the presence of the accurate timing gear, avoids contact between the threads and with the surrounding housing, consenting the pump to handle considerable amount of sand. The power is transmitted by the gears rather than threads, which are lightened by such duty, thus promoting longer pump life. Moreover the double volute design avoids axial forces during operation. Afterwards, the text will refer only to twin-screw pumps regarding multiple-screw pumps.

5.9.1. Twin-screw pumps

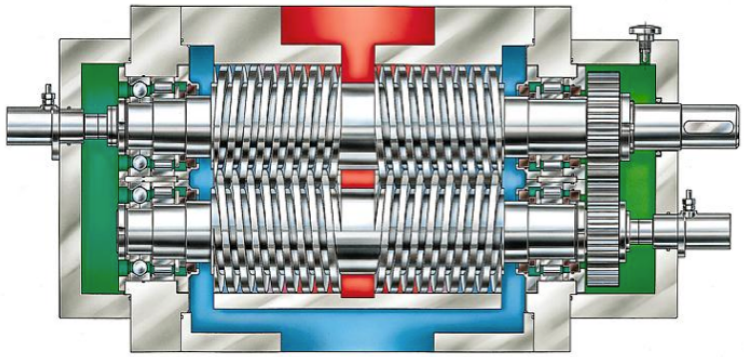

Fig.70: Twin-screw section. Blue section are the suction channels, whereas the red ones show the outlet flow. Green surfaces are filled with lubricant.

Twin-screw pumps are two meshed screws, which rotate in opposite directions; it can be assimilated to two single-rotor screw pumps operating in parallels. The upward picture shows the fluid path: after the common inlet, the flow is splitted to the outboard ends of the two pumping elements and is conveyed to the pump center. The two pump elements are, in practice, pumps connected in parallel.

Beyond the pump its self, there is a set of auxiliary components:

- Electrical motor;
- Cooling system;
- Oil refilling;
- Instrumentation.

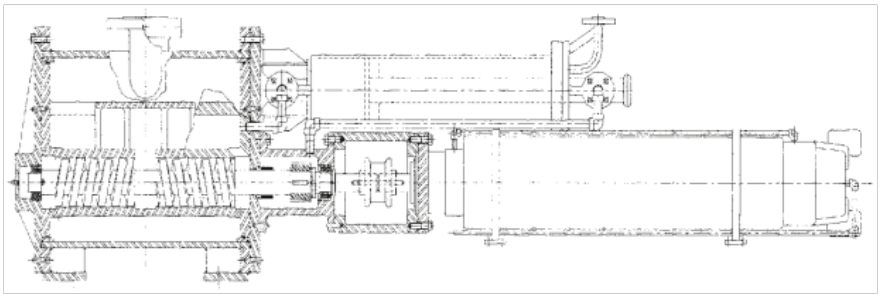

Fig.71: Twin screw system section: pump module (left) and electrical motor (right).

There are mainly two different types of twin-screw pump:

- Internally geared;
- Externally geared.

In the former, gears and bearings are located inside the pumping environment, this allows a simple design and a compact machine. This solution is possible only if the elaborated fluid can be used as lubricant. In oil industry external gear is preferred: timing gears and the rotor support bearings located outside the pumping environment and are oil-bath-lubricated. This allows the pump to elaborate a broad variety of fluids and to use appropriate materials for the required application, leading to an enhancement in reliability. Below, a simple analysis concerning manufacturing materials can be appreciated.

The timing gears can be either spur or helical, herringbone, hardened-steel gears with tooth profiles designed for an efficient drive of the rotors. Anti-frictional radial bearings are usually heavy-duty roller type, while the thrust bearings, which locate the rotors axially, are either double-row, ball-thrust or spherical-roller types. The following table shows different manufacturing materials for each component.

	Casing	Screws	Screw Coating
Material	Cast iron	Cast Iron heat-treated	Nickel-based alloys
	Ductile iron	Alloy steel	Tungsten carbide
	Cast steel	Stainless steel	Chrome oxide
	Stainless Steel	Monel	Ceramic
	Bronze	Nitralloy	

Tab.5: Common material used for surface multiphase pumps

The difference between a single-phase twin-screw pump and a multiphase one is the number of locks or chambers. An elevated number of chambers allows to decreases the pressure step per chamber, therefore the slip flowing through the thread clearances.

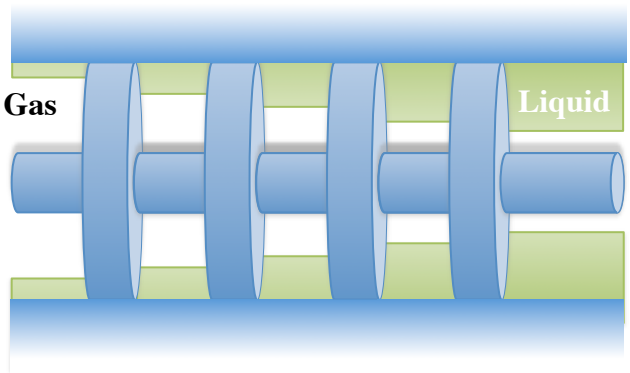

Fig.72: Simplified illustration of phase distribution along the pump shaft.

Indeed backflow in clearances is absolutely reduced in multiphase conditions and even a small amount of recirculated liquid is enough to provide such sealing and enable the screw pump to operate with GVF approaching 100%. The amount of

liquid required in order to cool down and seal the screws is, for example, from 3% to 6% in volume of the total gas inflow (although this value is highly affected by fluid properties, such as heat capacities and viscosities). At 100% GVF this liquid is not available, therefore liquid flux can be driven into the pump, produced in a separator body or recirculated back when the outflow is almost all gas.

5.9.1.1. Brief History

Firsts twin screw pumps were developed in 1934 for handling high viscous fluids in single-phase conditions. Only after 1980 this technology has be adapted for multiphase duties, by reducing the pitch and increase the number of locks. In 1989 the first multiphase twin screw pump was deployed in Malaysia by Shell, followed by the first operational subsea TSP in 2005. Nowadays, there are three TSPs working in subsea projects. A wider application is in high viscosity fluids handling, as heavy-oil.

5.9.1.2. Theory

5.9.1.2.1. Pressure

The intermeshed threads form many enclosing chambers, sometimes called locks, which trap the fluid and, while the pump is rotating, convey it to discharge. In most of the cases, the pump has no inbuilt volume ratio, therefore the outlet pressure is dictated by the pressure in the discharge environment. Ideally, there would not be any pressure gradient in the pump, but just a pressure step in the last chamber, the only working chamber, thus all previous ones would be useless.

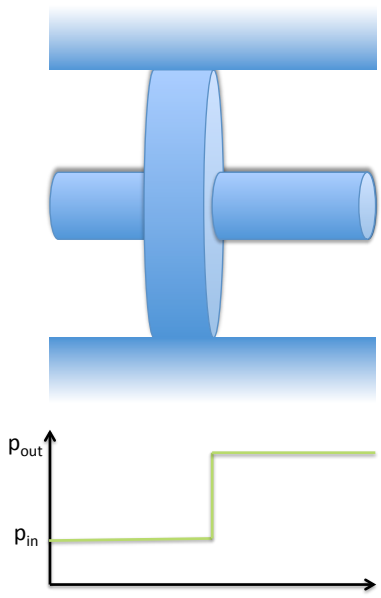

Fig.73: Ideal volumetric pumping: ideal volumetric pump (top) and ideal pressure profile (bottom).

However, the pump is very far from being ideal, indeed backflow occurs through clearances between moving parts. This backflow, usually referred as slip flow, depends on and determines the pressure in each chamber; indeed the fluid tends to migrate to chambers at lower pressure, but at the same time the pressure in each chamber is mainly determined by the mass amount in the chamber its self, as real gas equation shows:

$$p = \frac{z \cdot m \cdot R^* \cdot T}{V}$$

p = *pressure*

m = *fluid mass*

z = *compressibility factor*

R^* = *ideal gas constant divided by molecular weight*

T = *temperature*

V = *volume*

In the locks, the chamber volume and the ideal gas constant are always the same during the pumping process; as first analysis, the temperature can be considered steady as well (not verified at high GVF); therefore the pressure increase along the pump axis is mainly due to a mass increase in the chamber, due to slip flow.

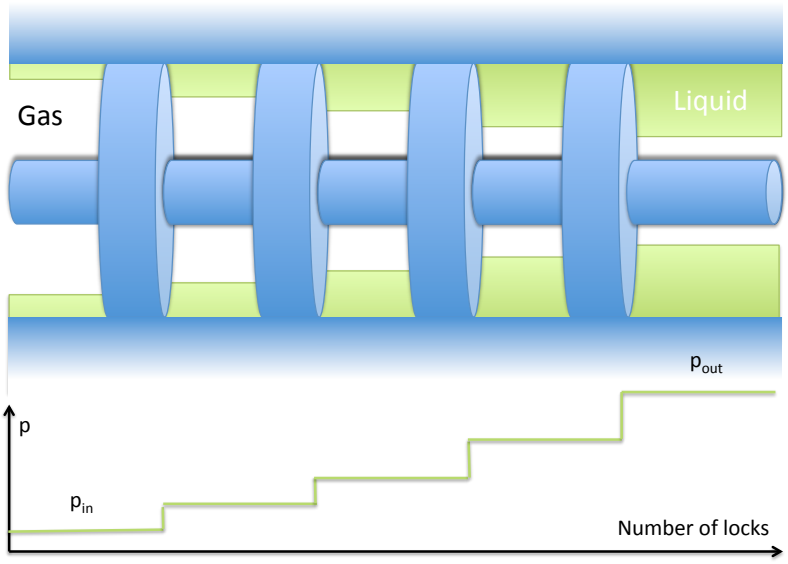

Fig.74: Real pumping process: actual pump (top) and actual pressure profile.

The pressure distribution across the screw, even depends from the GVF value. Ideally we have two main situations:

- Liquid pumping at GVF=0%
- Gas compression at GVF=100%

The pressure increase by pumping a pure liquid is linear, while compressing a gas is not. When a multiphase stream is boosted a third situation occurs: the liquid phase tends to accumulate in high pressure chambers (closer to discharge), decreasing the available space for gas therefore:

$$V_{gas} = V_{ch} - V_{liq}$$

$$p = \frac{z \cdot m \cdot R^* \cdot T}{V_{gas}} = \frac{z \cdot m \cdot R^* \cdot T}{\left(V_{ch} - V_{liq}\right)}$$

The pressure boost is mainly provided in last chambers, resulting in an exponential pressure profile. The following picture shows the pressure profile for different GVF values: for a liquid single-phase flow, the profile is linear and get steeper increasing GVF till a maximum is reached. This is due to both gas compression and liquid accumulation in last chambers (which provides further compression to the gas phase). Beyond this limit, the liquid fraction is very low and the accumulation effect is negligible: the pressure profile gets closer to pure gas one. The following picture shows such relationship between the pressure profile and GVF.

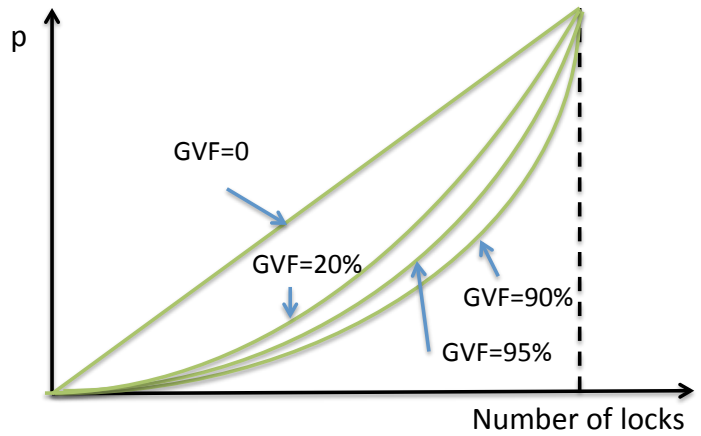

Fig.75: Pressure distribution.

5.9.1.2.2. Temperature

During the boosting process gas raises its temperature, while liquid does not. The temperature distribution along the screw depends from:

- GVF;
- Pressure ratio;
- Heat exhange with the machine;

The former two parameters represent the main variables of the process. If adiabatic boosting was occurring the final temperature would depend only on the pressure ratio and on specific heat ratio for the gas and the pressure difference for the liquid. However, gas and liquid are mixed together and mass and heat transfer occurs. The final temperature is the adiabatic mixing temperature and is closer to the adiabatic boosting temperature of the phase with higher heat capacity. Heat capacity is defined as the product between constant pressure specific heat and mass.

$$C = M \cdot c_p = V \rho c_p$$

$$\frac{C_{liq}}{C_{gas}} = \frac{V_{liq}\rho_{liq}c_{liq}}{V_{gas}\rho_{gas}c_{p,gas}} = \frac{\left(V_{tot} - V_{gas}\right)\rho_{liq}c_{liq}}{V_{gas}\rho_{gas}c_{p,gas}} =$$

$$= \left(\frac{1}{GVF} - 1\right)\left(\frac{\rho_{liq}c_{liq}}{\rho_{gas}c_{p,gas}}\right) = \left(\frac{1 - GVF}{GVF}\right)\left(\frac{\rho_{liq}c_{liq}}{\rho_{gas}c_{p,gas}}\right), \; with \; \left(\frac{\rho_{liq}c_{liq}}{\rho_{gas}c_{p,gas}}\right) \gg 1$$

Where:

C = heat capacity

M = mass

V = volume

c = specific heat

c_p = specific heat at constant pressure

GVF = gas volume fraction

For example, a pump stage operating at 30 bar provides a pressure boost of 20 bar. For a common oil, a reasonable value for specific heat can be 2,1 kJ/kgK. Similarly, for a common natural gas mixture a value of 2,7 kJ/kgK may be assumed. With these data a following table has been built to show the adiabatic mixing temperature at the equilibrium for different GVF.

	Gas	Liquid
cp[kJkgC]	2,7	2,1
β	1,667	1,667
Tout[°C]	51,1	10
ρ[kg/m^3]	25,64	775,1

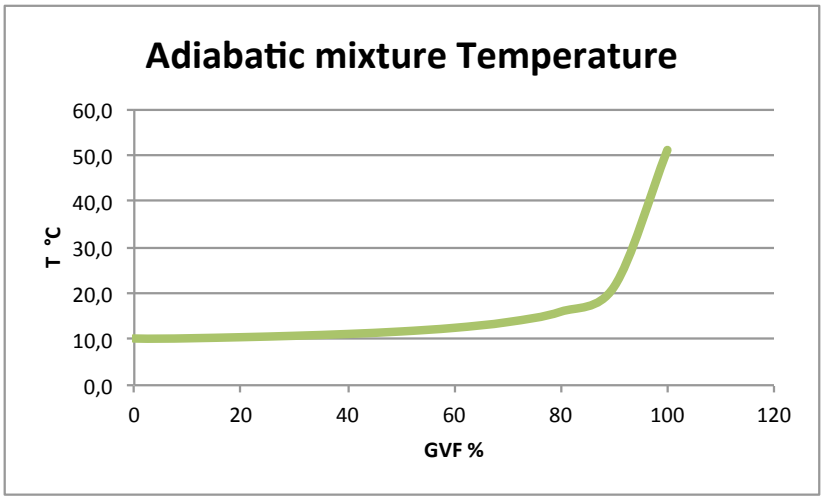

Tab.6: Mixture adiabatic temperature against GVF.

The table shows that the adiabatic mixing temperature raises and gets closer to the gas-phase one with increasing GVF. For a wide range of GVF values the temperature increase is moderate.

A thermal equilibrium in twin-screw boosters can be reached very quickly: as shown by Ruschel (Ruschel & Schlücker, 2010), phases are not divided, though quite well mixed by the intermeshing movement of threads, providing a wide contact surface which strongly enhances heat and mass transfer. Mass transfer comes with evaporation heat, which further improves the heat exchange.

Moreover the pump is very far from being completely adiabatic, indeed the water temperature can be as low as 3-5°C. The casing is usually made of steel and rarely insulated. Therefore this further reduces the flow temperature, which will be lower than the adiabatic one and closer to liquid one.

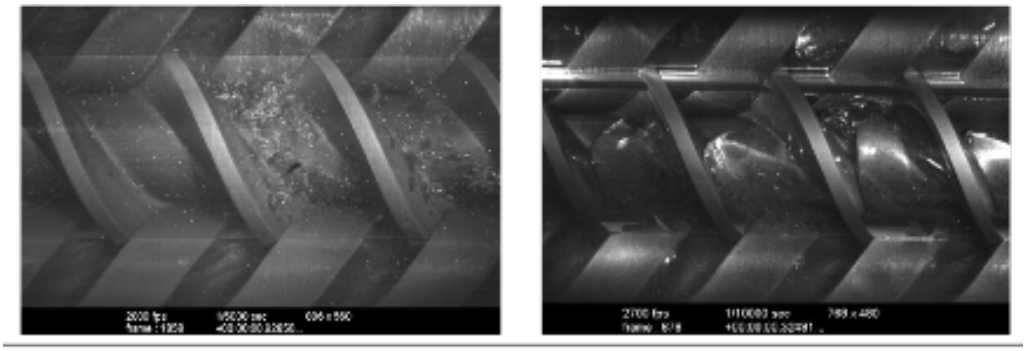

Fig.76: Camera acquired pictures of multiphase multiple-screw pump.

For the foregoing reasons, often isothermal compression is assumed even at considerably high GVF values, which simplifies the pump analysis.

5.9.1.2.3. Volumetric flow and slip flow

Twin-screw boosters are displacement machines and, as such, they ideally delivery constant volumetric rate per revolution defined equal to the displacement volume, defined by the geometric dimensions of the machines. Therefore for an ideal booster:

$$Q_{th} = V_{disp} N$$

Q_{th} = *ideal volumetric flow rate*

V_{disp} = *displacement volume*

N = *number of revolutions per unit time*

Though, the presence of slip due to backflow in clearances reduces the actual flow rate, which is the unique flow loss occurring in the machine. Therefore a volumetric efficiency is defined:

$$\eta_v = \frac{Q_{act}}{Q_{th}} = \frac{Q_{th} - Q_{slip}}{Q_{th}} = 1 - \frac{Q_{slip}}{Q_{th}}$$

Where:

η_v = *volumetric efficiency*

Q_{slip} = *slip flow (volumetric)*

Q_{act} = *actual volumetric flow*

The volumetric efficiency raises with a reduction of the slip flow. The former depends on the pressure difference under which the machine is operating: higher pressure boost leads to higher slip flow. A possible way for reducing slip flow is reaching lower values of tolerance in clearances dimensions: this strongly reduces the cross section area through which backflow occurs. Slip flow is strictly related to fluid viscosity: in narrow channels capillarity effects are stronger for high viscosity fluids due to thicker velocity boundary layers. For a laminar flow over a flat plate, Blasius has found an approximate solution for the boundary layer thickness:

$$t = \frac{5x}{\sqrt{\mathrm{Re}_x}} = \frac{5x}{\sqrt{\frac{\rho x u}{\mu}}} = \frac{5x}{\sqrt{\rho x u}}\sqrt{\mu}$$

t = boundary layer thickness

x = distance from the edge

Re = Reynold number

μ = dynamic viscosity

ρ = fluid density

u = fluid velocity

As can be noticed in the foregoing expression, boundary layer thickness raises with dynamic viscosity. For such reason, slip flow is strongly reduced by fluid viscosity and twin screw boosters are very suitable for high viscosity fluids.

Similarly, a possible solution for reducing slip flow is injecting high viscosity fluid in the main stream in order to reduce slip flow. Based on these observations, Chan (Chan, 2009) proposed a design of through-casing injection, a system which allows to inject some liquid directly inside the locks.

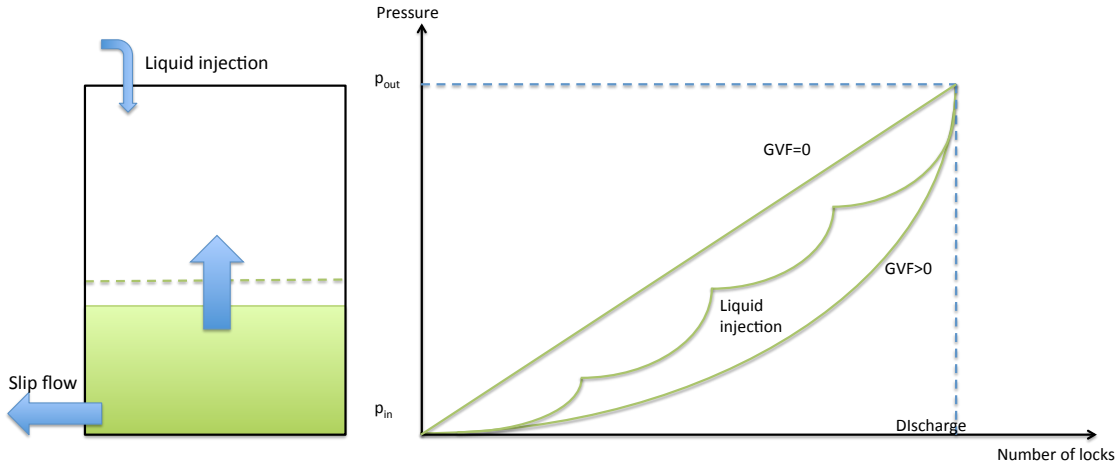

Fig.77: High viscosity liquid injection: mixture compression due to liquid compression and related pressure profile.

Performances of such design strongly depends on the injector location: when liquid is injected, the available volume for gas phase is reduced, therefore the chamber pressure increases. As can be seen in the picture above, if liquid is injected in any chamber beyond the suction, pressure difference among locks increases, enhancing the slip flow. The optimal solution is liquid injection directly into the pump suction.

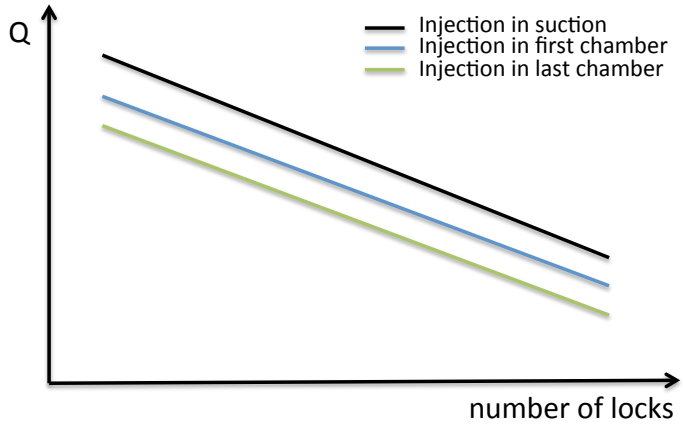

Fig.78: Effect of injection point location on total flow rate.

Twin-screw boosters are very sensitive to sand content, indeed performances of these machines are closely related to clearances dimensions, because they are closely related to the slip flow rate. If a flow stream has a high gas content and it is not purified before the pump suction, sand is hydraulically transported along the screw even through clearances by backflow, wearing the threads tips, as shown in the picture below.

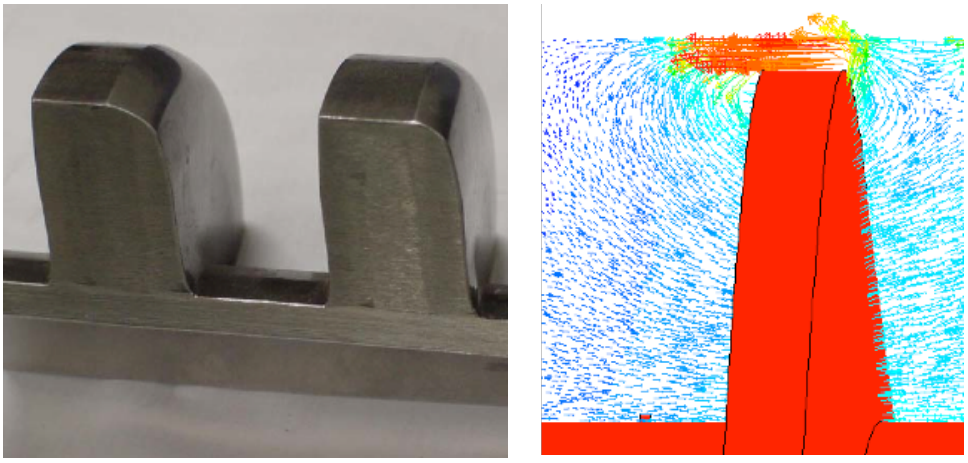

Fig.79: Sand erosion effect on screw edges (left) and sand velocity map.

Therefore, use of TSPs in wells with high sand content should be avoided or an upstream sand trap should be deployed. This sensibility to sand erosion limits the effective clearance: subsea boosting raw fluid always deals with small sand amounts. Thus, geometrical clearances cannot be excessively reduced.

5.9.2. Progressing cavity pumps

Progressing cavity pumps are single-rotor, single-ended screw pumps. The rotor and the stator are both helical and are set to create a cavity, which moves from suction to discharge by means of the shaft rotation, conveying the fluid. Usually the rotor is made of steel covered with hardened material, as chromium, resistant to abrasion. Both elastomer and steel can be suitable for the stator construction, depending on the application; If the rotor thread is eccentric to the axis of rotation, a steel housing can be built; otherwise an elastomer stator must be used.

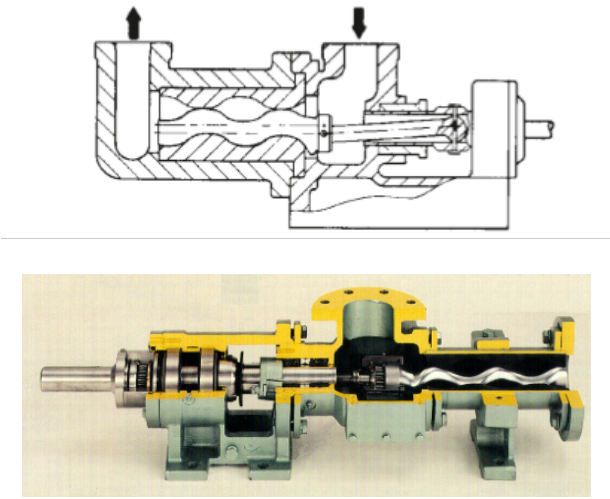

Fig.80: Progressing cavity pump.

Since its very first days, the progressing cavity pump has shown a suitable behavior in boosting both compressible and non-compressible fluids. Indeed, the first model has been invented by René Moineau, a pioneer of aviation, in 1930. Firstly thought as compressor for jet engines, René understood that such system was also effective in liquid pumping. It is very widespread in high viscosity fluid pumping and only in 1979 the first downhole PCP has been deployed for heavy oil extraction. Since early 80s, progressing cavity pumps have shown great reliability as downhole artificial lift method, but none subsea application has been reported due to their ability to handle fluid with a gas content up to 33%. They are quite suitable for high pressure duties thanks to their high number of sealing cavities, which reduces backflow occurring in clearances. They mostly fear high sand content streams, which are very dangerous for the elastomer stator due to wear action, and high temperatures, which degrade the elastomer properties. This occurs when the pump is operating at high GVF and the liquid phase is not able anymore to absorb the heat generated by gas-phase compression. Dry-running is absolutely to be avoided in order to prevent unexpected failures.

The steel housing solution does not suffer such operational problems; indeed it is much more resistant to wear effect and can operate at higher temperatures (then higher GVF) up to 200°C. The stator is hydroformed and it is made of the same metal used for the rotor in order reduce thermal expansions and contractions which may affect the effective clearances dimension. On the other hand the steel stator cannot seal as much as the elastomer can, thus it is less suitable to high pressure boost applications. This solution resembles the twin screw one.

5.9.2.1. Theory

The pumping mechanism is absolutely similar to the twin screw one, indeed the pump simply conveys the fluid from suction to discharge. If the stator could perfectly seal the trapped fluid, just one cavity would be necessary to accomplish the boosting duty. However, this does not happen and backflow occurs through the stator and rotor contact line. The mass increment in the lock leads to a pressure increment too. Therefore, if a high pressure boost is desired, more cavities are required for maintaining high volumetric efficiencies.

Differently from twin screw pumps, slip flow phenomena is much more weaker thanks to the great sealing capacity of the elastomer, thus are more suitable for high pressure boost duties.

5.10. Multiphase boosters comparison

Gong Hua&Al (Hua, Falcone, Teodoriu, & Morrison, 2011) have already performed a complete overview and comparison between different multiphase pumps. Even if the following paragraphs will often refer to their research, a further analysis is proposed for pump selection depending on the application.

5.10.1. Subsea

The main challenge in this field occurs between Helico-Axial and Twin-Screw pumps. The main difference between these excellent pumps is that TSP are volumetric pumps and HAP are dynamic pumps. Therefore TSP volumetric rate ideally does not depend from the pressure difference, but only from the pump geometry and speed. HAP flow rate and pressure boost are strongly linked each other and suction conditions strongly affect pump performance. Both pumps shown their capability to handle streams with a high gas content up to 100%, thus GVF does not represent a limit; however, twin screw pumps are less GVF sensitive than helico-axial ones, which provide lower pressure boost at lower fluid density. Even if TSPs can show some advantages compared to HAPs, they are avoided by operators for subsea applications because of their reliability; indeed the main requirements for subsea applications are:

- Flexibility to a wide range of operational conditions (both pumps can satisfy this requirement). Only for viscosity fluids, twin-screws are more suitable;
- Reliability: TSP are quite sensible to sand content and have two counter-rotating shafts, thus have the double of radial bearings, thrust bearings and seals. All these components are subject to failure and reduce the pump reliability. HAPs are advantaged from this point of view;
- Weight: pump module weight is very important in case of failure. Indeed, the pump must be repaired or substituted as soon as possible, which cannot be done on the seafloor. HAPs are much lighter, thus are easier to be retrieved.

Foregoing advantages of helico-axial vs twin-screw pumps are the main reason because successfully field projects account respectively 15 vs 3.

Subsea	TSP	HAP
GVF	0-100% (with external fluid recycle)	0-100% (with buffer tank or flow mixer)
Δp bar	100	200
Vol. flow bbl/day	1200000	22000-450000
Sand content tolerance	Low	High
Fluid viscosity (μ) cP	>0,55	2<μ<4000
min. Suction pressure	1	2,76

Tab.7: Main features comparison of TSPs an HAPs for subsea duties.

5.10.2. Down-hole

In down-hole applications, pressures are usually higher and gas contents usually lower. Therefore, even hybrid centrifugal and progressing cavity pumps can be interesting: they can be even placed upstream to a ESP, which provides most of the required pressure boost. Hybrid centrifugal pump can handle mixture with a GVF up to 70%, thanks to the split-vane design and mixed flow geometry which prevents gas from accumulating within vanes. HAPs, whose fluid flows almost axially, can tolerate higher GVF (75%). Progressing cavity pumps (PCP) are suitable only for high viscosity fluids and low GVF (up to 33%) applications, due to temperature limits. PCPs with metal stator will probably become widespread, thanks to their ability to reach high GVF and their limited weight; however they actually have been deployed just in one project, Bohai Bay(China). Downhole twin screws are an adapted version of subsea twin screws. They are slimmer, vertically designed to optimally fit the system requirements. They can handle GVF fractions up to 100% and high viscosity fluids, although they strongly fear sand content. For down applications, Twin screw pumps do not require fluid recycling for clearances sealing and lubrication. Even in downhole applications, customers have shown to prefer rotodynamics pumps rather screw ones, thanks to their reliability properties, which ensure longer operating time without unexpected failures and maintenance.

Downhole	TSP	HAP	MVP	PCP
GVF %	0-98	0-75	70	33*
Vol. flow BBL/day	450000	5000-9000	18000	6200
Sand content tolerance	Low	High	High	Medium
Maximum temperature °C	350	232	210	120

*Tab.8: Main features comparison of multiphase boosters for downhole duties. *(elastomer stator).*

6. Simulation Tools

6.1. OLGA

OLGA (Oil and Gas Simulator) is a dynamic, mono-dimensional simulator which models the thermo-hydraulic behavior of multiphase fluids. The model was conceived in 1979 at Institute for Energy Technology (IFE) of Norway by Dag Malnes and Kjell Bendiksen and developed at Tiller laboratory in Trondheim (Norway) through experimental validation of low pressure air/water flow. In 1980 the software acquired his actual denomination OLGA and has been further developed until 1983, when the first version has been released. The software has been implemented in Fortran code, in partnership with StatOil, which financed the project and provided frequent experimental feedback.

6.1.1. The model

Olga solves mass, momentum and energy conservation equations for the multiphase mixture in different ways:

- Mass conservation equation is applied to gas, liquid bulk and liquid droplets. Then mass balances for each phase is coupled with each other through interfacial mass transfer;
- OLGA solves only a combined gas phase/liquid droplets equation and a separate one for liquid phase for momentum conservation;
- The energy balance is applied to the whole mixture and the phase temperature is assumed to be the same for all phases.

Hence, OLGA solves six conservation equations:

- Gas-phase mass balance equation:

$$\frac{\partial}{\partial t}\left(V_g\rho_g\right) = -\frac{1}{A}\frac{\partial}{\partial z}\left(AV_g\rho_g u_g\right) + \Psi_g + G_g$$

- Liquid-phase mass balance equation:

$$\frac{\partial}{\partial t}\left(V_L\rho_L\right) = -\frac{1}{A}\frac{\partial}{\partial z}\left(AV_L\rho_L u_L\right) - \Psi_g\frac{V_L}{V_L+V_D} - \Psi_e + \Psi_d + G_L$$

- Liquid droplets mass balance equation:

$$\frac{\partial}{\partial t}\left(V_D\rho_L\right) = -\frac{1}{A}\frac{\partial}{\partial z}\left(AV_D\rho_L u_D\right) - \Psi_g\frac{V_D}{V_L+V_D} + \Psi_e - \Psi_d + G_D$$

Where A is the pipe cross sectional area, Ψ_g the mass rate between liquid and gas phases, Ψ_e the entrainment rate of liquid droplets in gas phase and Ψ_d the deposition rate of liquid droplets in liquid phase. G represents the presence of mass sources in each phase.

Defining a gas fraction R_s at equilibrium conditions it is possible to calculate the inter-phase mass transfer rate:

$$R_s = \frac{m_a}{\left(m_a + m_L + m_D\right)}$$

$$\Psi_g = \left\{\left[\left(\frac{\partial R_s}{\partial p}\right)_T \frac{\partial p}{\partial t} + \left(\frac{\partial R_s}{\partial T}\right)_p \frac{\partial T}{\partial t}\right] + \left[\left(\frac{\partial R_s}{\partial p}\right)_T \frac{\partial p}{\partial z}\frac{\partial z}{\partial t} + \left(\frac{\partial R_s}{\partial T}\right)_p \frac{\partial T}{\partial z}\frac{\partial z}{\partial t}\left(\frac{\partial \rho_g}{\partial R_s}\right)_{p,T}\right]\right\}\left(m_g + m_L + m_D\right)$$

The first term represents the phase transfer due to a local change in the thermodynamic conditions; the second one represents a phase transfer due to mass flow from one section to one other.

The momentum conservation would be determined by the resolution of each phase momentum equation, however the gas and liquid droplets ones are merged up in order to simplify the calculation. Indeed, this leads to the resolution of two equations:

- Gas-phase+liquid droplets momentum balance equation

$$\frac{\partial}{\partial t}\left(V_D\rho_L u_D + V_g\rho_g u_g\right) =$$
$$= -\left(V_g + V_D\right)\frac{\partial p}{\partial z} - \frac{1}{A}\frac{\partial}{\partial z}\left(AV_D\rho_L u_D^2\right) - \lambda_L\frac{1}{2}\rho_g u_g\left|u_g\right|\frac{S_g}{4A} -$$
$$-\lambda_i\frac{1}{2}\rho_g u_r\left|u_r\right|\frac{S_i}{4A} + \left(V_g\rho_g + V_D\rho_D\right)g\cos\alpha + \Psi_g\frac{V_L}{V_L + V_D}u_\alpha + \Psi_e u_i - \Psi_d u_d$$

- Liquid-phase momentum balance equation

$$\frac{\partial}{\partial t}\left(V_L\rho_L u_L\right) =$$
$$= -\left(V_L\right)\frac{\partial p}{\partial z} - \frac{1}{A}\frac{\partial}{\partial z}\left(AV_L\rho_L u_L^2\right) - \lambda_L\frac{1}{2}\rho_L u_L\left|u_L\right|\frac{S_L}{4A} +$$
$$+\lambda_i\frac{1}{2}\rho_g u_r\left|u_r\right|\frac{S_i}{4A} + \left(V_L\rho_L\right)g\cos\alpha - \Psi_g\frac{V_L}{V_L + V_D}u_\alpha - \Psi_e u_i + \Psi_d u_d - V_L d\left(\rho_L - \rho_g\right)g\frac{\partial V_L}{\partial z}\sin\alpha$$

Where α is the pipe inclination from the vertical axis, S_g, S_i and S_L, are the wetted perimeters of the gas, interface and liquid. The inlet angle for the mass source is assumed orthogonal to the pipe wall.

- Energy balance equation;

$$\frac{\partial}{\partial t}\left[m_g\left(E_g + \frac{1}{2}u_g^2 + gh \right) + m_L\left(E_L + \frac{1}{2}u_L^2 + gh \right) + m_D\left(E_D + \frac{1}{2}u_D^2 + gh \right) \right] =$$
$$= -\frac{\partial}{\partial z}\left[m_g u_g\left(H_g + \frac{1}{2}u_g^2 + gh \right) + m_L u_L\left(H_L + \frac{1}{2}u_L^2 + gh \right) + m_D u_D\left(H_D + \frac{1}{2}u_D^2 + gh \right) \right] + H_s + Q$$

Where E is the internal energy, h the elevation, and H enthalpy. The letter "S" stands for mass source. Q is the heat exchanged with the surrounding environment. OLGA requires only the external heat transfer coefficient as input, indeed it is able to calculate the internal one from physical and flow conditions.

6.1.2. Numerical solution scheme

The equations system can be resolved once all the boundary conditions are given and the initial conditions are defined. Then, the program divides the pipeline into several sections of similar length. Sections are connected to each others by boundary conditions: the outflow of one section is the inflow of the next one. The software identifies two main types of variables:

- Boundary variables (velocities, mass flows, fluxes,);
- Volume variables (pressure, mass, phase fraction and temperature);

The formers are measured at the beginning of each section, while the latters are measured in the middle of the section.

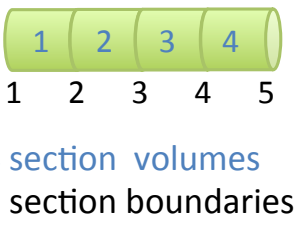

Fig.81: OLGA discretization process.

This discretization allows lighter and simpler algorithms; as the number of sections tends to infinity, the algorithm is describing the real pipeline. Therefore, by increasing the number of sections the calculation precision increases, but the computational time increases with the square of the sections number. Indeed, while the number of arithmetic operations per time step increases proportionally to the number of sections, the time step decreases.

6.1.3. OLGA simplified pump model: method and assumptions

OLGA considers the pump performances a function of pump differential pressure ΔP, flow rate Q, speed N, inlet gas volume fraction GVF, and the pump inlet pressure p_i. The simplified centrifugal pump in OLGA is intended for quick, approximate modeling. These appears very useful when the software has to match different flow-pressure characteristic curves. In these cases the time, the preprocessor takes to find an initial and approximate steady state equilibrium point, is approximately the 70% of the simulation time. Thus, simple pump modeling appears very useful when more wells are connected together. The OLGA simplified pump model uses a linearized approximation to the local behavior of a real centrifugal pump, and shall be used only for small excursions from its specified local operational point. The model requires, hence, rated pump conditions, such as flow rate, differential pressure, efficiency and speed. Then, these informations are used to determine the real pressure increase through the following simple equations:

$$\Delta P_o = \Delta P_r \left(1 + D_1 \left(N - N_r \right) + D_2 \left(Q - Q_r \right) \right) \left(1 - D_3 \alpha \right)$$

$$\eta = \eta_r \left(1 + E_1 \left(N - N_r \right) + E_2 \left(Q - Q_r \right) \right) \left(1 - E_3 \alpha \right)$$

$$\frac{\Delta P}{\rho} = \frac{\Delta P_0}{\rho_0}$$

where:

ΔP_o = Pump pressure increase at rated density [bar]

ΔP = Pump pressure increase [bar]

N = Pump speed [rpm]

Q = Flow rate [m3/s]

α = Gas volume fraction

η = Pump efficiency

ρ = Specific density [kg/m3]

$D_{1,2,3}$ = Input coefficients for pressure increase

$E_{1,2,3}$ = Input coefficients for efficiency

Subscripts: r = rated

Setting the coefficients $D_{1,2,3}$ and $E_{1,2,3}$ equal to zero, the pump will operate at constant head. Constant flow rate pump can be simulated by roughly iterating the typed ΔP_r or assume some value for D_1 and let a controller determine the necessary speed.

The power to the fluid is calculated in the following manner:

$$P = \dot{m}\Delta H = \dot{m}\frac{\left(H_{iso} - H_{in}\right)}{\eta}$$

Where

H_{in} = inlet enthalpy

H_{iso} = iso-entropic outlet enthalpy

$\dot{m}$ = the mass flow rate.

ΔH = actual enthalpy change

Then shaft power is simply the power required by the fluid (P) corrected by the mechanical efficiency η_m:

$$P_{shaft} = \frac{P}{\eta_m}$$

Pump torque TH can be determined as follow:

$$TH = \frac{P_{shaft}}{\omega}$$

Where:

$$\omega = \frac{2\pi N}{60}$$

6.2. PVTsim

PVTsim is a software developed for fluid characterization, which combines both theoretical models and experimental datas. This unique feature allows to reach optimal results with acceptable complexity and effort. The software requires a composition of different species which can be real components or pseudo-components. Each component is defined by accentric factor, normal boiling point, molecular weight (for pseudo-components), critical volume, coefficients of ideal gas heat capacity polynomial, ideal gas absolute enthalpy at 273.15 K, melting point temperature, enthalpy of melting, PNA (paraffin-naphthenic-aromatic) distribution (for pseudo-components). Pseudo-components usually represent a class species which share a common feature; this is very useful when many components can be modeled by a single one with average properties weighted on concentration, definitely simplifying the fluid characterization. Pseudo-components are especially used when composition are experimentally acquired and they are divided by carbon atom number (C1, C2, ..., C19); they can also characterize a group of species which have carbon atom number higher than a certain value (C7+, C10+... C20+).

Once defined the fluid composition, equation of state must be chosen in order to calculate the phase equilibrium. Most used equations are:

- Soave-Redlich-Kwong (SRK);
- Peng-Robinson (PR);
- Modified Peng-Robinson (PR78).

They all share a cubic relationship between p and V, inherited by the Van der Waal equation of state:

$$p = \frac{RT}{V-b} - \frac{a(T)}{(V+\varepsilon b)(V+\sigma b)}$$

$$a(T) = \Psi \frac{a(T_c) R^2 T_c^2}{p_c} \qquad a(T_c) = \Psi \frac{R^2 T_c^2}{p_c} \qquad b = \Omega \frac{R T_c}{p_c}$$

Eq. of State	$\alpha(T_r)$	σ	ϵ	Ω	Ψ	Z_c
vdW (1873)	1	0	0	1/8	27/64	3/8
RK (1949)	$T_r^{-1/2}$	1	0	0.08664	0.42748	1/3
SRK (1972)	$\alpha_{SRK}(T_r; \omega)^{\dagger}$	1	0	0.08664	0.42748	1/3
PR (1976)	$\alpha_{PR}(T_r; \omega)^{\ddagger}$	$1 + \sqrt{2}$	$1 - \sqrt{2}$	0.07780	0.45724	0.30740

$$^{\dagger}\alpha_{SRK}(T_r;\ \omega) = \left[1 + (0.480 + 1.574\,\omega - 0.176\,\omega^2)\left(1 - T_r^{1/2}\right)\right]^2$$

$$^{\ddagger}\alpha_{PR}(T_r;\ \omega) = \left[1 + (0.37464 + 1.54226\,\omega - 0.26992\,\omega^2)\left(1 - T_r^{1/2}\right)\right]^2$$

Where p is pressure, T temperature, V molar volume, R the gas constant, b and a are equation of state parameters depending on critical properties.

After having defined both composition and equation of state, it is possible to perform directly in PVTsim some simple process simulations, which allow to check the fluid properties and validate the fluid characterization. Among these, are very useful tools:

- Flash simulation;
- Phase envelope calculation;
- Hydrate existence curve calculation.

Then, the fluid can be saved and exported to another process simulator. OLGA, for instance, requires physical properties tables plotted as function of pressure and temperature and, to this purpose, PVTsim's file is converted into a ".tab" file.

The following paragraphs briefly describes the algorithms used to perform the main simulations.

6.2.1. Flash model

PVTsim is able to perform different types of flash, which must be specified, and requires the flash specifications (pressure and temperature), then the software estimates the molar compositions of each component in each phase. The phase equilibrium is defined by the free Gibbs energy minimization, thus by the phase fugacity coefficients equivalence. The number of phases, is going to be determined, is the one with lower Gibbs potential.

$$0 = \Delta G = \sum n_i \mu_i = \sum n_i \left(\mu_i^0 (T_0, p_0) + RT \ln \frac{f_i}{f_i^0} \right)$$

Where G is the Gibbs potential, μ chemical potential and f is the fugacity coefficient. The 0 stands for standard state, while i for the component considered.

$$\ln f_i^\alpha = \ln f_i^\beta = \ln f_i^\gamma$$

The greeks letters identify the involved phases. The phase with lower fugacity will grow, while the others will disappear till an equilibrium is reached.

During a p-T flash, liquid and gas phases can be easily identified by their densities: the liquid has much greater density than gas. However, if single phase is the flash outcome, there is no generally accepted definition to identify it as gas or liquid. The software recognizes the phase as liquid when pressure is lower than the critical pressure and temperature lower than the bubble point temperature or if pressure is above the critical pressure and temperature lower than the critical temperature. On the other hand, gas is identified when pressure is lower than the critical pressure and temperature higher than the dew point temperature or if pressure is above the critical pressure and the temperature higher than the critical temperature.

6.2.2. Phase envelope determination

Phase envelopes are constant phase fraction curves plotted for different couples of pressure and temperature values. Phase fraction values range from 0 to 1 and can be built in PVTsim environment as follow: PVTsim finds equilibrium points at constant temperature and phase fraction by matching one equation on equilibrium factors (gas and liquid phase fractions ratio $k_i = y_i/x_i$) and one on mass balance. After an equilibrium has been determined, the software finds the second point through temperature and equilibrium factors k_i derivatives respect to the pressure. Then equilibrium points and corresponding derivates extrapolation is used to determine the remaining envelope curve. The algorithm starts from one envelope bundle to the other, which are user specified.

6.2.3. Hydrate modeling

PVTsim is able to determine hydrate existence field and the amount it is likely going to form at certain thermodynamic conditions. The software takes into account many variables such as:

- Thermodynamic inhibitors;
- Dissolved salts;
- Hydrate structures and their affinities with guest molecules.

As for the flash calculation, hydrate formation is determined by Gibbs free energy minimum, thus by the chemical potentials equivalence. PVTsim model states a hypothetical and intermediate thermodynamic state in order to simplify the transition from pure water into hydrate. If hydrate structure has a lower chemical potential, water solidifies into ice, then ice is filled with guest molecules.

$$pure\ water \rightarrow\ ice \rightarrow hydrate$$

$$\mu^H - \mu^W = \left(\mu^H - \mu^I\right) + \left(\mu^I - \mu^W\right)$$

In such way, two different mechanisms can be divided and analyzed. Indeed, the chemical potential difference between ice and water quantifies the tendency of water to solidify, which PVTsim determines as follows:

$$d\left(\frac{\mu^I - \mu^W}{R_g T}\right) = -\frac{\Delta h}{R_g T^2} + \frac{\Delta v}{R_g T} dp$$

Where h is molar enthalpy, R the gas constant and v the molar volume. The former equation takes into account volume and enthalpy as the two antagonist variables which determines the phase equilibrium.

The chemical potential difference between hydrate and ice expresses the guest molecules drift towards the hydrate lattice. PVTsim models this mechanism as an adsorption process:

$$\mu^H - \mu^I = R_g T \sum_{i=1}^{n_c} v_i \ln\left(1 - \sum_{k=1}^{n} y_{k,i}\right)$$

v_i is the number of cavities of type I and $y_{k,i}$ is the possibility that the component k is trapped in the cavity i. n_c is the number of cavities per hydrate crystalline cell, while n is the number of component in the mixture. The probability factor $y_{k,i}$ is determined by the Langmuir isotherm model.

The overall process is governed by the two mechanisms resultant, which is outlined by the chemical potential difference between hydrate and water. When this value is lower than zero, hydrate is going to form, while if higher, is not. A hydrate phase equilibrium curve represents the temperature and pressure values in which the chemical potential difference is zero and divides those in which the difference is respectively higher and lower than zero.

6.3. Aspen HYSYS

HYSYS is the most widespread process simulator in the world. It provides huge amounts of functions both under steady state and transient conditions. The software has been used for the multiphase pump model development. The model uses the following process elements:

- Mixer; the mixer receives as input many different streams and join them into a unique outlet stream. The outlet pressure is either the average either the lowest pressure between the fed ones, depending on the operator specifications;

- Flash tank; flash tank performs a enthalpy -pressure flash and splits the phases into two different streams. Flash pressure can be either an average either the lowest between fed ones, minus the pressure loss across the vessel. Enthalpy as well is average between the feeds. Optionally, it is possible to consider heat flux, which warms up or cools the vessel;

- Compressor&pump; both compressor and pump require an inlet, an outlet and an energy stream. They also need an adiabatic efficiency, which Hysys uses to determine the outlet enthalpy after having calculated the isentropic one. The following paragraph describes the algorithm used for real compression simulation;

- Choke valve; choke valve simply requires a pressure difference to operate and laminates the fluid which changes its temperature due to Joule-Thompson effect;

- Tee: the tee operation splits one feed stream into multiple product streams with the same conditions and compositions and is used for simulating pipe tees and manifolds.

And the following logical functions:

- Set; this logical operator reads any parameter to one stream and sets it to another stream. Both streams are user specified;

- Adjust; adjust is a key logical function in HYSYS. Indeed, it requires an object variable and an adjusted variable. The object variable requires a target value which can be either set by the user either equalized to another stream value. Then the adjust changes the adjusted variable until the object variable reaches the target value. The adjust, due to its iterative nature, has many different calculation options such as integration time step, tolerance (between the target value and the adjusted one) and the maximum number of iterations. If multiple Adjusts are used, their solutions must be found simultaneously. In this case, each Adjust result immediately influences the others; HYSYS uses the

modified Levenberg-Marquardt algorithm to simultaneously vary all the adjustable parameters defined in the Adjusts until the desired specifications are met;

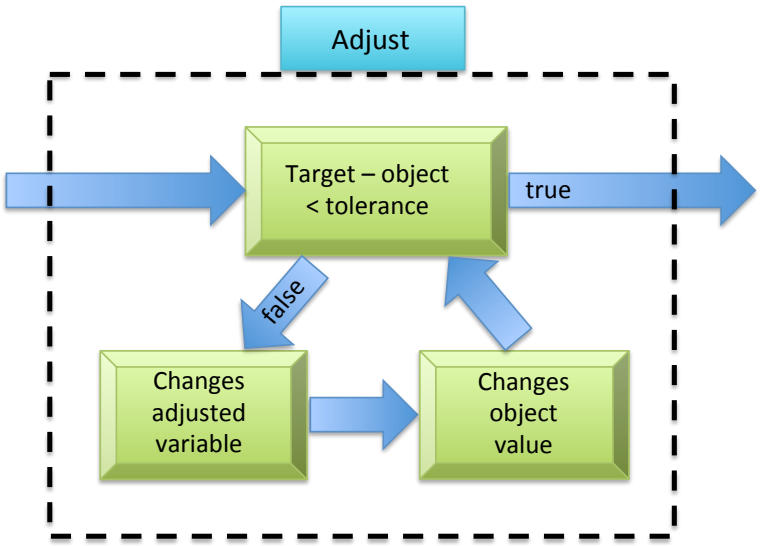

Fig.82: Adjust logical solving procedure.

- Recycle; HYSYS is not able to identify a recycle and stops instead of proceeding in the calculation, due to lack of informations. The Recycle operator provides such informations and allows the simulation to go on. The logical block requires some assumed values, which are initially used during the calculation and are changed until convergence is reached. The convergence process can be divided as follows:

  - HYSYS uses the conditions of the assumed stream and solves the Flowsheet up to the calculated stream;
  - HYSYS then compares the values of the calculated stream to those in the assumed stream;
  - Based on the difference between the values, HYSYS modifies the values in the calculated stream and passes the modified values to the assumed stream;
  - The calculation process repeats until the values in the calculated stream match those in the assumed stream within specified tolerances.

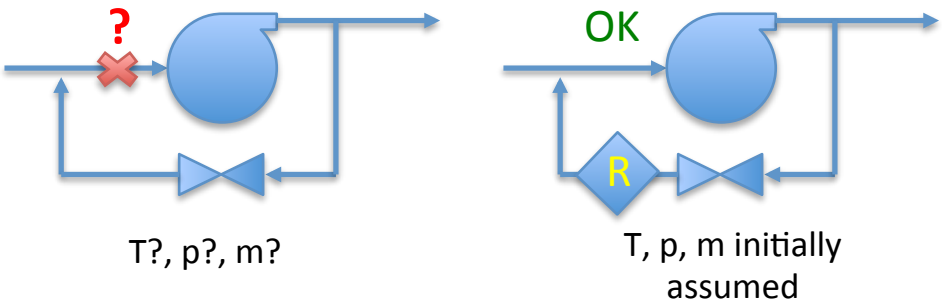

Fig.83 :HYSYS Recycle logical operator purpose in solving the HYSYS flowsheet.

6.3.1. Shultz method

The Schultz method (Schultz 1962), which HYSYS is actually using for compressor modeling, is based on following a simple polytropic path from inlet to discharge conditions.

$$PV^n = C$$

Where n determination is based on the conditions at the beginning and end of the polytropic path. P is pressure and V volume.

This equation is combined with the definition of polytropic head

$$H = \int V\,dP$$

That upon integration between P_1 and P_2 gives

$$H = \frac{n}{n-1}\left(P_2V_2 - P_1V_1\right)$$

$$H = Z_1RT_1\left(\frac{n}{n-1}\right)\left[\left(\frac{P_2}{P_1}\right)^{\frac{n-1}{n}} - 1\right]$$

The polytropic efficiency can then be calculated from:

$$\eta_{pol} = \frac{h_2 - h_1}{H}$$

While iso-entropic compression does not depend on the compression path (as all functions of state), real compression is not reversible and it must be path-dependent instead of endpoints dependent. To compensate this effect, Shultz introduced a correction factor usually called the polytropic head:

$$H = f\frac{n}{n-1}\left(P_2V_2 - P_1V_1\right)$$

Where f is the polytropic head factor and is defined as:

$$f = \frac{h_2 - h_1}{\frac{n}{n-1}\left(P_2V_2 - P_1V_1\right)}$$

Which for an isentropic compression/expansion gives $H = h_2 - h_1$ and $\eta = 1$.

7. Multiphase Twin-Screw Model

7.1. Introduction

In the backward description of OLGA simplified multiphase pump model was highlighted the lack of theory in such model, where the pump behavior is simply described by a single line. This is useful during system calculations, when the software has to match the wells characteristics, the system ones, and the pump one. Such task is really hard to be achieved by the software, which takes huge amount of time (roughly one hour) to find an approximated steady state solution. Therefore more complex pump models should be avoided during system simulations.

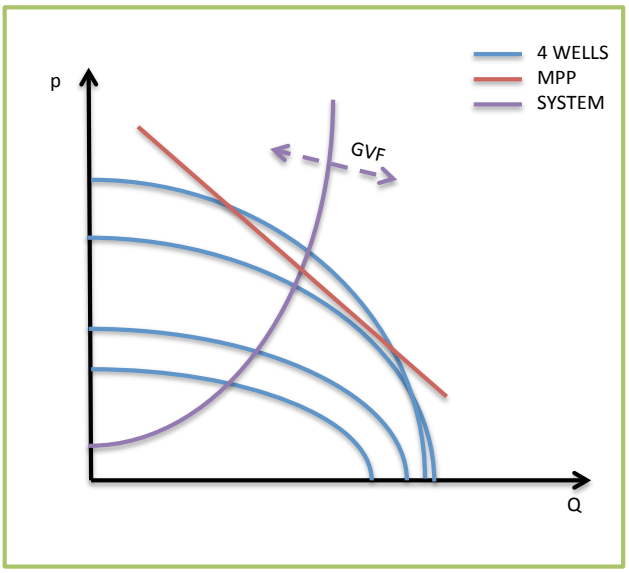

Fig.84: System hydraulic matching between wells, pump and system characteristic curves.

However, the simplified model is very far from describing the pump real behavior, thus the pump speed, required power and efficiency. Manufacturers provide pumps characteristics for each pump even for multiphase duties, though these characteristics are for air-water mixtures. Multiphase pumps are very susceptible to gas void fractions, fluid viscosities and densities; nonetheless the ideal required power for gas compression depends on the gas specific heat at constant pressure. As can be easily intuited, pumps characteristics with air-water mixtures cannot estimate pump working conditions. Moreover, suction conditions are strongly affected by pump position across the system and pump load: closer the pump will be to the wells, lower will be the suction GVF, higher will be the pump load (e.g. pressure boost), higher will be the suction GVF.

In this dissertation a simple method to estimate a twin screw pump behavior is proposed, indeed rotodynamic pumps are too complex to be described by a simple model.

7.2. The multiphase pumping process

Multiphase pumping is absolutely a complex topic. During this physical process nothing can be assumed steady: pressure, temperature and phase fractions change. However, mechanical transient periods are quicker than thermal ones, thus it is possible to divide the multiphase pumping process into different steps. When the fluid enters in a new chamber, pushed in by the rotor thread, it faces a higher pressure environment. Suddenly the fluid increases its pressure till equalizing the environment one and the vapor phase increases its temperature, as it occurs in all compression processes. Then, the fluid does not increase its pressure any more till it is pushed into the next chamber and phases can interact with each others at constant pressure for most of the revolution period 1/N. Gas phase condensates and provides sensible and latent heat to the liquid one. If the liquid amount is sensibly higher than the gas one, it is able to absorb such heat, thank to its higher heat capacity, and no overall temperature increase is observed. Although, when GVF approaches 60%, liquid phase cannot face such task anymore and temperature increases along the screw. Once gas and liquid phases have reached thermal equilibrium, the fluid enters into the next pump stage or chamber. Thus the pumping process, which is assumed adiabatic, can be divided as follows:

- Adiabatic compression of both phases;
- Constant pressure heat and mass exchange between phases.

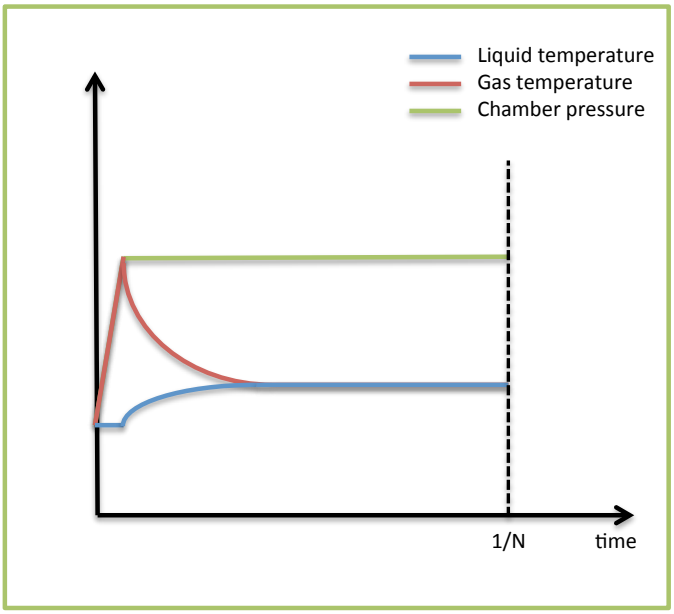

Fig.85: Chamber pressure, liquid and gas temperature profiles during the multiphase compression process in a twin screw pump. N is the rotational speed and 1/N is the fluid residence time.

7.3. Pressure built up profiles

If multiphase twin screw pumps were ideals, single stage machines would be required to accomplish the pumping task. Indeed, without any backflow occurring through clearances, the fluid would automatically reach the outlet pressure, as soon as exiting the pump discharge. However, pressure difference across the pump leads the fluid to recirculate from high pressure environments to lower pressure ones through clearances, reducing volumetric efficiency. In order to reduce backflow, more stages are required because pressure is increased gradually and pressure difference per stage is lower. Backflow, or slip flow, strongly affects the pump performances and determines the pressure profile across the pump, which determines the former in return: backflow and pressure profile are strongly linked to each other. Such relationship can be expressed by a single multiphase equation, which expresses slip flow as a function of pressure profile, as explained in the following pragraph.

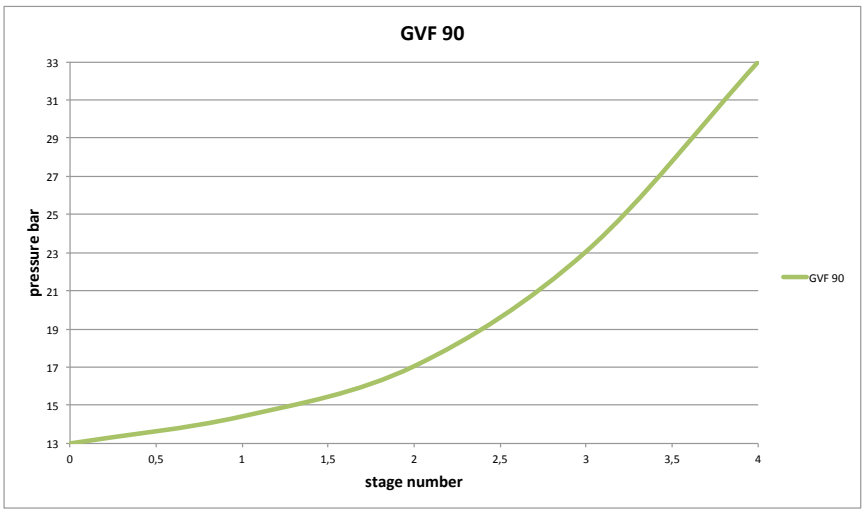

Chart 1: Model predicted pressure profile for a 90 GVF air-water mixture.

7.4. Slip Flow Model for Twin Screw Pumps

The first predicting models were proposed by Vetter and Winchek (1993, 2000). They simplified the pump spindle-geometry to a series of parallel disks, which divide the machine into sealed chambers. Slip flow was assumed everywhere as liquid single phase and gas compression was due to liquid inlet into the chamber and assumed isothermal. Egashira (Egashira, Shoda, Tochikawa, & Furukawa, 1998) has been the first to understand the importance of slip flow in multiphase pumps and to develop a numerical model for predicting the pump performance from experimental data on slip flow. He assumed liquid slip flow only in peripheral gaps, imaging the liquid pushed round to the liner by centrifugal forces. Rabiger (Räbiger, Maksoud, Ward, & Hausmann, 2006), developed for

the first time a 3D leakage flow model able to predict the fluid temperature and density distributions inside the gaps. No phase assumptions were taken while modeling gap flow. Afterwards, he proposed a thermodynamic model, in which pressure profiles are predicted from slip flow datas generated from previous model. In 2010, Ruschel A. and Schlücker E. (Ruschel & Schlücker, 2010) investigated gap flow with high-speed camera techniques and demonstrated that slip flow in clearances is multiphase and no phase separation is occurring in the chamber, thanks to the mixing action of the intermeshed threads.

There are mainly three different types of clearances through which back flow is occurring:

- Peripheral gaps between screw tip and casing;
- Radial gaps between screw tip and screw rotor;
- Flank gaps between the thread flanks.

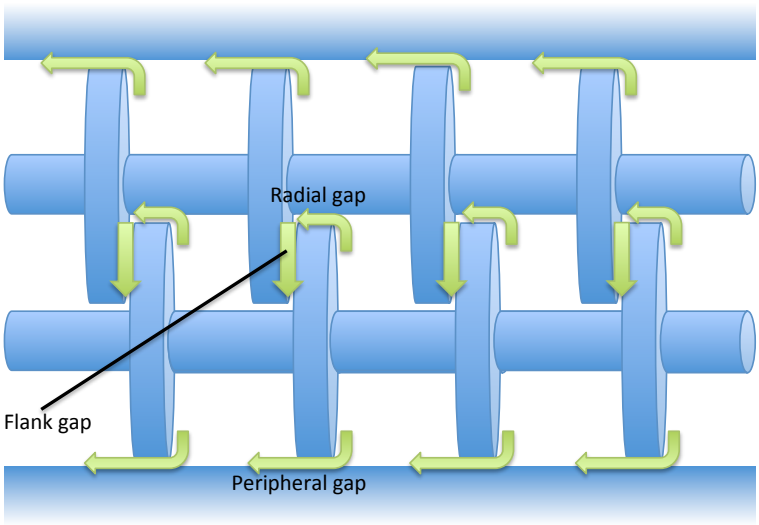

Fig.86: Slip flow paths in a multiphase twin-screw pump.

In this dissertation, gap flow is driven by pressure difference, as electric current is driven by voltage differential: there are different flow paths which slip flow can follow, the amount of flow passing through each clearance depends even by the disposition of other clearances. Indeed, if two clearances are operating in parallel, slip flow splits in two different streams, whose flow rate depends on the flow resistance which each path has; indeed, slip flow tends to pass through the clearances with lower resistance, as it occurs in an electrical circuit. The total slip flow is the sum of all streams flowing though clearances:

$$Q_{slip} = \sum_{1}^{n} \frac{1}{R_i} \Delta p$$

Q_{slip} = *slip flow*

R = *flow resistance*

Δp = *pressure difference*

Peripheral gaps are in parallel with the radial and flank ones and flow is splitted according to flow resistances. Let consider the inner fluid path: fluid can enter the clearance all along the intermeshed thread tip or from the radial gap; then, the fluid flows through the thread flanks and can exit from the flank outlet or from the radial outlet.

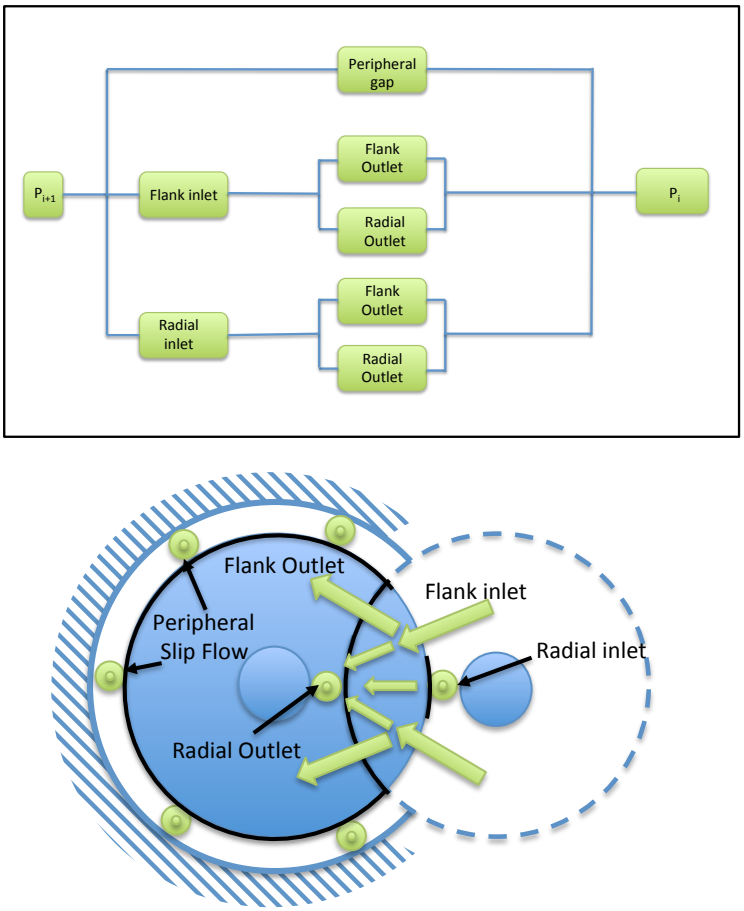

Fig.87: Frontal conceptual view of a twin-screw chamber and slip flow preferential paths. Thicker green arrows illustrate the preferential paths, while thinner ones illustrate least preferred ones.

Due to lower resistance, flank inlet/flank outlet is the preferential path. Indeed, radial inlet and radial outlet have high frictional losses and fluid tends to avoid them, hence:

$$Q_{slip} = \sum_{1}^{n} \frac{1}{R_i} \Delta p \simeq \left(\frac{1}{R_{peripheral}} + \frac{1}{R_{flank,inlet} + R_{flank,outlet}} \right) \Delta p$$

Slip flow is generally modeled as fluid flow into a narrow channel between two flat plates. Initially, single liquid-phase flow was assumed, but such model was underestimating back-flow. Afterwards, multiphase models were developed using Lockhart-Martinelli correlation, developed in 1949 (E Loth, 2006); it was the very first correlation developed for multiphase flow in horizontal pipes. Even if it is not very accurate, it is very widespread because no phase-holdup informations are required in order to determine the multiphase pressure drop, which is proportional to the one occurring as if there was only one phase flowing through the same channel.

$$\left(\frac{dp_{MP}}{dx} \right) = \Phi_L^2 \left(\frac{dp_{SP,L}}{dx} \right) = \Phi_G^2 \left(\frac{dp_{SP,G}}{dx} \right)$$

Φ = *Lockhart-Martinelli factor*

$$\left(\frac{dp_{SP,L}}{dx} \right) = \frac{1}{2} f_{SP,L} \rho_L \frac{u_{SP,L}^2}{D_H}$$

$$\left(\frac{dp_{SP,G}}{dx} \right) = \frac{1}{2} f_{SP,G} \rho_G \frac{u_{SP,G}^2}{D_H}$$

f_{SP} = *Single-phase Fanning friction factor*

For a smooth pipe in turbulent regime, Fanning factor is determined as follows:

$$f_{SP} = \frac{0{,}066}{\mathrm{Re}^{0{,}25}}$$

Where

$$\mathrm{Re} = \frac{\rho D_H u_{SP}}{\mu}$$

The Lockhart-Martinelli factors are determined as it follows:

$$\Phi_L^2 = 1 + CX + X^2$$

$$\Phi_G^2 = 1 + C\frac{1}{X} + \frac{1}{X^2}$$

Where

$$X = \left[\frac{\left(\frac{dp_{SP,G}}{dx}\right)}{\left(\frac{dp_{SP,L}}{dx}\right)}\right]^{0,5}$$

C is an empirical constant which depends on the flow regime. Chisholm ("Critical and Subcritical Oil/Gas/Water Mass Flow Rate Experiments and Predictions for Chokes," 2006) found the following values for each combination of flow condition, experimentally verified for the air-water couple:

Liquid	Gas	C
Turbulent	Turbulent	20
Turbulent	Laminar	12
Laminar	Turbulent	10
Laminar	Laminar	5

Tab.9: Chisholm's empirical factor values for Lockhart-Martinelli coefficient prediction.

Lockhart-Martinelli model takes into account that usually multiphase pressure drop is usually much higher than single phase one, indeed, for the same pressure drop for both phases, X is equal to 1 and the multiphase pressure drop is 20 times higher than single phase ones. Furthermore, Lockhart and Martinelli developed another correlation to match the multiphase multiplier Φ and the liquid holdup required for obtaining the occurring pressure drop:

$$\alpha_L = \left(\frac{1}{\Phi_L^2}\right)^{1/3}$$

In a twin screw, liquid holdup is equal to:

$$\alpha_L = \frac{V_L}{V_{ch}} = \frac{V_{ch} - V_G}{V_{ch}} = 1 - GVF$$

Then:

$$\Phi_L^2 = \frac{1}{\alpha_L^3} = \frac{1}{(1 - GVF)^3}$$

Finally:

$$\left(\frac{dp_{MP}}{dx}\right)=\Phi_L^2\left(\frac{dp_{SP,L}}{dx}\right)=\frac{1}{(1-GVF)^3}\left(\frac{dp_{SP,L}}{dx}\right)=\frac{1}{(1-GVF)^3}\frac{1}{2}f_{SP,L}\rho_L\frac{u_{SP,L}^2}{D_H}=$$

$$=\frac{1}{2(1-GVF)^3}f_{SP,L}\rho_L\frac{1}{D_H}\left(\frac{Q_{SP,L}}{A}\right)^2=\frac{1}{2(1-GVF)^3}f_{SP,L}\rho_L\frac{1}{2\delta}\frac{(1-GVF)^2Q^2}{(\delta l)^2}=\frac{1}{4}\frac{1}{(1-GVF)}f_{SP,L}\rho_L\frac{Q^2}{l^2\delta^3}$$

$$\Delta p_{frictional}=\frac{1}{4}\frac{1}{(1-GVF)}f_{SP,L}\rho_L\Delta x\frac{Q^2}{l\delta^3}$$

Where:

A = *Cross sectional area*

l = *width*

δ = *height*

Δx = *length*

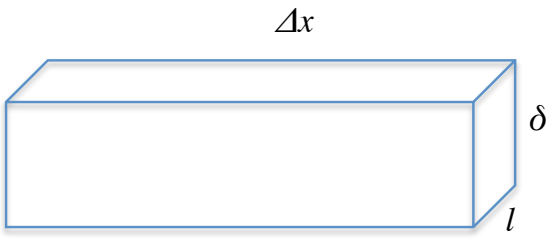

Further pressure dissipations must be taken into account:

- Inlet pressure drop;
- Outlet pressure drop.

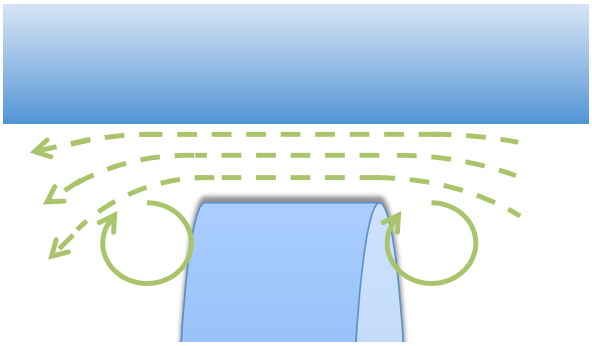

Fig.88: Hydraulic irreversibilities (eddies) along the slip flow path.

Concentrated pressure losses occur due to a sudden change in cross section area, which is followed by a quick change in fluid velocity. At gap inlet, velocity increases for the mass conservation law and kinetic energy increases as well. For energy conservation, pressure decreases providing the required kinetic energy for respecting the energy and mass balances. Fluid velocity decreases at the outlet, but vortices, occurring due to a sharp cross section increase, dissipate all the differential kinetic energy.

$$\Delta p_{in} = \frac{1}{2}\left(0{,}5\rho\frac{Q^2}{(l\delta)^2}\right)$$

$$\Delta p_{out} = \frac{1}{2}\left(\rho\frac{Q^2}{(l\delta)^2}\right)$$

$$\Delta p_{conc} = \frac{1}{2}\left(1{,}5\rho\frac{Q^2}{(l\delta)^2}\right) = 0{,}75\rho\frac{Q^2}{(l\delta)^2}$$

Then

$$\Delta p_{tot} = \Delta p_{frictional} + \Delta p_{Conc} = \frac{1}{2}\left[\frac{1}{2}\frac{1}{(1-GVF)}f_{SP,L}\rho_L\Delta x + 1{,}5\rho\delta\right]\frac{Q^2}{l^2\delta^3}$$

The former expression is valid for multiphase and uniform flow into a narrow channel between two parallel plates and can be used to model slip flow through each gap-path with the following hypothesis:

- Gaps GVF is equal to the one in the inlet chamber;
- Circumferential gap can be flattened thanks to high D_{tip}/δ ratio;
- Flank-path can be modeled as an equivalent channel between two flat plates, with $s_f = A_f / l_f$;

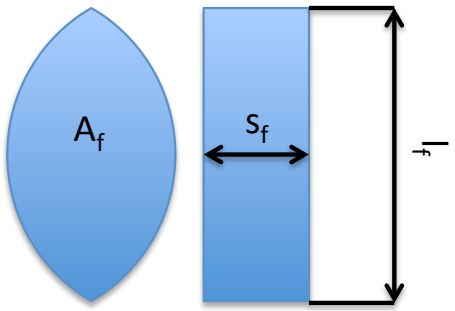

Fig.89: Equivalent flank surface, depth(s_f) and width (l_f).

Then slip flow rate is given by the following:

$$Q_{tot} = \sqrt{2\Delta p_{tot}\left[\frac{l_{circ}^2\delta_{circ}^3}{\frac{1}{4}\frac{1}{(1-GVF)}f_{SP,L}\rho_L\frac{s_{circ}}{2} + 1{,}5\rho\delta_{circ}} + \frac{l_f^2\delta_f^3}{\frac{1}{4}\frac{1}{(1-GVF)}f_{SP,L}\rho_L s_f + 1{,}5\rho\delta_f}\right]}$$

As can be seen in the former expression, slip flow can both increase and decrease with GVF increment (as long as multiphase flow is occurring); this is due to the very nature of frictional pressure losses in multiphase Lockhart-Martinelli correlation. Backflow is strictly correlated to the fluid properties, thus optimum point is determined by the suctioned mixture composition and usually lays in multiphase conditions. Both single-phase conditions have lower performances (see picture 90).

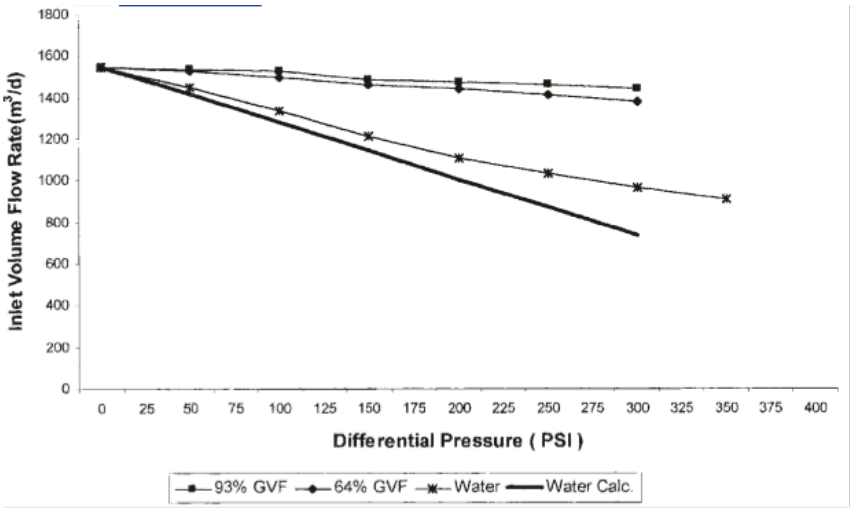

Fig.90: Experimental multiphase twin-screw pump performance points (Karassik et al., 2001).

The following graph relates pump performance with GVF. Data have been obtained using the pump model described in this chapter.

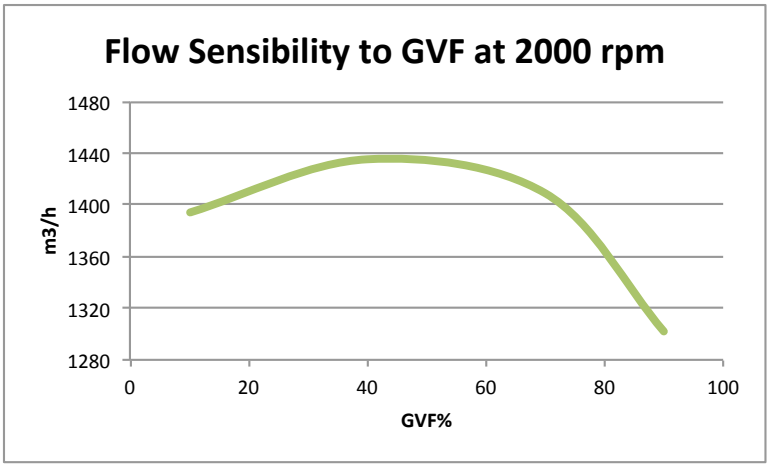

Chart 2: Model sensibility to GVF variations at 2000 rpm.

7.5. The Model

The pump was divided into stages, represented by the volume limited by the rotor diameter, the pump casing and the meshing threads.

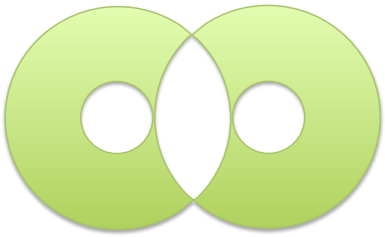

Fig.91: Chamber volume (green).

Pressure is constant in each chamber and phases are in equilibrium. No heat loss was considered and the pump was assumed adiabatic. Slip flow occurs through the thread tip diameter-casing clearance and through the meshed threads. When the fluid enters in a new chamber, phases are adiabatically compressed separately and no heat and mass transfer is occurring. Then, phases can interact in next chamber, where slip flow is occurring. Slip flow determines the pressure profile along the pump.

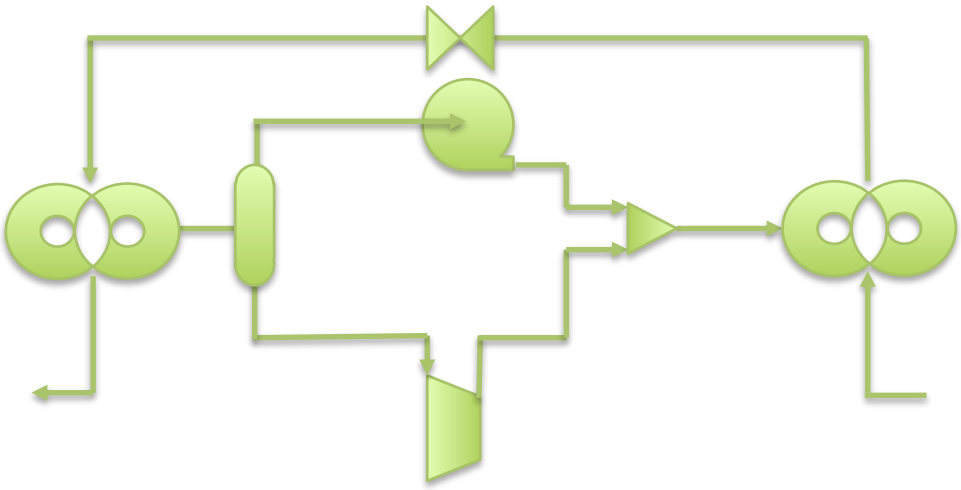

Fig.92: Model's multiphase compression process per pump stage.

These physical transformations can be described by HYSYS process components, where are occurring in continuous at the pump speed N:

- The pump chamber *i* is represented by a simple stream, in which the fluid is thermodynamically in equilibrium at T and p. The volumetric flow rate is equal to the chamber volume multiplied by the pump speed. ($Q[m^3/h] = V[m^3] \times N[rpm] \times 60$);
- Phases are separated in a iso-enthalpy flash;

- Vapor phase is compressed into a compressor as the liquid one is pumped in a pump;

Phases are mixed up together in a mixer with the slip flow stream coming from the *i*+1 chamber, then slip flow going to *i*+1 chamber is separated from the main stream in a splitter.

Eventually, the fluid enters in the *i*+1 chamber, which has the same volume of previous chamber *i*.

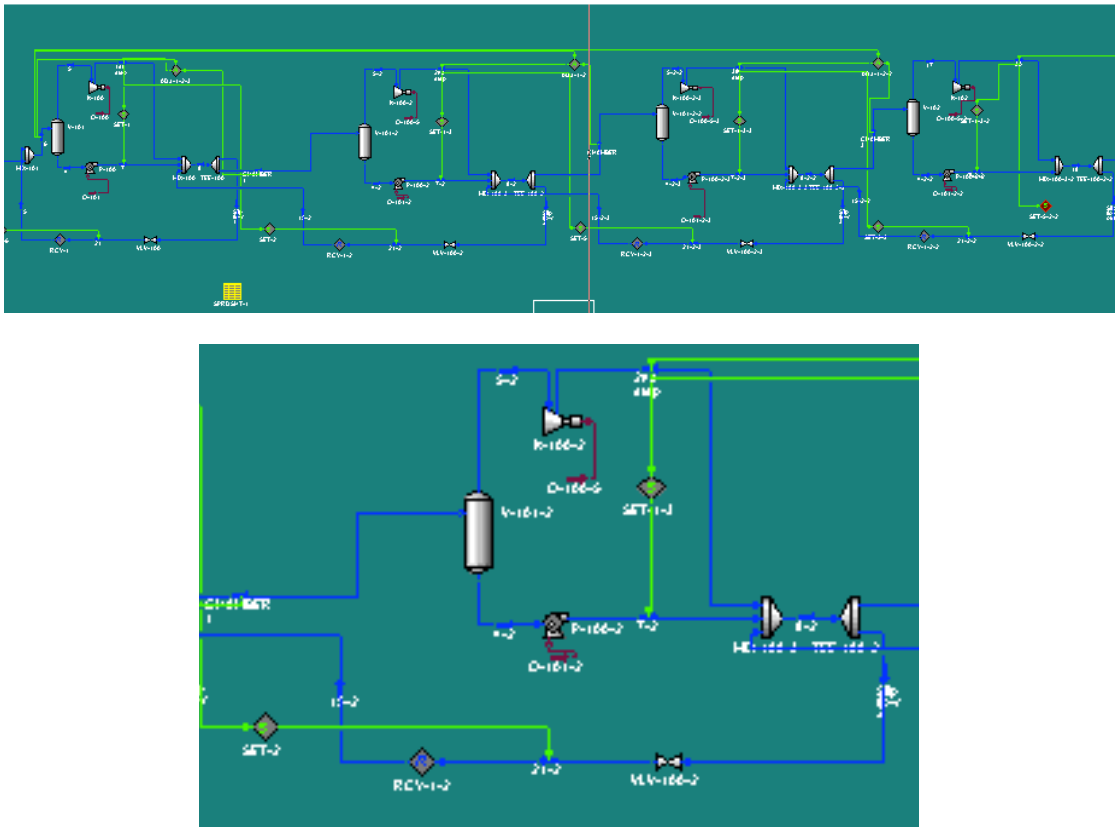

Fig.93: HYSYS flowsheet view of the twin-screw pump model. Pump overview (top) and single stage focus (bottom).

Through the HYSYS Adjust logic operator, it is possible to equalize all the volumetric flow rates to the inlet one, which is fixed by the pump geometry and speed. The Adjust will vary the stage pressure, which changes both inlet and outlet slip flows.

7.6. Model Calibration

The model aims to represent the behavior of a generic multiphase twin screw pump and, in order to achieve its purpose, requires the geometric dimensions of the modeled pump. Number of stages, tip screw diameter and rotor diameter can be obtained by manufacturers, however the clearance height must be deducted from any operating point of the pump: the real pump is run at known inlet conditions, speed, pressure difference and flow rate. The model receives as input the inlet conditions, pressure difference and gives as output the required pump speed to elaborate the given flow rate, at given inlet conditions, under given pressure increase. If the output speed is higher than the real one, the clearances equivalent height must be reduced, oppositely must be increased. Once the model is able to represent the pump behavior at one given point, it should be able to do it under different working conditions, as pressure difference, inlet GVF, fluid composition and flow rate.

The model was calibrated with a 70% GVF air-water mixture at 12 barg of inlet pressure. The real pump (Bornemann) elaborates 819 m^3/h at 1200 rpm under 10 bar of pressure difference. The resulting equivalent clearances height, required to represent the pump operating point, was registered equal to 0,6 mm.

p_{in}	12	barg
T_{in}	24	°C
GVF_{in}	70	%
Δp	10	barg
Volumetric flow rate	819	m^3/h
Speed	1200	rpm
Clearance height	0,6	mm

Tab.10: Geometrical dimensions of the simulated pump.

7.7. Model Validation

Once clearances equivalent height is known, the model should be able to predict the pump performances appropriately; hence, the model was tested under different operating conditions and compared with the real pump behavior. Then constant speed curves were plotted in a differential pressure-flow rate diagram. The comparison has been performed under three different rotational speeds (1200, 1600, 2000 rpm). In such comparison, it is essential to not neglect that the real pump is not able to produce the ideal flow rate, even under none differential pressure. Indeed, some fluid is always trapped into the meshed threads, due to eddies effect, and the available volume for the conveyed fluid is reduced.

Therefore, flow rate under none differential pressure, will be lower than ideal one.

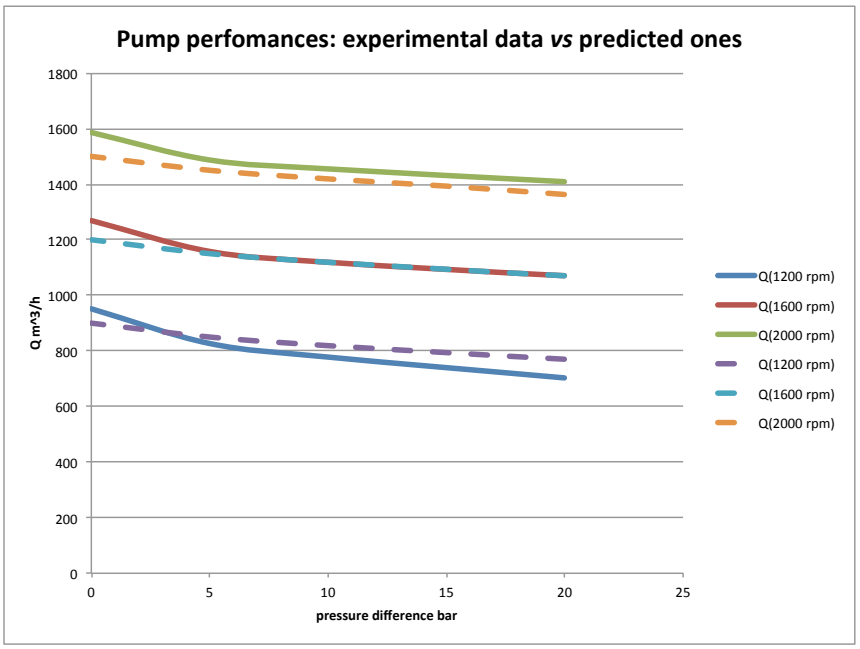

Chart 3: Experimental and model predicted values matching and comparison. Continuous lines stand for model predicted trends, while dashed ones for manufacturer provided ones.

The previous graph shows almost a good agreement with the manufacturer datas. As mentioned above, the first difference which comes up is that predicted flow rate is always higher than real one under none differential pressure. This is due to eddies occurring between meshed threads which trap some fluid, reducing the pump capability.

The model has been further tested and an additional analysis has been carried out, plotting and individuating the errors committed by the model.

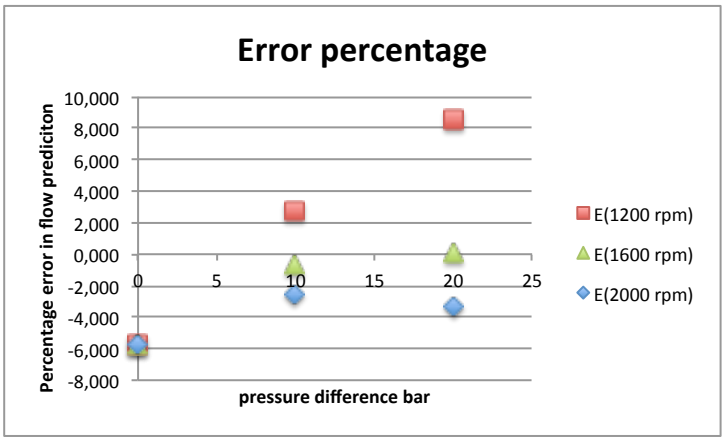

Chart 4: Model percentage errors in flow prediction.

The highest percentage error (8,6%) is occurring at 1200 rpm and 20 bar of differential pressure. Under none differential pressure the model commits the same error independently from rotational speed. This is due to the model inability to model eddies inside the meshed chambers. Standard deviation has been determined equal to 4,7%. If the pump is operating with differential pressures higher than 5 bar, the standard deviation is 4,1%.

Max. Error	8,6	%
St Deviation (full operating range)	4,7	%
St Deviation (Δp>5 bar)	4,1	%

Tab.11: Model errors in pump performance prediction.

The pump model can be considered reliable when a 70% GVF air-water mixture is used, although none verification was performed outside this range. Indeed, manufacturer datas were available only for this mixture. In order to assess the model reliability outside the experimental data validation range, it has been compared with former literacy outcomes. For instance, the pump sensibility to GVF fluctuations has been compared with Rabiger results (Räbiger et al., 2008))and (Xu, 2008) ones. Despite the comparison is simply qualitatively performed, it shows great agreement between results: the pressure profile is linear when pure liquid is fed to the pump, while it gets steeper increasing the gas volume fraction, until a maximum is reached; then, liquid accumulation effect becomes sensibly lower and pressure profile gets closer to the pure gas one. The first graph below shows the pump model results and have been compared with the following ones.

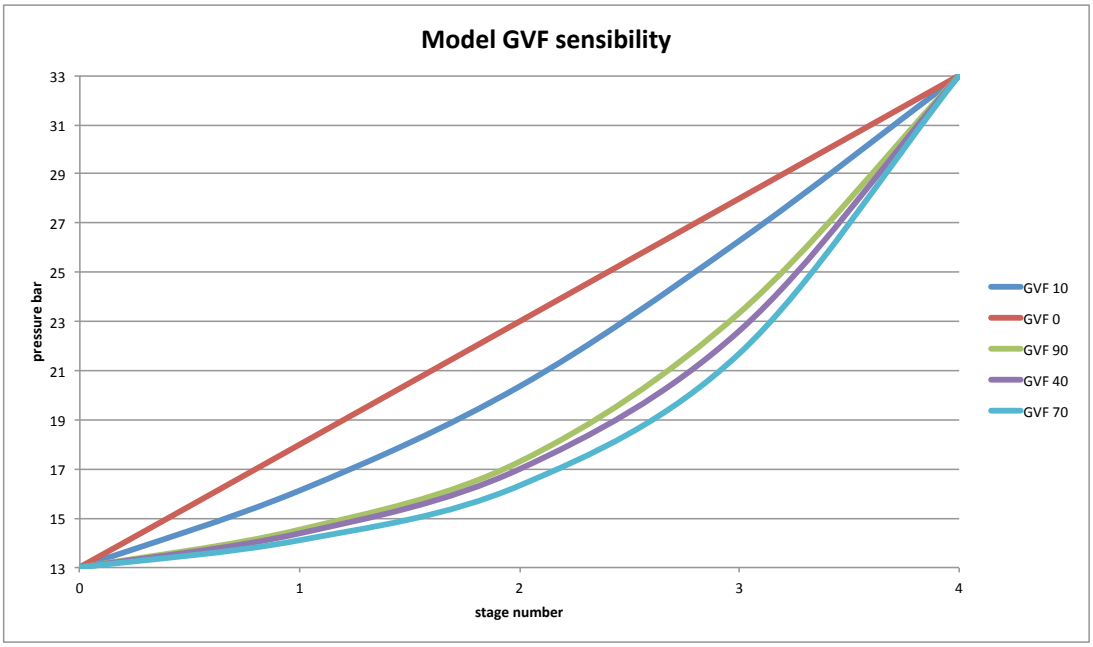

Chart 5: Model pressure distribution along pump shaft: sensibility to GVF variations.

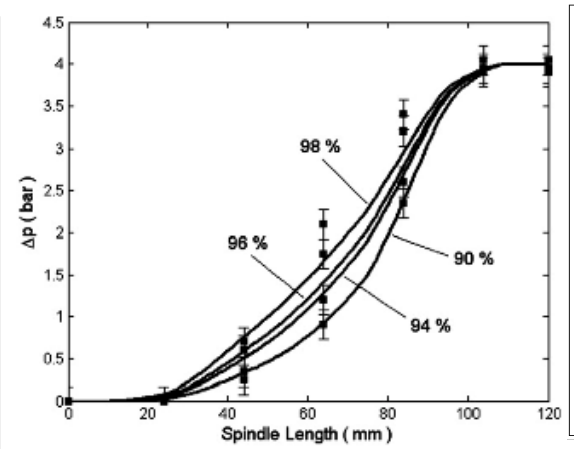

Fig. 7. Experimental data points at different GVFs and a rotational speed of 290 rpm compared to calculated pressure distributions.

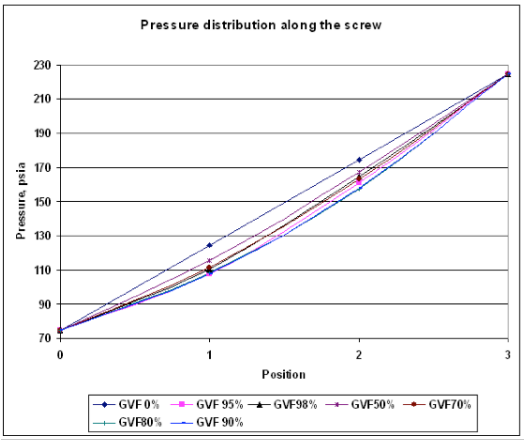

Fig. 3.22—Pressure distribution along the screw at 1700 rpm, suction pressure 60 psig and differential pressure 150 psi

Fig.94: Other pressure distributions along pump shaft: sensibility to GVF variations from (Räbiger et al., 2008) *and from* (Chan, 2009).

7.8. Conclusion on the model reliability

The model has been experimentally verified for a 70% GVF air-water mixture. In order to further assess the proper behavior under different inlet GVFs, the model was successfully compared with previous academic results (Räbiger et al., 2008) (Xu, 2008)). However, no validation has been carried out for a hydrocarbon mixture, in particular for the one later analyzed. Indeed, this type of mixture has definitely different viscosities and GVF strongly changes with pressure, thus along the screw. The pump behavior will depend on the fluid properties, which change during compression process. No experimental datas were found for a hydrocarbon mixture useful for validating the model under these conditions, although the model was created on this very purpose. Hence, further investigation shall be carried out to assess the model reliability with the considered fluid, although it has been created with strong theoretical fundamentals and prediction has not been committed to experimental data elaboration. Thus, the method used to build up the model is very far from being inductive, where general laws are derived from specific cases, while is almost completely deductive (from general and known laws it reaches logical conclusions). Assumptions taken during the model creation were made independently from the suctioned fluid, thus, it is reasonable to entrust the pump performance prediction to the model even with hydrocarbon mixtures. In the following chapters, the model is used to predict the pump performance under different working conditions to assess which are the pump deployment benefits and which is its best location along the tieback. Due to the high differential pressure requirements, the effective clearance height has been reduced to 0,3 mm in order to achieve acceptable pump performances.

8. System Analysis: simulation setup

8.1. System overview

In this dissertation, the advantages of multiphase boosting for deepwater oilfields are analyzed throughout the simulation of a four wells field with long tieback coupled with a multiphase pump. Furthermore, pump position and differential pressure effects on the system behavior has been investigated throughout the oilfield life. The evaluation of benefits due to pump deployment on the system performance has been carried out by comparing and analyzing the following key parameters:

- Flow stability and field operational range;
- Oil recovery;
- Thermal behavior (during a shutdown);
- Specific power consumption;
- Field restart velocity.

The analyzed system is located in west Africa and is made of 2 producing blocks, each one with two wells. The blocks are connected by 2,5 km of multiphase subsea insulated flowline in Daisy Chain configuration, then the fluid is conveyed to the FPSO (Floating, Production, Storage and Offlanding) riser base through a 15,5 km insulated tieback. The field is expected to operate nine years and water is injected in three of four wells, in order to maintain the reservoir pressure. Water is transported through an auxiliary water line departing from the FPSO riser base. FPSO is located in 1250 m of water depth and connected to the 15,5 km flowline by a flexible and insulated riser.

The field has been analyzed in three characteristic years which represent the most critical design conditions:

- First producing year: at the beginning of its producing life, the oilfield has enough pressure to self flow and watercut is minimum. This is expected to be the most critical year for transient operation and shutdown conditions, because water is the phase with highest heat capacity;
- Last year: reservoir has been strongly exploited and much water has been injected to sustain pressure. Water phase strongly differs from oil and gas ones in physical and chemical properties, thus its effects on the system must be evaluated;

- Third year: another sample has been evaluated to extend the analysis to the intermediate years. Third year has been taken as representative sample rather than the fourth or fifth ones because oil production shrinks during oilfield life.

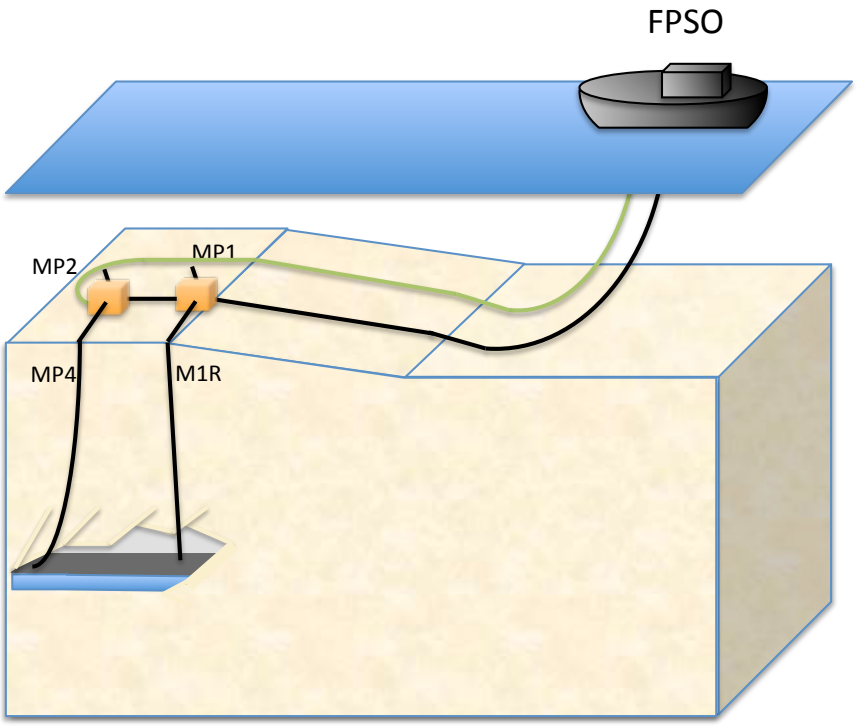

Fig.95: Simulated system conceptual layout.

Different production solutions have been evaluated for the analyzed system, providing a higher number of benchmarks and wider range of production scenarios, each one showing characteristic features and advantages.

The first production strategy evaluated is with self-flowing wells: production is entrusted to the reserve energy which draws out the fluid and drives it to the processing facility. The main advantages of this solution are simplicity and low CAPEX, thanks to the absence of further equipment. However, this solution has low production rates due to the high backpressure on the wells.

Secondly, two multiphase pumps operating in parallel, initially placed at riser base, then at manifold, were considered and analyzed. In both cases the pumps reduce the back pressure on the wells, thus enhance the oil extraction. Pumps operate at constant head (or constant pressure difference at nominal density), thus the pumps were simulated at three different rated pressure boost: 30 bar, 60 bar, 90 bar. The two pumps have the same volume, equal to half of the modeled pump one. Because the two pumps are operating at half of their capacities, hereafter it will be referred both to pump or pumps without distinction.

Furthermore, gas lift has been evaluated in order to reduce backpressure on the wells. Indeed, the geodetic pressure loss across the riser is the product of fluid average density and height change. As mentioned above, the FPSO is floating in 1250 m of water depth, therefore, small changes in density value can mean strong changes in pressure drop across the riser. The main critical feature of subsea gas lift is temperature: gas is compressed to 300 bar at sea level, then injected in the gas lift line, which is very far from being insulated, and conveyed to riser base, where can be assumed in thermal equilibrium with the environment water (roughly 4°C). Before joining the oil line, gas is expanded in a choke, where reaches the system pressure and cools down to -15°C due to Joule-Thompson effect. In such conditions, even small gas lift/conveyed oil ratios can strongly reduce the stream temperature and be threatening for flow assurance due to hydrates formation.

Last production strategy is the combination of gas lift at riser base and multiphase pump, which has been located either at riser base either at manifold in two different scenarios. When pump is located at riser base, the gas injection occurs afterward the pump, in order to avoid inlet GVF too high and power wastes. A first analysis was performed to individuate the most opportune gas flow rate to fit the system requirements in such scenario. However, optimal gas flow rate depends on the producing year and on the number of flowing wells: under turndown conditions higher amounts of gas are required to properly lift the liquid phase through the riser.

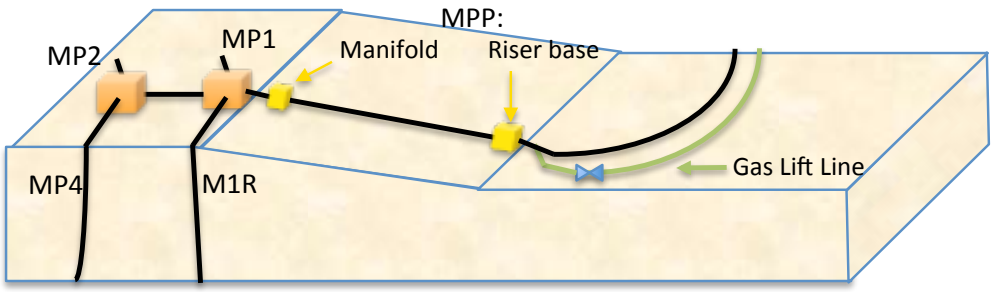

Fig.96: Pump locations and gas lift injection point in the simulated system.

This solution couples the technologies of both artificial lift methods, but not their advantages and their disadvantages. Indeed, decreasing too much the backpressure on the wells, the gas content in the main pipeline increases as well. Friction losses increase with gas content, as cooling speed does under transient conditions. However, the hydrate formation threat sharply falls in this production scenario, thanks to the MPP double effect: the amount of gas, required to lift up the produced fluid, will be lower compared to the scenario without the pump. In such scenario the pump provides heat to the fluid, which increases the temperature before being mixed with the cold gas stream and further decreases the exposure to hydrate formation at riser base.

Each production strategy was analyzed under steady state conditions in the first year, in the third year and in the last one. In the first year, all transient conditions (i.e. shutdown) are harsher, therefore all production strategies were tested under transient conditions. Furthermore, were considered the cases in which one or more wells must be shut down due to unforeseen failure. The system works at part load and such condition is known as turndown. During turndown, flow rate is strongly reduced and slugging may occur; furthermore, the reduction in flow rate means a reduction in fluid speed, thus an increase in characteristic residence time, which means lower temperatures. In turndown operations, if an unexpected shutdown occurs, the system is very exposed to hydrates formation, because starts to cool down from lower steady state temperatures. Therefore, it is very important to analyze the system behavior under partload and estimate the period of time that the fluid takes to reach the hydrate formation temperature, thus the period of time the field operators have to inject methanol and dead oil in the pipes. In the following years transient conditions are expected to be less threatening for flow assurance, however hydraulic analysis must be performed during turndown conditions, in order to estimate and avoid severe slugging conditions. Shutdown operations were performed only from stable flow conditions. The table below shows the simulations performed per each year per production strategy.

	Year	I year					
	Pump Position	Riser			Manifold		
Natural flow	Steady state	x					
	Shutdown	x					
	Turn down I well	x					
	shutdown	x					
	II well	x					
	Shutdown	x					
MPP	Steady state	x	x	x	x	x	x
	Shutdown	x	x	x	x	x	x
	Turn down I well	x	x	x	x	x	x
	shutdown			x			x
	II well	x	x	x	x		x
	shutdown			x			x
GL	Steady state	x		x		x	
	Shutdown	x		x		x	
	Turn down I well	x		x		x	
	shutdown	x		x		x	
	II well	x		x		x	
	shutdown			x			
MPP+GL	Steady state	x	x	x	x	x	x
	Shutdown	x	x	x	x	x	x
	Turn down I well	x	x	x	x	x	x
	shutdown			x			x
	II well	x	x	x	x	x	x
	shutdown						

Tab.12: Simulations performed during the first producing year.

	Year	III year					
	Position	Riser			Manifold		
Natural flow	Steady state			x			
	Shutdown			x			
	Turn down I well			x			
	shutdown						
	II well			x			
	Shutdown						
MPP	Steady state	x	x	x	x	x	x
	Shutdown	x	x	x	x	x	x
	Turn down I well	x	x	x	x	x	x
	shutdown		x	x		x	x
	II well	x	x	x	x	x	
	shutdown						
GL	Steady state		x			x	
	Shutdown		x			x	
	Turn down I well		x			x	
	shutdown			x			
	II well		x				
	shutdown			x			
MPP+GL	Steady state	x	x	x	x	x	x
	Shutdown						
	Turn down I well	x	x	x	x	x	x
	shutdown						
	II well	x	x		x	x	
	shutdown						

	Year	IX year					
Natural flow	Steady state			x			
	Shutdown						
	Turn down I well			x			
	shutdown						
	II well			x			
	Shutdown			x			
MPP	Steady state	x	x	x	x	x	x
	Shutdown	x	x		x	x	x
	Turn down I well	x	x	x	x	x	x
	shutdown		x	x		x	x
	II well	x	x	x	x	x	x
	shutdown		x	x		x	x
GL	Steady state		x			x	
	Shutdown			x			
	Turn down I well		x			x	
	shutdown			x			
	II well		x			x	
	shutdown			x			
MPP +GL	Steady state	x	x	x	x	x	x
	Shutdown						
	Turn down I well	x	x	x	x	x	x
	shutdown						
	II well	x	x	x	x	x	x
	shutdown						

Tab.13: Simulations performed during the third (first table) and ninth (second table) producing year.

8.2. Production wells

All tubings have the same inner diameter of 12,43 cm and a surface rugosity of 0,15 mm. Reservoir temperature is supposed to remain steady during the field producing life and equal to 62°C, while reservoir pressure changes due to field exploitation and is sustained by water injection, which increases the total water fraction in the reservoir. The four wells have really different reservoir energies, some are so prone to production that can choke the others. Therefore, flowing bottom hole pressure must be kept constant for each well in order to ensure proper field exploitation and flow equilibrium between wells. Such task is performed by a controller placed on each tubing, which opens or chokes a wellhead located valve. The following table resumes the well datas during the field life.

	WELL	Reservoir Temperature	Reservoir Pressure	Total water Fraction	Flowing Bottom Hole Pressure*
		°C	bara	%	bara
I year	I WELL	62	167.3	0.031%	152.3
	II WELL	62	194.0	0.422%	188.8
	III WELL	62	193.9	0.080%	164.6
	IV WELL	62	204.7	0.001%	195.5
III year	I WELL	62	175.0	52.68%	150.3
	II WELL	62	176.6	62.97%	146.4
	III WELL	62	205.3	38.09%	163.9
	IV WELL	62	188.9	9.84%	175.8
IX year	I WELL	62	190.8	84.06%	157.4
	II WELL	62	158.3	83.63%	144.4
	III WELL	62	228.7	81.45%	187.4
	IV WELL	62	168.0	82.44%	146.9

Tab.14: Wells properties.

The tubing has not been considered insulated and has been modelled as follows:

Material	Thickness	Capacity	Conductivity	Density
	inches	J/kgK	W/m K	kg/m3
Carbon steel	0,304	434	45	7832
Gas	2,0625	2000	1000	1
Cement	1	900	5.88	2400
Formation	53,36	1256	1,59	1256

Tab.15: Tubing layers properties.

8.3. Insulated flowline

The produced fluid is conveyed to riser base through an insulated 8 in (174,5 mm) flowline which should minimize heat losses during transport. The main pipeline is not perfectly horizontal but has a gradient of 1°, which is considered constant along the line.

Material	Thickness	Capacity	Conductivity	Density
	mm	J/kgK	W/m K	kg/m3
Carbon steel	22,2	490	45	7850
Aerogel	19,5	1046	0,015	130
Air	15,4	1050	0,19	1,3
Carbon steel	17,5	1256	1,59	1256

Tab.16: Insulated flowline layers properties.

8.4. Flexible Jumpers

Flexible jumpers are used to connect wells to manifold and the pump to the rest of the system; in such way the pump can be removed easily and the flow line can be pigged.

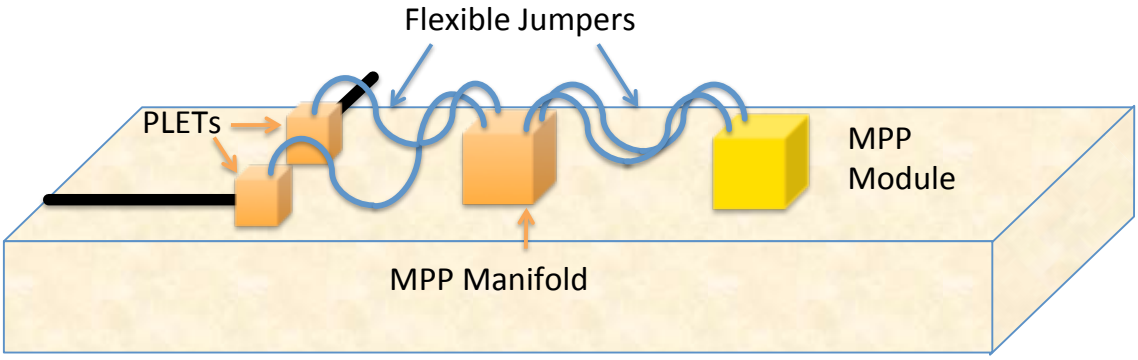

Fig.97: Multiphase pump connection system layout.

Flexible pipes are made of steel layers and insulation layers. Layers are un-bonded and can move freely from the others, which allows excellent flexibility. Each one has a different task from the others; for instance, the external sheath, which is made of HDPE (High Density Poli Ethylene), protects the pipe from abrasion, seawater penetration and steel from corrosion, while the intermediate layers, made of the same material, protect the steel layers from abrasion during thermal elongation (each coating moves respectively to the others creating shear stresses on the contact surface). Such insulator materials are temperature sensitive and can commonly operate up to 130°C. The following table shows the flexible jumper cross sectional structure which has been used in the simulation.

ID (mm)		152.40		
Roughness (m)		0.813		
Material	Thickness [mm]	Capacity J/kg.°C	Conductivity W/m.K	Density kg/m3
Duplex 2205	7.35	502	100	4847
PVDF Solef 60512 Copolymer	4.00	1200	0.2	1770
PVDF Solef 60512 Copolymer	7.00	1200	0.2	1770
Carbon Steel	8.00	460	45.35	7850
Polypropylene	0.30	1800	0.215	900
Carbon Steel	5.99	460	45.35	7850
Polypropylene	0.30	1800	0.215	900
High Strength Glass Filament	2.03	1200	0.2	1770
Polypropylene	0.30	1800	0.215	900
Carbon Steel	5.99	460	45.35	7850
Polypropylene	0.30	1800	0.215	900
High Strength Glass Filament	2.03	2512	0.45	697
Polypropylene	0.30	1800	0.215	900
HDPE(Yellow)	13.00	2400	0.5	950
PP Syntactic Foam, 2134m WD	7.00	200	0.15	670
PP Syntactic Foam, 2134m WD	7.00	200	0.15	670
PP Syntactic Foam, 2134m WD	7.00	200	0.15	670
PP Syntactic Foam, 2134m WD	7.00	200	0.15	670
Polypropylene	0.30	1800	0.215	900
PP Syntactic Foam, 2134m WD	7.00	200	0.15	670
PP Syntactic Foam, 2134m WD	7.00	200	0.15	670
PP Syntactic Foam, 2134m WD	3.50	200	0.15	670
PP Syntactic Foam, 2134m WD	3.50	200	0.15	670
Fabric	0.41	1334	0.6	840
HDPE(Yellow)	15.00	2400	0.5	950

Tab.17: Flexible jumper layers properties.

8.5. Flexible riser

As flexible jumpers, flexible risers are made of different un-bonded sheaths. A simple catenary riser has been chosen for the analyzed field whose cross section is shown in the table below.

ID (mm) :		203.2		
Roughness (m) :		0.813		
Material	Thickness	Capacity	Conductivity	Density
	[mm]	J/kg.°C	W/m.K	kg/m3
Duplex_2205	8.4	502	100	4847
PVDF_Solef_60512_Copolymer	4	1200	0.2	1770
PVDF_Solef_60512_Copolymer	8	1200	0.2	1770
Carbon Steel	10.01	460	45.35	7850
PA_12_Yellow (PA11P20)	1.52	1.19	0.24	1020
Carbon Steel	7.01	460	45.35	7850
PA_12_Yellow (PA11P20)	1.52	1.19	0.24	1020
Carbon Steel	7.01	1200	0.2	1770
Polypropylene	0.3	1800	0.215	900
High_Strenght_Glass Filament	2.03	2512	0.45	697
Polypropylene	0.3	1800	0.215	900
HDPE_yellow	13	2400	0.5	950
PP synthatic foam	5	200	0.15	670
PP synthatic foam	5	200	0.15	670
PP synthatic foam	5	200	0.15	670
PP synthatic foam	5	200	0.15	670
Polypropylene	0.3	1800	0.215	900
PP synthatic foam	5	200	0.15	670
PP synthatic foam	5	200	0.15	670
PP synthatic foam	5	200	0.15	670
PP synthatic foam	5	200	0.15	670
Fabric	0.41	1334	0.6	840
PA_12_Yellow (PA11P20)	13	1.19	0.24	1020

Tab.18: riser layers properties.

8.6. Tubing Profiles and Flowlines Bathymetry

Overall system profile is represented in the following picture for different paths, except from MP2 and MP4 which share the same profile.

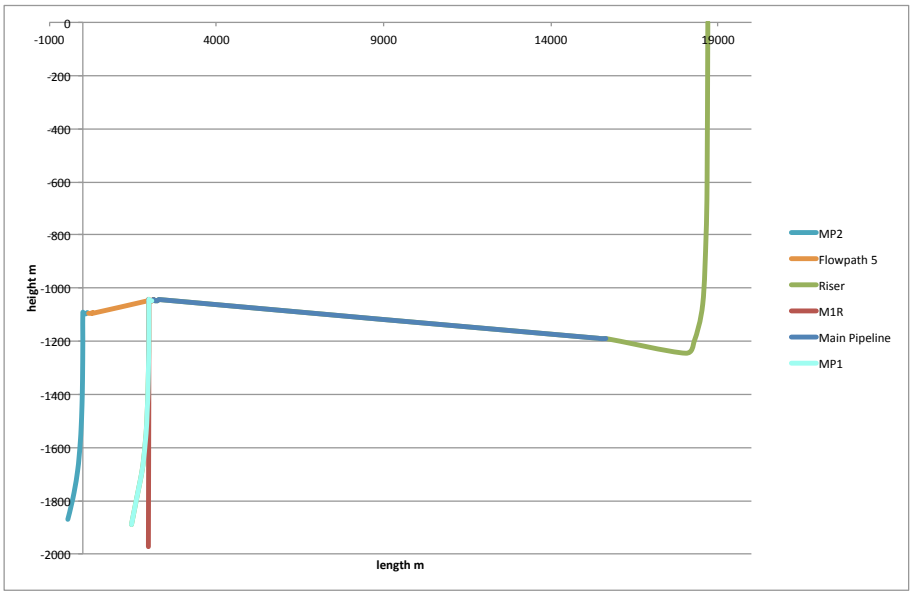

Chart 6: Subsea system bathymetry.

8.7. OLGA Implementation

The system has been implemented in OLGA environment, using the previous geometry, pipe cross sections and field datas. The following picture shows the field layout in OLGA.

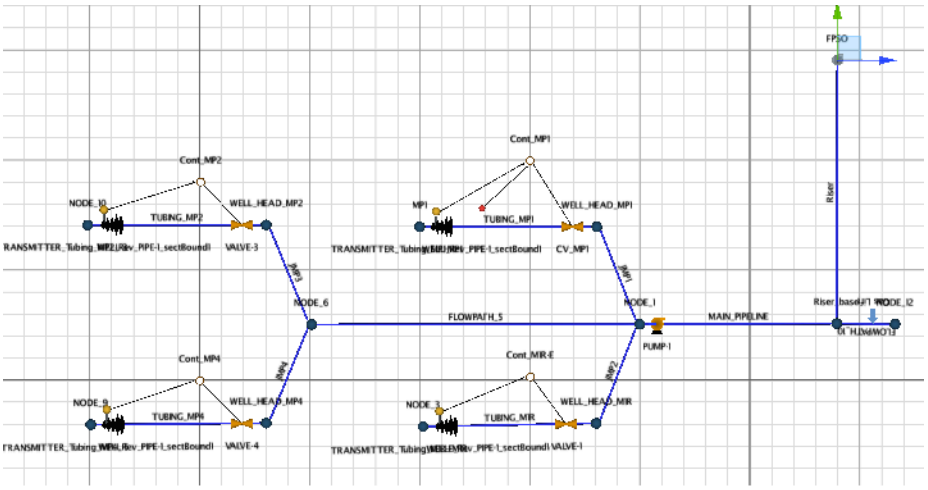

Fig.98: OLGA simulated system layout.

Simulations have been run changing the operating conditions and the outcomes are analyzed in the following chapter.

9. Results Analysis

9.1. Flow stability and system operability Analysis

The first analysis is focused on determining all the stable operating conditions of the system in the different scenarios. This is very important to lead and perform the following analysis only for possible operating conditions. Indeed, would be nonsense to perform a comparison of technical solutions which can not be accomplished. Furthermore, by means of defining an operability map for each producing scenario, it is possible to understand the flexibility and the operation limits of each technology and producing strategy.

		Natural flow
I year	Steady state	slugging
	Turn down I well	slugging
	II well	slugging
III year	Steady state	stable
	Turn down I well	slugging
	II well	slugging
IX year	Steady state	Not flowing
	Turn down I well	Not flowing
	II well	Not flowing

Tab.19: Natural flow operability map.

	Flow rate in MMscf/d	10	15	20
I year	Steady state	stable	stable	stable
	Turn down I well	stable and choked	stable and choked	stable and choked
	II well	slugging	stable and choked	stable and choked
III year	Steady state	stable	stable and choked	stable and choked
	Turn down I well	slugging	stable and choked	stable and choked
	II well	slugging	stable and choked	stable and choked
IX year	Steady state	slugging	stable and choked	stable and choked
	Turn down I well	slugging	stable and choked	stable and choked
	II well	slugging	stable	stable and choked

Tab.20: Gas lift operability map.

	Year		MPP					
	Position		Riser			Manifold		
	bar		30	60	90	30	60	90
I year	Steady state		stable	stable	stable	stable	stable	stable
	Turn down	I well	slugging +choke	slugging +choke	slugging +choke	slugging	slugging	slugging
		II well	slugging	slugging +choked	slugging +choked	slugging +choked	slugging +choked	slugging +choked
III year	Steady state		slugging	slug	stable	slugging	slugging	stable
	Turn down	I well	slugging	stable	stable	slugging	stable	stable +chocked
		II well	slugging	slugging +choke	slugging +choke	slugging alla fine	Sluggin +choke	slugging +choked
IX year	Steady state		slugging	stable	stable +choked	stable	stable	stable +choked
	Turn down	I well	slugging	stable	stable +choked	slugging	stable	stable+ choked
		II well	slugging	stable	stable +choked	slugging	stable +choked	stable +choked

Tab.21: MPP operability map.

	Year		MPP+GL					
	Position		Riser			Manifold		
	bar		30	60	90	30	60	90
I year	Steady state		stable	stable	stable	stable	stable +choked	stable +choked
	Turn down	I well	stable +choked	stable	stable	stable +choked	stable +choked	stable +choked
		II well	slugging	slugging +choked	stable +choked	slugging +choked	stable +choked	stable +choked
III year	Steady state		slugging	slugging	stable +choked	slugging	stable +choked	stable +choked
	Turn down	I well	slugging	sluggingch oked	stable +choked	slugging	slugging+ choked	stable +choked
		II well	slugging +choked	stable +choked	stable +choked	y half choked	stable +choked	stable +choked
IX year	Steady state		slugging	slugging	slugging	slugging +choked	stable +choked	Slugging
	Turn down	I well	slugging +choked	slugging +choked	stable +choked	slugging +choked	stable +choked	stable +choked
		II well	slugging +choked	stable +choked	stable +choked	slugging	slugging +choke	stable +choked

Tab.22: MPP+GL operability map.

Natural flow wells can ensure stable flow only in few cases and none acceptable solution was found under turn down operations. The reservoir energy is not able to overwhelm the frictional losses occurring along the tieback and the geodetic head across the riser, as expected.

Other artificial lift methods show to have stable solution under many different operating conditions. However, in many cases the back pressure was excessively reduced and wellhead valves had to choke the stream down, in order to maintain a steady fluid production profile at the processing facility. When all wellhead

valves are choked, any further attempt to reduce backpressure on wells is worthless. Thus should be avoided any situation in which gas or power is wasted.

9.1.1. GL

Gas lift appears to be the best solution from a flow stability analysis point of view, indeed it is able to cover all the potential operational conditions. Flow rates higher than 15 MMscft/d are useless, because the flow stability is ensured and all wellhead valves are choked. The optimum flow rate is not steady and depends on the operational conditions. Indeed, during the first year under nominal and turn down I conditions, the gas flow rate should be higher than 20 MMscf/d, while for the rest of situations it lays between 10 and 15 MMscft/d.

9.1.2. MPP

The multiphase pump greatly fits the system requirements under nominal conditions, but struggles under turndown ones; indeed, during the first year, none stable turndown solution was found and during the third one the system is not able to operate under turn down II condition. The pump inability of working at part load can be easily explained as follows: the pump compresses the vapor phase and reduces the overall density thus decreases the fluid velocity. During nominal conditions, an increase in pump differential pressure increases the fluid density and simultaneously increases the flow rate so that the fluid velocity is steady. Such equilibrium is not satisfied during a turn down. When one or more wells are shut down, flow rates are sensibly lower, which has two main effects on the system:

- Firstly, the fluid velocity sharply falls, enhancing slugging across the riser;
- Secondly, frictional losses decrease with the square of fluid velocity. During turndown, back pressure is lower than in nominal conditions and system complete choking is easier to reach. Once all wellhead valves are choked, no flow rate enhancement follows to any further decrease in back pressure, although the fluid afterward the pump has been compressed. Thus, under turndown conditions, the further pressure energy, given by the pump, leads to choking and slugging. Indeed, in natural flow and gas lift scenarios (where the pump is absent), none “slugging+choking” solutions were found, as can be deducted from previous tables.

The manifold located pump solution shows to have a slightly wider range of operation, although both locations appear to share the same problem under turndown conditions. Therefore, the system must be equipped with gas lift in order to exploit the field in all the remaining situations.

9.1.3. MPP+GL

Once understood that the pump is not able to run in some turndown conditions, the pump has been coupled with gas injection at riser base. Different combinations of flow rates and pump pressure increases were performed and 10 MMscf/day appeared to be the most satisfactory during the first year under nominal conditions. However, the opportune gas flow rate sensibly changes with operating conditions, as it is demonstrated by the following statement. Indeed, during turn down conditions such sharp backpressure reduction appears to be unreasonable and excessive, leading the wellhead valves to choke down the flow rate.

Even in the MPP+GL scenario, displacing the pump from riser base to the upstream manifold slightly extends the system operational range, although can not solve the strategy limits.

9.1.4. Optimal flow stability scenarios

In the following tables are reported the optimal gas flow rate and rated pressure difference for each scenario. Such analysis has not been performed for the MPP +GL scenario in which both optimal rated pressure boost and gas flow rate change simultaneously. However, an overall and rough rule can be followed in order to find the best system solution: slugging occurs due to the liquid inability to climb up the riser pushed by buoyancy forces, thus a minimum kinetic energy is required at the beginning of the riser. For the analyzed system, the kinetic energy can be raised by promoting the flow rate (thus pump rated pressure difference and gas lift flow rate). If the system has each wellhead valve choked, the only way to avoid slugging is to reduce the rated pump pressure difference (which just compresses the fluid) and increase the gas flow rate.

		GL [MMscf/d]
I year	Steady state	20+
	Turn down I well	20+
	II well	10÷15
III year	Steady state	10÷15
	Turn down I well	10÷15
	II well	10÷15
IX year	Steady state	10÷15
	Turn down I well	10÷15
	II well	10÷15

Tab.23: Optimal gas injection rate per scenario.

			MPP [bar]	
			Riser	Manifold
I year	Steady state		90+	90+
	Turn down	I well		
		II well		
III year	Steady state		90+	90+
	Turn down	I well	90+	60÷90
		II well		
IX year	Steady state		60÷90	60÷90
	Turn down	I well	60÷90	60÷90
		II well	60÷90	30÷60

Tab.24: Optimal rated differential pressure per scenario.

9.2. Oil Recovery Analysis

9.2.1. MPP

All the production strategies have been simulated under nominal operating conditions. However, steady state was not reached in all simulations, in which an average value over time has been determined and used in the comparison. The table below shows the oil flow rate at standard conditions, which is the parameter of main interest.

	QOst bbl/d					
location	Riser			Manifold		
rated Δp bar	30	60	90	30	60	90
I year	24717	26220	26053	25154	26134	26168
III year	15243	17311	18078	15703	18406	19496
IX year		3373	3487		3366	3454

Tab.25: Steady state standard oil flow rate with pump deployment

As can be easily observed, the produced oil decreases year by year, due to reservoir exploitation, and increases with the rated pump pressure difference till a maximum is reached. When the pump provides a higher pressure boost, back pressure on wells decreases and wellhead pressure with it. When the wellhead pressure reaches its minimum nominal value, a wellhead located throttle valve is activated and keeps the pressure equal to the fixed one. Thus, a further back pressure decrease is hampered by the valve. The graphs below show the GVF and pressure trends for both pump locations. As can be noticed, the riser outlet pressure is steady, indeed it is a system requirement dictated by the downstream processing facility and the pressure built up profiles are obtained by adding back pressure from the pipe outlet to the pipe inlet.

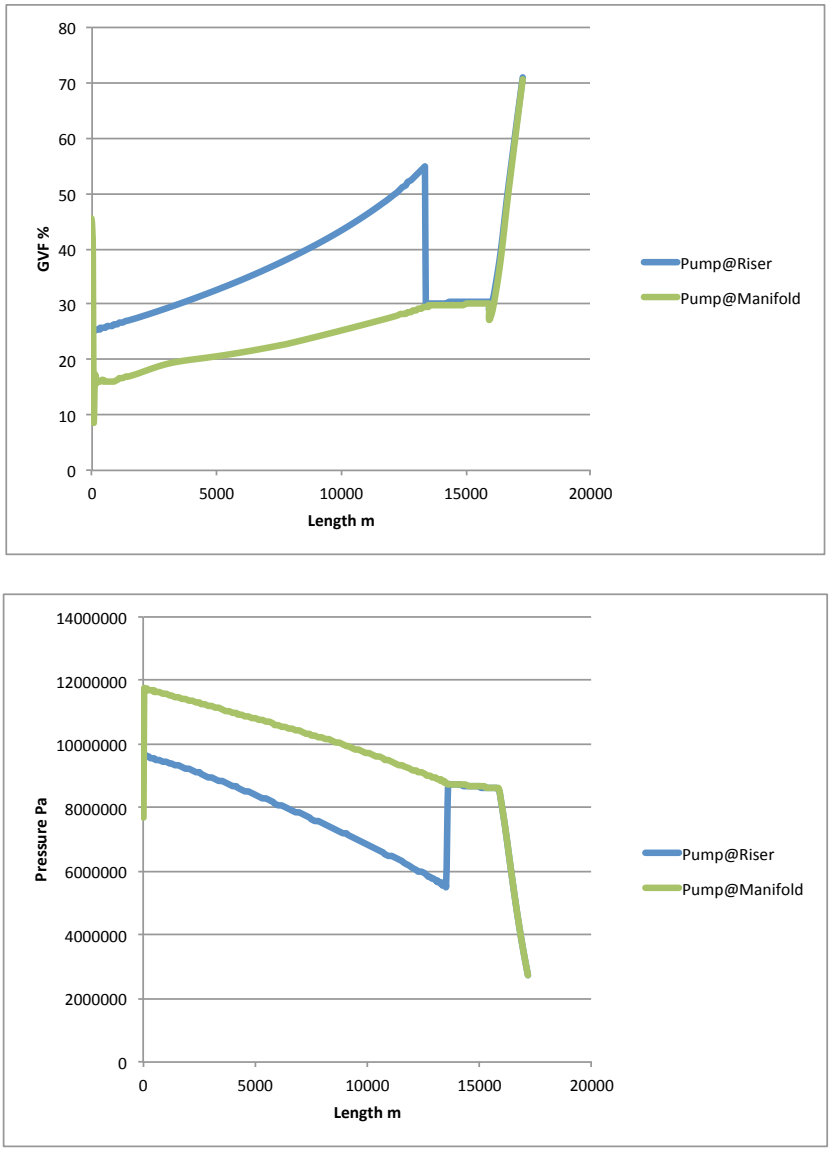

Chart 7: GVF and pressure profiles for both pump locations. (Rated differential pressure = 60 bar).

The manifold located pump shows to slightly produce more oil under the same pressure difference than the riser located one. Indeed, deploying the pump at riser base, the conveyed fluid travels along the main flowline at lower pressure, thus higher GVF, which means more frictional losses; if the pump is manifold located, the fluid is conveyed at higher pressure and at low GVF. Frictional losses increase the backpressure on the wells, thus reduce the field productivity. The table below shows the frictional losses occurring along the main producing flowline respectively with the pump located at riser base and at manifold, under 60 bar of rated pressure increase. Displacing the pump from riser base to manifold, it is possible to reduce the back pressure on wells of 11 bars.

Pump Δp rated	Δp @Riser	Δp @Manifold	Δ(Δp)
60 [bar]	41,8	29,9	11,8

Tab.26: Flowline frictional losses for both pump locations. (Rated differential pressure = 60 bar)

Although the manifold located pump shows such benefit, the riser located pump is able to overwhelm the frictional losses by increasing the rated pressure difference. This can be achieved only in the first and in the last year, while in the third one only the manifold located one provides the production peak.

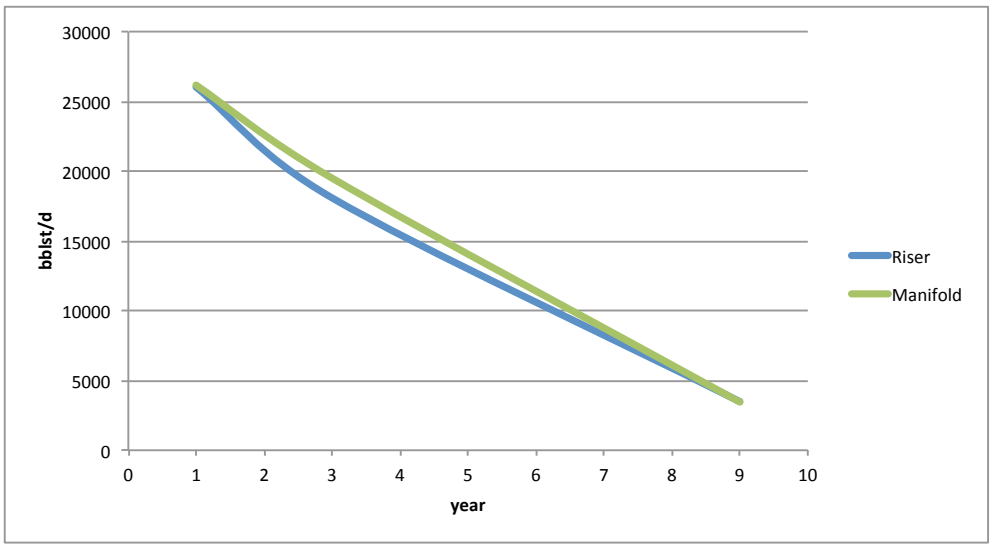

Chart 8: Steady state maximum standard oil flow rate with pump deployment

9.2.2. GL

In the following graphs GVF and pressure are plotted against the pipe length for the following producing scenarios:

- First year, MPP 60 bar rated and located at riser base
- First year, MPP 60 bar rated and located at manifold
- First year, gas injection of 15 MMscf/d at riser base

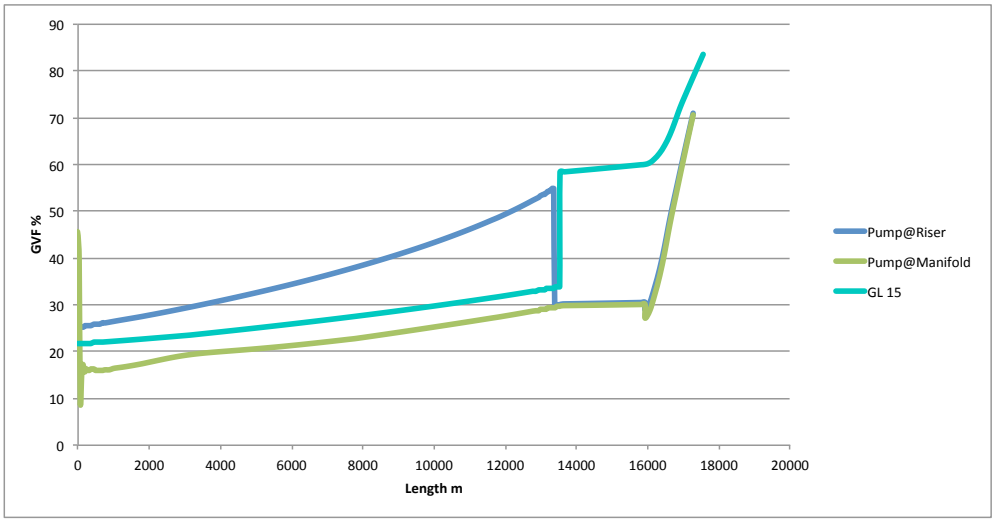

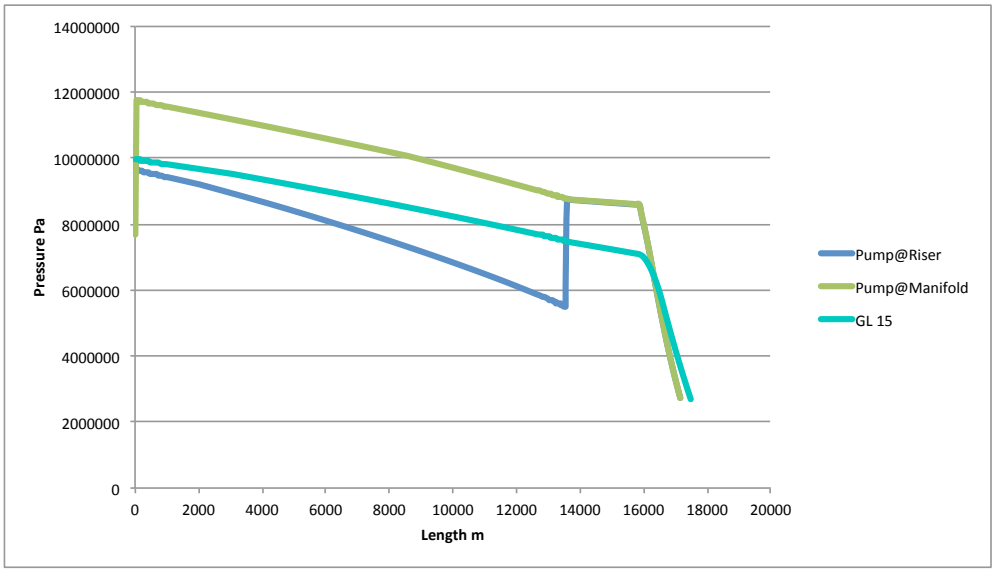

Chart 9: GVF and pressure profiles for both pump locations (Rated differential pressure = 60 bar) and gas lift (injected gas flow rate = 15 MMscf/d).

The second graph shows that the geodetic pressure increase across the riser is the same for both pump's scenarios, while is sensibly lower in the GL one. This is simply due to the enlighten of the fluid column in the riser, thanks to the gas injection. The following table resumes the average oil flow rates for each year and gas flow rate.

	Qost bblst/d		
	GL MMscf/d		
	10	15	20
I year	22869	23247	23425
III year	2287	3288	4789
IX year	1061	3253	3290

Tab.27: Standard oil flow rates during gas lift steady state operation.

9.2.3. MPP+GL

This combined production strategy was expected to have the best performances among all. However, the gas flow rate was chosen to optimally exploit the field during the first year, although during the following years it resulted over-dimensioned. Indeed, water cut increases year by year and the OLGA pump, which simulates a rotodynamic pump, becomes more effective due to higher inlet densities. Thus, because of the pump is decreasing backpressure on the wells more than in the first year, the required gas flow rate is sensibly lower. Most of the wells are operating below their BHFP (bottom hole flowing pressure) and are choked by the wellhead throttle valve.

QOst bbl/d					
Riser			Manifold		
30	60	90	30	60	90
25010	26239	26549	26440	26543	
3903	5530	4871	4022	4189	4272
	2918		3124	2723	

Tab.28: Standard oil flow rates during pump and gas lift steady state operation.

From an oil recovery analysis point of view, the pump location does not affect the system performances.

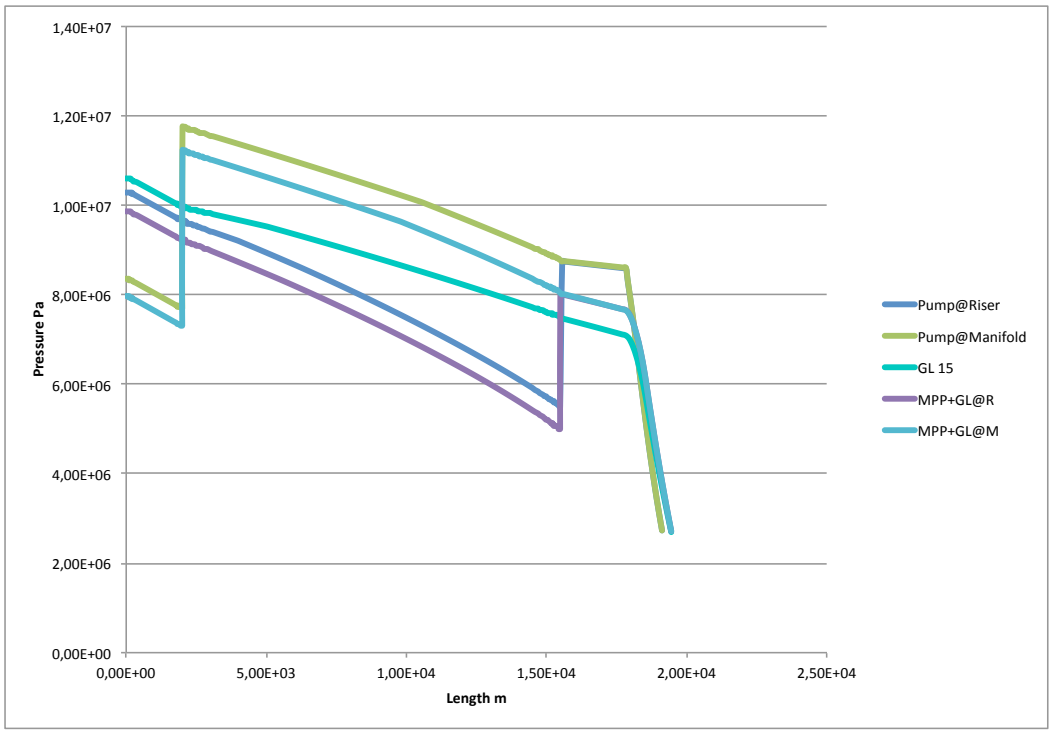

Chart 10: GVF and pressure profiles for both pump locations (Rated differential pressure = 60 bar), gas lift (injected gas flow rate = 15 MMscf/d) and pump-gas lift coupling (Rated differential pressure = 60 bar and injected gas flow rate = 10 MMscf/d).

9.2.4. Single well analysis

The analyzed system has very complex hydraulic behavior, which cannot be easily summed up. Indeed, each well has a different reservoir energy and can overwhelm the others and reduce the overall oil production: throttle valves prevent the weaker wells from inflow by choking the stream. The maximum production flow rate is obtained when a compromise, between choking the stronger and enhancing the weaker wells, is reached. Such phenomena can be observed when both artificial lift methods are active and back pressure is excessively drawn down. The wellhead valves choke the weaker wells completely avoiding fluid inflow.

		MPP Riser			MPP Manifold		
Δp rated [bar]		30	60	90	30	60	90
MP4	I year	22	22	22	22	22	22
	III year	24	24	24	24	24	24
	IX year	0	0	0	0	0	0
MP2	I year	11	11	11	11	11	11
	III year	5	8	9	5	11	15
	IX year	-2	10	10	-4	10	10
MP1	I year	9	9	11	10	10	11
	III year	5	5	11	6	6	17
	IX year	14	14	23	10	10	23
M1R	I year	5	5	5	5	5	6
	III year	7	8	8	7	8	8
	IX year	6	6	6	5	6	6

*Tab.29: Wells multiphase mass flow rates [kg/s] in MPP strategy. *Grey: slugging operation.*

		GL		
flow rate MMscf/d		10	15	20
MP4	I year	4	5	4
	III year	8	17	17
	IX year	4	22	22
MP2	I year	5	5	5
	III year	7	8	8
	IX year	5	6	6
MP1	I year	11	11	11
	III year	0	0	0
	IX year	11	11	0
M1R	I year	22	22	22
	III year	0	0	0
	IX year	22	0	0

*Tab.30: Wells multiphase mass flow rates [kg/s] in GL strategy. *Grey: slugging operation.*

		MPP+GL Riser			MPP+GL Manifold		
Δp rated [bar]		30	60	90	30	60	90
MP4	I year	8	17	17	8	17	17
	III year	8	17	17	8	17	17
	IX year	8	17	17	8	17	17
MP2	I year	7	8	8	7	8	8
	III year	7	8	8	7	8	8
	IX year	7	8	8	7	8	8
MP1	I year	0	0	0	0	0	0
	III year	0	0	0	0	0	0
	IX year	0	0	0	0	0	0
M1R	I year	0	0	0	0	0	0
	III year	0	0	0	0	0	0
	IX year	0	0	0	0	0	0

*Tab.31: Wells multiphase mass flow rates [kg/s] in MPP+GL strategy. *Grey: slugging operation.*

9.2.5. Oil recovery analysis: strategies comparison

Since the very first year, multiphase pump deployment has demonstrated to decisively promote oil recovery. Indeed, gas injection has really lower oil flow rates all over the time, especially during the third year, and its coupling with the pump has shown to be wasteful.

9.3. Thermal analysis

9.3.1. Shutdown operations

When a shutdown is performed the pressure distribution changes quite quickly from a dynamic profile (pump boost and friction losses) to a static one, which is univocally determined by flowline geometry and fluid density.

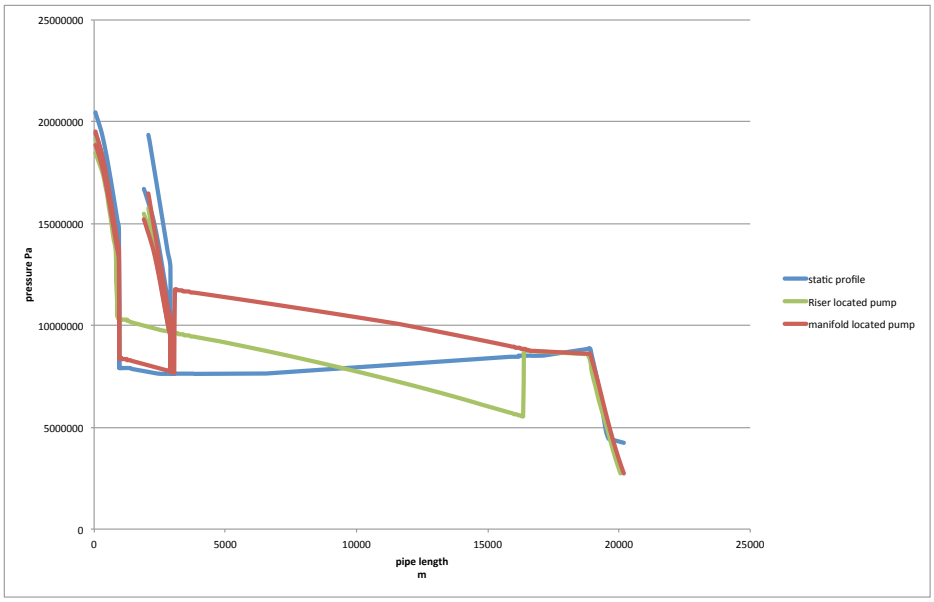

Chart 11: Pressure profile along flowline length during nominal operating conditions (dynamic pressure profile) and after a shutdown(static pressure profile).

On the other hand, temperature profiles change slower due to heat exchange with the external environment. Operators have limited amount of time to diagnostic any possible failure or problem and to take any initiative, due to hydrate formation, which can lead to solid plug formation. Before hydrate formation temperature is reached, the system should be either restarted or preserved. The time the system takes to reach the hydrate formation temperature (plus 3°C for conservative issues) is defined cool down time and represents a temporal limit for operators to take action. Common field practice foresees a first period for failures or problems detection and trouble shooting, which lasts between two and four hours. Then the system could be restarted or preserved, starting from the most critical components. Jumpers and the tubing upper parts are displaced with methanol for a period from two to four hours; such period is known as light touch time and is influenced by the number of wells and chemical injection philosophy. The service line of the analyzed system is able to convey 25 m^3/h of methanol, thus the tubings and jumpers (either wellhead located either pump located) fluid displacement should take 2 hours and 13 minutes. Eventually, the flowline is flushed with non-hydrate forming fluid, such as Diesel; this operation, known as system preservation, should avoid solid formation under an unlimited period of time. The time required to flush the entire flowline is obtained by dividing the

flowline length by an estimated average Diesel velocity of 2 m/s and multiplying by a conservative factor of 1,5, which takes into account mixing effects due to turbulences occurring in the pipe. The following table resumes the system specifications for shutdown operations. Two different minimum required cool down times have been highlighted because jumpers and rigid flowlines have very different Uvalue and thermal behavior.

no touch time	4	h
light touch time	2,21	h
preservation time	2,56	h
minimum cool down time for jumpers and tubing topsides	6,21	h
minimum cool down time for complete preservation	8,76	h

Tab.32: Critical times for operators promptness.

9.3.2. Hydrates formation curves

Hydrates existence envelopes have been generated using HYSYS and PVTsim only for the vapor phase. Vapor composition has been obtained through a flash simulation of the produced fluid at 30°C at different pressures. Then, each composition has been saturated with water and given as input to PVTsim, which produces the hydrates existence envelopes. The following graph shows the hydrates formation temperature as a function of pressure and flash pressure.

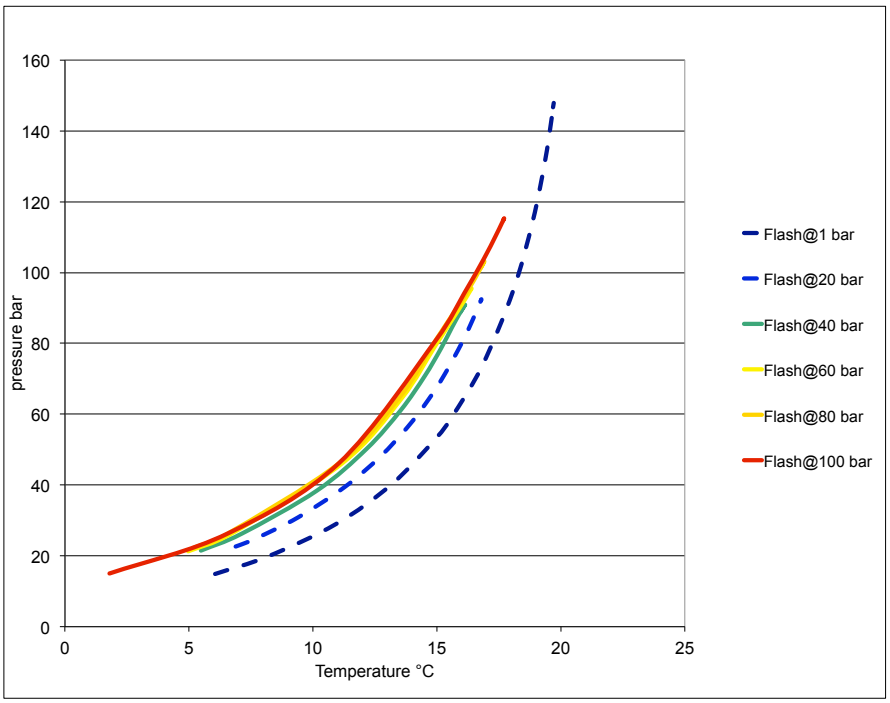

Chart 12: Hydrate formation envelopes for different gas compositions (lower flash pressures lead to heavier components in the vapor phase).

Flash pressure only affects the mixture composition: lower pressures mean heavier components in the gas mixture. As can be noticed from the plot, the hydrates existence field is not affected by the flash pressure when is performed above 40 bar. Such statement allows to make an extremely useful simplification: because points of greatest interest for flow assurance issues lay between 80 and 150 bar of static pressure, gas composition can be considered steady along the pipeline. Pressure profile is univocally related to geometry, thus it is possible to merge pressure-geometry and hydrate formation temperature-pressure relationships to build up a hydrate formation temperature-geometry one.

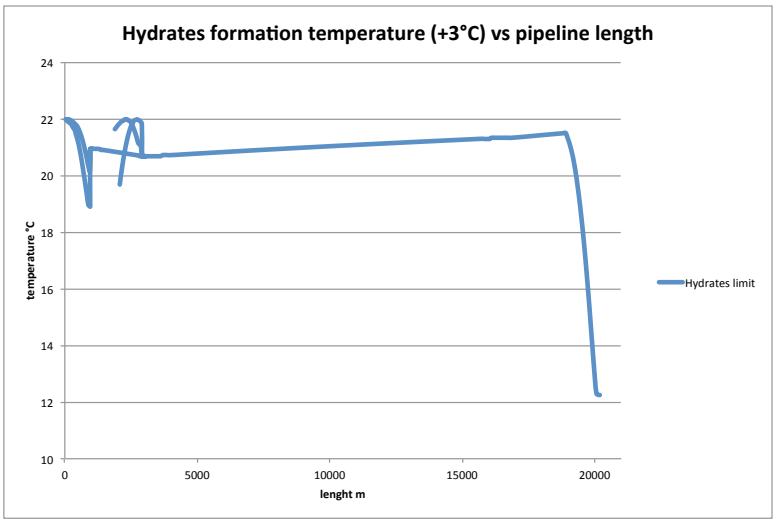

Chart 13: Hydrate formation temperature plotted against system geometry.

Such temperature profile is very useful because allows to find out easily and univocally the most critical points during shutdown conditions at each pipeline position, although in multiphase conditions none algorithm is able to predict the hydrates existence field properly. A further uncertainty cause is represented by operators promptness to react and face an unforeseen failure shutdown. Thus, two conservative decisions have been taken:

- Increase the hydrate formation temperature by means of a conservative factor of 3°C;
- Besides the hydrate formation curve determined at the system real pressure flash, the 1 bar envelope is also plotted against the geometry. This allows to further reduce the risk of wrong correlation predictions. The area encompassed between the two hydrate curves represents somehow the correlation uncertainty.

Two different available cool down times have been measured:

- Available cool down time at wellhead jumpers (ATW);

- Available cool down time at riser base jumpers (ATR).

This separation is necessary because the most threatened part of the system varies with the production strategy. For instance, when production is prompted by gas injection, the injection point will reach the hydrate formation temperature quicker; while if the multiphase pump is deployed at riser base, the most threatened part will probably be before the pump section (in fact, the pump provides also heat to stream).

9.3.3. MPP

Under steady state conditions, the pump provides heat to the main stream due to losses occurring in the pump itself. This represents a great advantage in subsea applications, where low temperature environments are widespread. The following picture shows the temperature along the main producing line and along the riser during steady state operation.

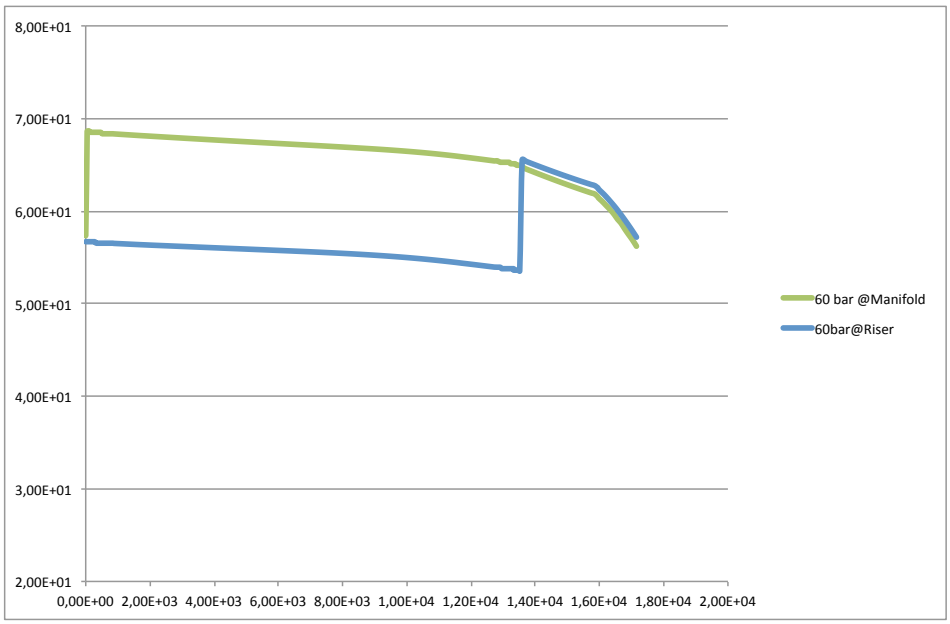

Chart 14: Steady state temperature profiles for both pump locations (rated differential pressure= 60 bar).

The manifold located pump ensures that the main flow line is kept at higher temperature, while the riser located scenario slightly provides a higher temperature increase, due to higher pump inlet GVF, thus more gas to be compressed. Another important difference is that, locating the pump at manifold, the GVF strongly decreases. Liquid has much higher heat capacity and increases the cool down time. In the figures below, temperature profiles are plotted against pipe length for different times during a shutdown.

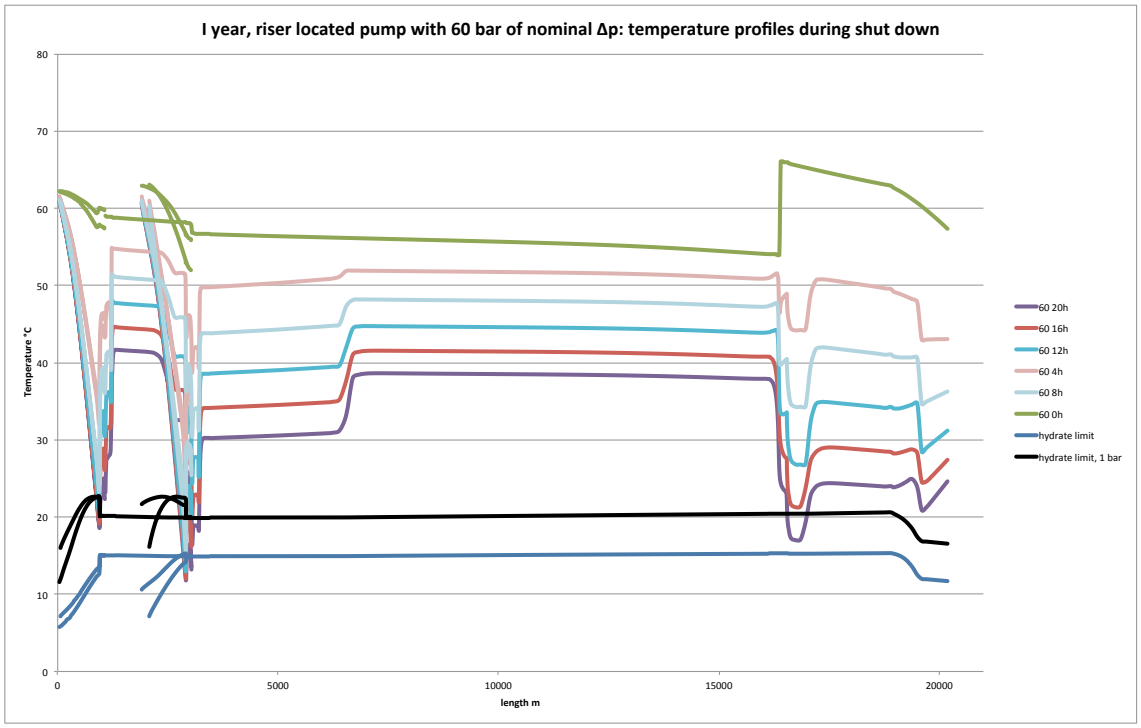

Chart 15: Temperature profiles and hydrate formation temperature during a shutdown. (I year, riser located pump with 60 bar of rated differential pressure).

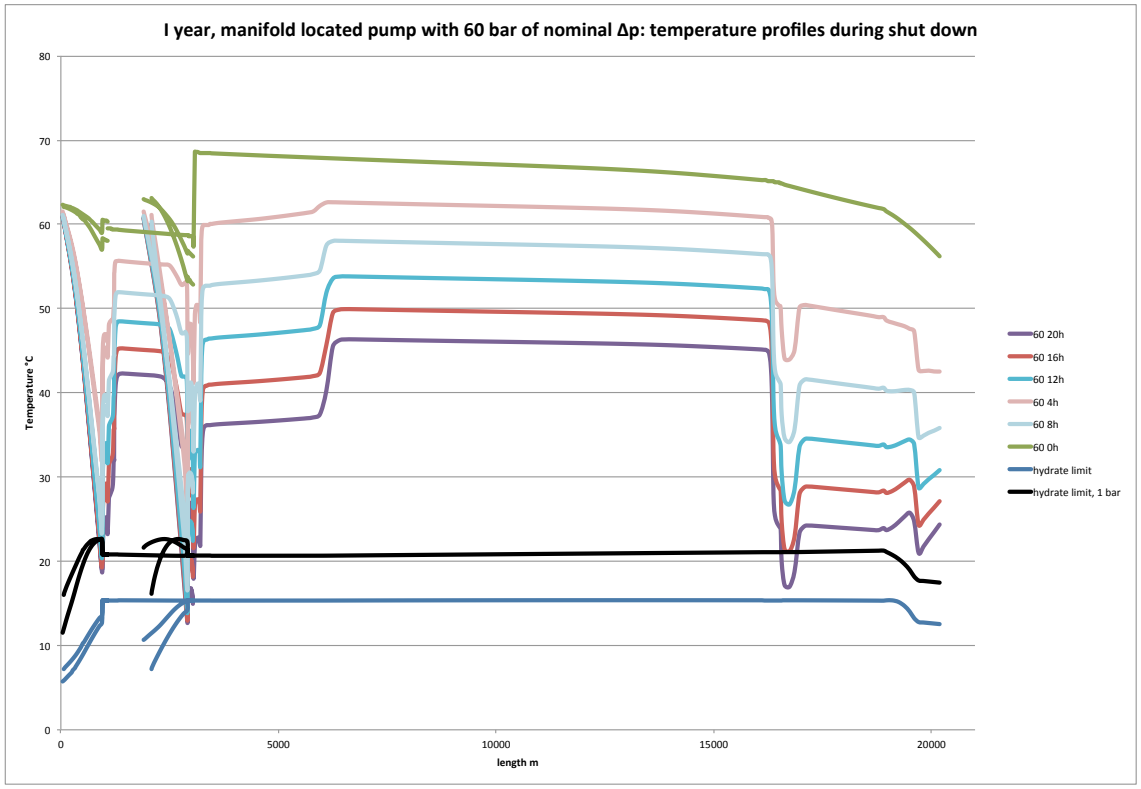

Chart 16: Temperature profiles and hydrate formation temperature during a shutdown. (I year, manifold located pump with 60 bar of rated differential pressure).

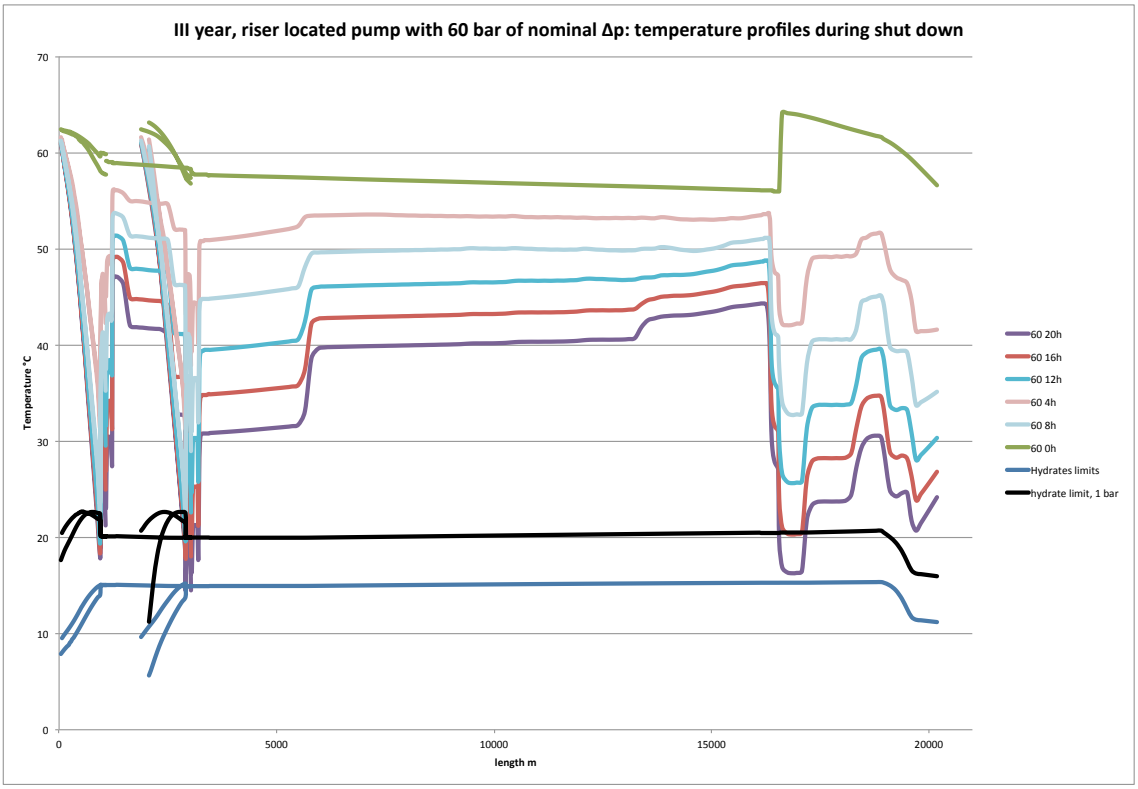

Chart 17: Temperature profiles and hydrate formation temperature during a shutdown. (III year, riser located pump with 60 bar of rated differential pressure).

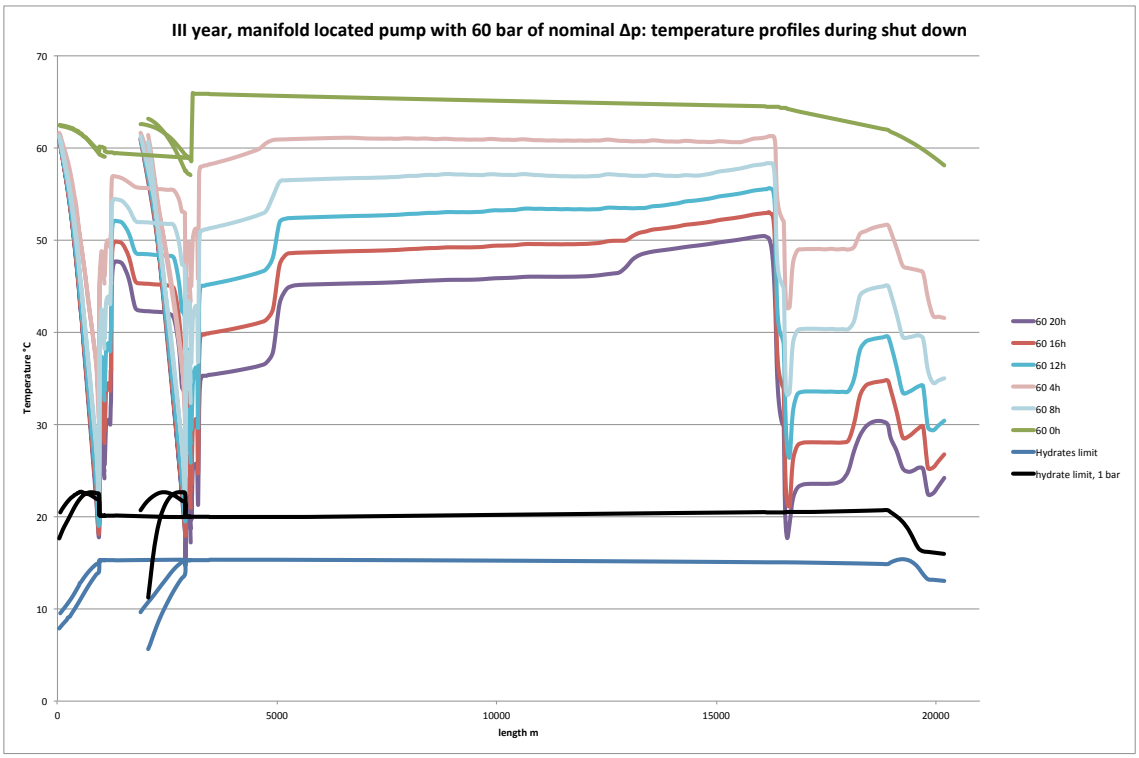

Chart 18: Temperature profiles and hydrate formation temperature during a shutdown. (III year, manifold located pump with 60 bar of rated differential pressure).

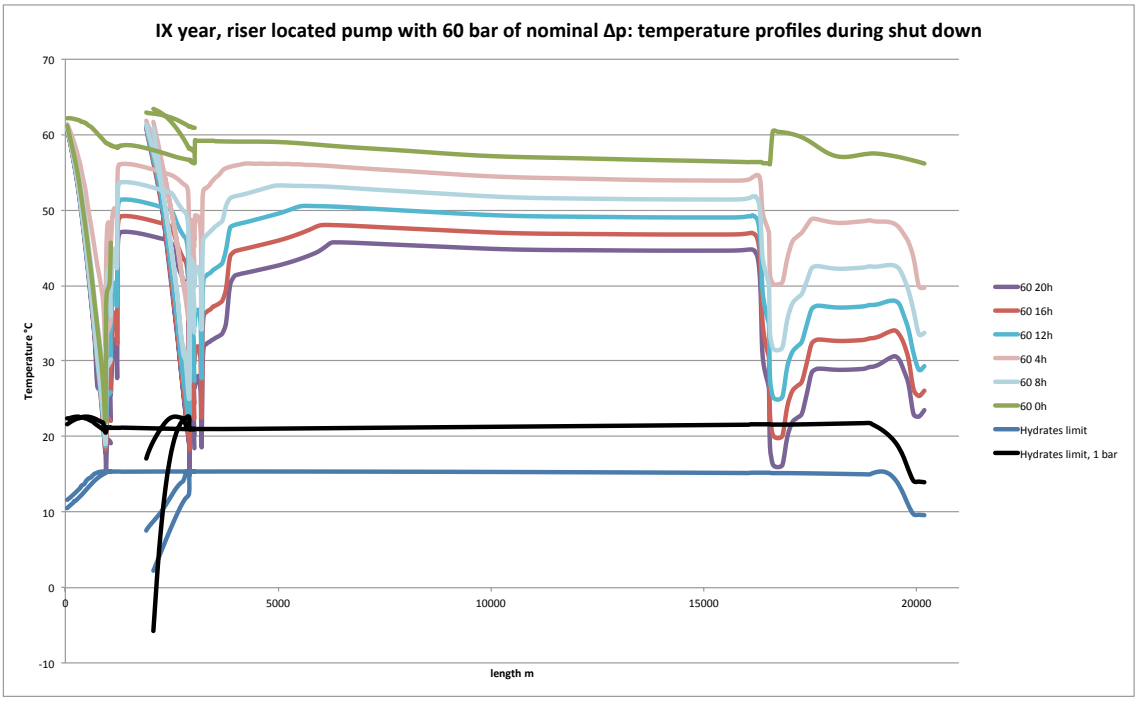

Chart 19: Temperature profiles and hydrate formation temperature during a shutdown. (IX year, riser located pump with 60 bar of rated differential pressure).

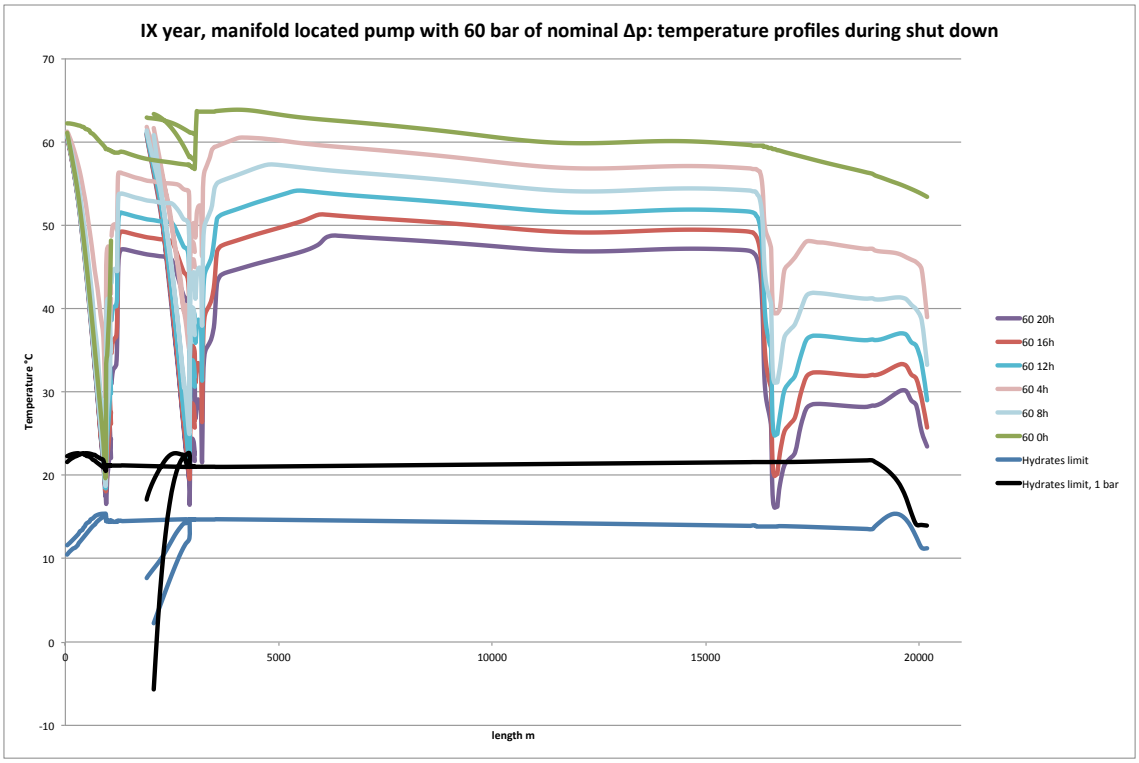

Chart 20: Temperature profiles and hydrate formation temperature during a shutdown. (IX year, manifold located pump with 60 bar of rated differential pressure).

Temperatures sharply drop where gas accumulates:

- Jumpers at riser base;
- Jumpers at manifold;
- Tubing topsides.

During shutdown conditions the most threatened section appeared to be at wellhead jumpers, where gas accumulates due to buoyancy effects and pipe geometry. Graphs also show hydrate limit (hydrate formation temperature plus 3°C for conservative issues) and hydrate limit at 1 bar (flash is performed at one bar). Thanks to higher water content, ATW increases during field exploitation, while contrary to what expected, ATR reduces with field life, even if the produced fluid has a higher heat capacity. While the fluid cools slower, the hydrate formation temperature steps up due to higher static pressure: the increased amount of water increases the geodetic pressure difference across the riser, raising the hydrate formation temperature of some Celsius degrees and neutralizing the larger heat capacity effect.

The manifold located pump scenario shows to have higher flow line temperatures, but lower ones at riser base jumpers. Although, keeping the line at higher pressures, gas amount is considerably lower and the system has higher heat capacity. The tables below show respectively the ATR and ATW for both pump scenarios after a shutdown from nominal and turndown operating conditions. The graphed value refers to the available cool down time when hydrate formation temperature is obtained flashing the fluid at 1 bar. This value is always lower due to higher concentration of lighter components.

		MPP: minimum cool down time (h) for riser base jumpers					
	Position	Riser			Manifold		
	bar	30	60	90	30	60	90
I year	Steady state	20(14)	20+(17)	20+(18)	20+(15)	20+(17)	20+(18)
	Turn down I well						
	II well						
III year	Steady state		20+(16)	20+(17)	20(15)	20+(17)	20+(18)
	Turn down I well		20+(15)	20+(18)		20+(17)	20+(18)
	II well						
IX year	Steady state		20(14,5)		20 (14)	20 (15)	20+(16)
	Turn down I well		20 (15)	20 (15)		20+(16)	20+(17)
	II well		20(15)	20+(16)		20+(16)	20+(17)

Tab.33: Riser base cool down times (those obtained considering the 1 bar hydrate formation temperature are reported in brackets) in the MPP strategy.

		MPP: minimum cool down time (h) for well head jumpers					
	Position	Riser			Manifold		
	bar	30	60	90	30	60	90
I year	Steady state	9(5)	9(6)	9(7)	6,5(4)	10(7)	9,5(6)
	Turn down I well						
	II well						
III year	Steady state		20(6)	19(8)	20(7)	20(8)	20(9)
	Turn down I well		20+(8)	20+(9)		20(8)	20+(8)
	II well						
IX year	Steady state		20(11)		20+(10)	20+(11)	20+(9,5)
	Turn down I well		20+(11)	20+(11)		20+(11)	20+(12)
	II well		20+(10)	20+(11)		20+(10)	20+(10)

Tab.34: Jumper base cool down times (those obtained considering the 1 bar hydrate formation temperature are reported in brackets) in the MPP strategy.

Shutdowns from turndown conditions were expected to be more challenging due to lower flow rates during steady state conditions, thus lower heat capacity. Results show astonishing long cool down times during turndown conditions. Such unexpected outcome is due to a profile temperature increase during steady state conditions. When stronger wells are closed (which are farther than weaker ones), backpressure sensibly decreases on weaker wells. The produced fluid crosses faster the tubing than in nominal conditions and has to travel a shorter distance to reach the manifold. As a result, the fluid reaches the manifold at higher temperature and travels warmer. This surprising outcome is well explained in the following graph, where temperature is plotted against pipe length.

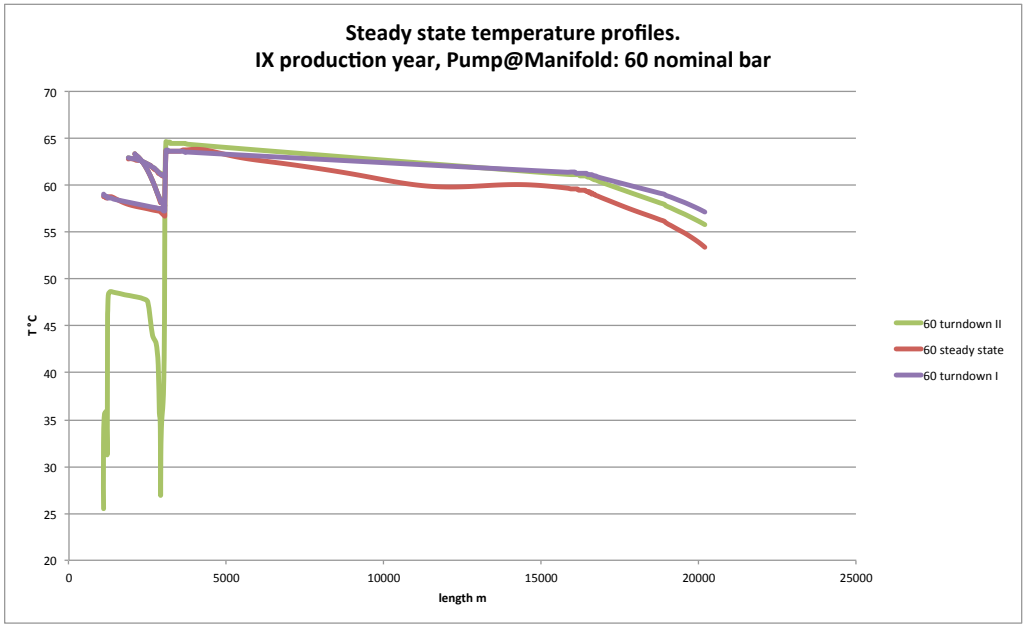

Chart 21:Temperature profiles during nominal, turndown I and turndown II operational conditions.

Some ATWs are sensibly lower than what expected (reported in red in the ATWs table). When nominal pressure difference is increased, longer ATWs are expected (due to higher flow rates); although, if backpressure is excessively reduced, wellhead valves choke the stream causing a temperature reduction (Joule-Thompson effect) at the downstream wellhead jumpers. Consequently, ATWs are sensibly reduced when wells are choked.

It is very important to highlight that if 1 bar hydrate curve is used to calculate ATWs, the available cool down time is sometimes lower than the required one (6,21h). This condition is particularly challenging during the first year, when both pump locations have one single available safe solution (90 bars at riser base and 60 at manifold).

9.3.4. GL

Gas injection occurs at -15°C and represents a further threat to hydrates formation by reducing the cool down time under shutdown conditions. The table below reports the temperature reduction occurring after gas injection.

	ΔT °C		
GL MMscf/d	10	15	20
I year	5,43	7,79	10,05
III year		8,54	11,63
IX year		7,14	6,91

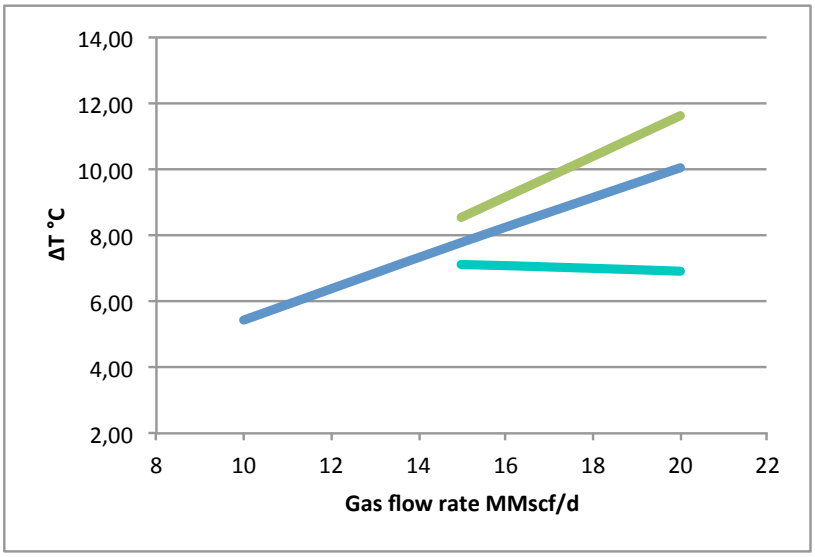

Tab.35: Temperature reductions due to cold gas injection at riser base.

As expected, increasing the amount of injected gas, the temperature decreases linearly. The year, in which the strongest temperature reduction has been observed, is the third one, when the water cut is still moderate and flow rates are

slightly lowers than the first year, meaning higher injected gas-produced oil ratios.

Besides the mixture temperature decrease, there is a further threat to hydrate formation when cold gas is injected at riser base: increasing the amount of gas in the mixture, the hydrate existence range widens to higher temperatures. The graph below shows the temperature profiles at 4 hours intervals after the shutdown and hydrate formation temperature. As soon as gas is injected, fluid temperature drops while hydrate forming temperature steps up.

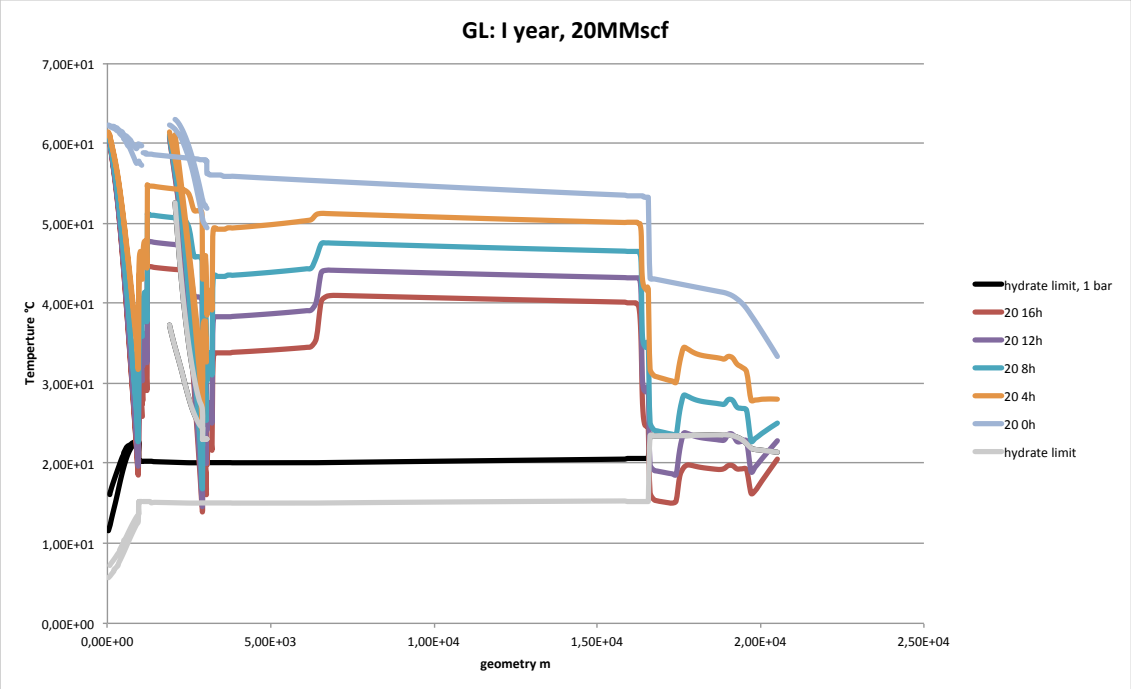

Chart 22: Temperature profiles and hydrate formation temperature during a shutdown. (I year, gas flow rate =20MMscf/d).

Shutdown simulations were performed only starting from stable flow conditions and cool available down times are reported in the table below. Bracketed values refer to ATWs calculated when 1 bar hydrate curve is used.

		Gas injection rate MMscf/d			
		10	15	20	
I year	Shutdown from ss	9,5	9	8	Available cooldown time (hours) at riser base jumpers
	Shutdown from td I	7			
	Shutdown from td II		2		
III year	Shutdown from ss	8	8	8	
	Shutdown from td I		8		
	Shutdown from td II		8		
IX year	Shutdown from ss		9		
	Shutdown from td I		10		
	Shutdown from td II		10		

Tab.36: Riser base available cool down times (those obtained considering the 1 bar hydrate formation temperature are reported in brackets) in the MPP strategy.

		Gas injection rate MMscf/d			
		10	15	20	
I year	Shutdown from ss	12(7)	12(7)	12(7)	Available cooldown time (hours) for wellhead jumpers
	Shutdown from td I	12(7)			
	Shutdown from td II		12(7)		
III year	Shutdown from ss	12(7)	12(7)	12(7)	
	Shutdown from td I		12(7)		
	Shutdown from td II		12(7)		
IX year	Shutdown from ss		12(7,5)		
	Shutdown from td I		12(7,5)		
	Shutdown from td II		12(7,5)		

Tab.37: Jumper available cool down times (those obtained considering the 1 bar hydrate formation temperature are reported in brackets) in the MPP strategy.

As expected, ATRs decrease with gas injection rates, while ATWs remain almost steady. While ATWs have been calculated with two different hydrate curves, ATRs have been determined using the gas lift hydrate curve. For such reason, depending on which hydrate curve is used in determining ATWs, it is possible to individuate the most threatened section. It is possible to conclude that both sections are equally exposed to hydrate formation. If ATWs are determined with 1 bar hydrate curve, all flow conditions are borderline (available cool down time slightly longer than required one), thus caution must be always kept.

Concerning riser base section, during the first year shutdowns from turndown sharply reduces the cool down time from 9,5 to 7 and 2 hours respectively, which is not acceptable. Unexpected results come from the third and ninth years, where no difference can be appreciated between shutdowns from nominal conditions, turndown I and turndown II; due to excessively low backpressure, all wellhead valves are choked to ensure nominal flow rate to the processing facility. When

one or two wells are shut down, others can increase their production, leading to the same overall flow rate. Therefore, the hydraulic conditions at riser base are roughly the same and the shutdown simulations lead to the same outcome. The following plot highlights the previous statement: temperature profiles exactly superpose each other.

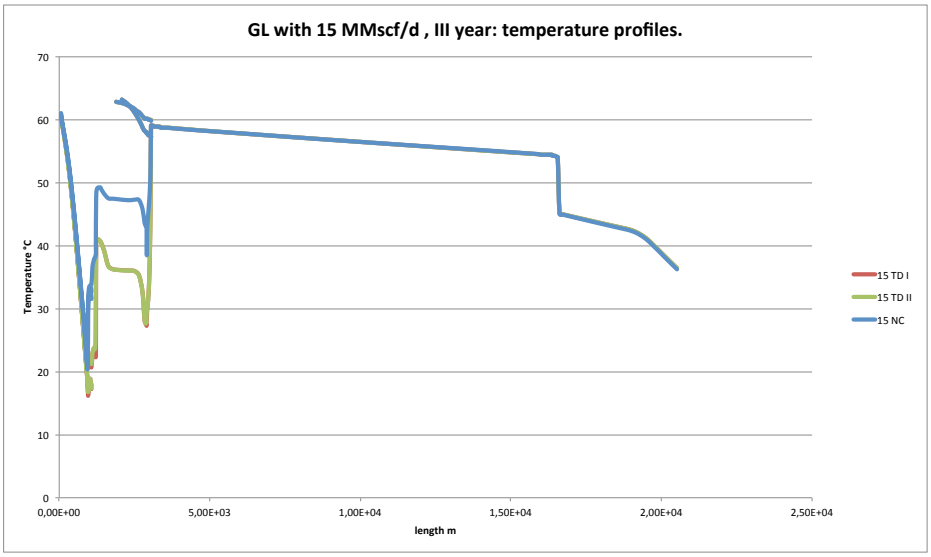

Chart 23: Temperature profiles during nominal, turndown I, turndown II operations (III year, gas injection rate: 15 MMscf/d)

The same situation occurs in the IX year, although in the nominal conditions scenario, the system cools faster than in turndown ones. In the following graph temperature profiles are plotted and superpose each others except after gas injection; no reason was found which could justify such asymmetry, although the small difference in temperature values (3,4%) could be neglected.

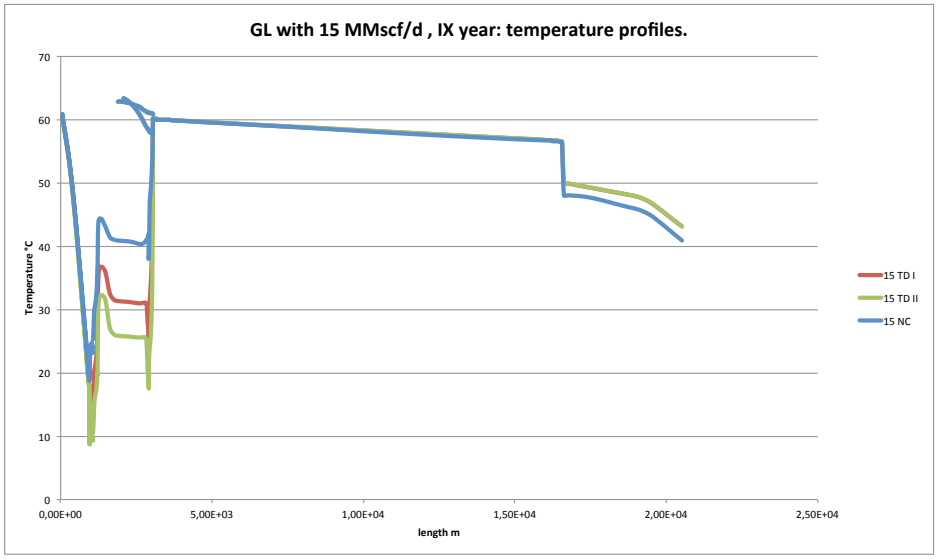

Chart 24: Temperature profiles during nominal, turndown I, turndown II operations (III year, gas injection rate: 15 MMscf/d).

9.3.5. MPP+GL

The MPP+GL scenario appears to be an intermediate solution between the MPP and GL ones. Indeed, while the pump supplies heat to the stream, the gas injection cools it down; this conflict is particularly evident when the pump is riser base located and a weird temperature peak is observed. The charts below display temperature profiles for both pump locations under a shutdown.

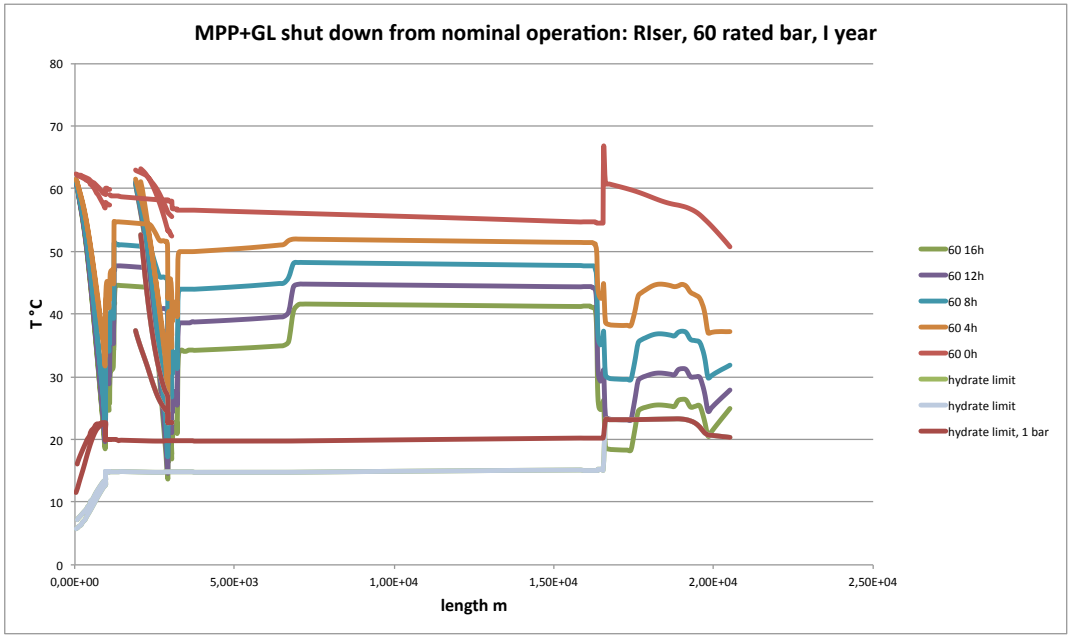

Chart 25: Temperature profiles and hydrate formation temperature during a shutdown. (I year, riser located pump with 60 bar of rated differential pressure and gas flow rate =5 MMscf/d).

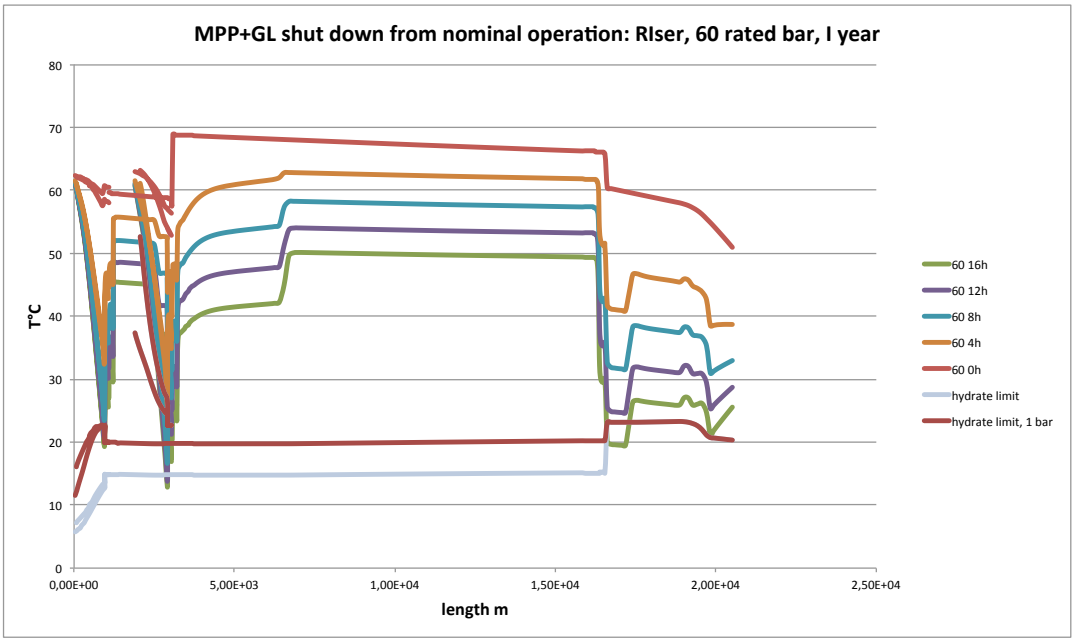

Chart 26:Temperature profiles and hydrate formation temperature during a shutdown. (I year, manifold located pump with 60 bar of rated differential pressure and gas flow rate =5 MMscf/d).

The pump location has not heavily affected the thermal behavior at riser base, indeed the fluid is more heated if compressed riser base, while it is less cooled if conveyed liquid, thus compressed at manifold. The table below demonstrates the former statement, showing that increasing the pump pressure difference, the ATR sensibly improves; ATWs are approximately steady and stricter than ATRs, particularly if 1 bar hydrate curve is used.

	Shutdown:MPP+GL cool down times(h) from nominal conditions					
Position	Riser			Manifold		
bar	30	60	90	30	60	90
Risebase jumpers	11	12	13	12,5	13	
Wellhead jumpers	12(7)	12(7)	12(7)	11,5(6,5)	11,5(6,5)	

Tab.38: Wellhead and riser base available cool down times.

9.3.6. Thermal analysis: strategies comparison

Gas injection badly affects the thermal behavior, by reducing the initial temperature, the fluid heat capacity and increasing the hydrate formation temperature. Gas injection can be joined by pump deployment, reducing the detrimental effects on the system. The best solution is achieved with the pump alone, although it is not able to cover all the producing conditions; indeed, during the first year, the pump cannot operate stably under turn down I and II. Sole GL allows stable flow under such conditions, during which extreme caution must be taken. An interesting outcome comes from the cool down time sensibility to hydrate formation temperature: a small increase in the hydrate formation temperature leads to a strong reduction in the available cool down time. This statement is simply determined by the energy conservation equation for the system:

$$\frac{\partial U}{\partial t} = -hS(T_s - T_w) \approx V\rho c_v \frac{\partial T_s}{\partial t}$$

Where

U= internal energy of the system

T_s= system temperature

T_w = water temperature

h= overall heat transfer coefficient

S= heat transfer surface

V= system volume

If a considerable amount of time has passed (i.e. 4 hours), it is possible to assume that fluid distribution along the system remains almost steady (phases stratified in accordance with buoyancy forces) and mixture phases simply depend on temperature. Considering a section of the analyzed system during a limited temperature range (from 1 to 5 °C), it is possible to neglect phase changes and assume h and c_v steady; thus it is possible to integrate the separated variables between two different hydrate formation temperatures and the respective available cool down times.

$$\frac{dT_s}{(T_s - T_w)} = -\frac{dt}{\frac{\rho c_v}{h}\frac{V}{S}}$$

$$\ln\left(\frac{(T_{s,hl} - T_w)}{(T_{s,hl,1bar} - T_w)}\right) = -\frac{(t_{hl} - t_{hl,1bar})}{\tau}$$

$$T_{s,hl} = T_w + (T_{s,hl,1bar} - T_w)e^{-\left(\frac{t_{hl} - t_{hl,1bar}}{\tau}\right)}$$

Where

$T_{s,\,hl}$ = system hydrate formation temperature + 3°C

$T_{s,\,hl,\,1\,bar}$ = system hydrate formation temperature (vapor composition at 1 bar flash) + 3°C

$t_{,\,hl}$ = available cool down time when $T_{s,\,hl}$ is chosen as limit temperature

$t_{,\,hl,\,1\,bar}$ = available cool down time when $T_{s,\,hl,\,1\,bar}$ is chosen as limit temperature

τ = system time constant

The previous formula demonstrates there is an exponential relationship between hydrate formation temperature and the available cooldown time. It is not in the interest of this dissertation to find out which is the law regulating heat transfer in the analyzed system, rather to point out and highlight the huge uncertainty which rules in the hydrate formation temperature prediction. This uncertainty spectrum affects the cool down time determination and is univocally amplified by the previous heat transfer law. It is reasonable, then, to take the most conservative measures to ensure the system safety and reliability.

9.4. Power Analysis

In order to deeply understand the very components, which underlie and influence the energetic system behavior, power analysis has been divided into two different sections:

- Shaft power analysis;
- Electrical power analysis.

The first section compares different technologies, whose power performances are affected just by thermodynamics and hydraulics. The second section takes into account the pump position and electrical losses along the umbilical system.

9.5. Shaft analysis

9.5.1. MPP

MPP shaft power increases with pump pressure difference, flow rate and inlet GVF. During the field life, water cut increases while oil production decreases. These two concurring effects determine a maximum shaft power point, which was observed during the third producing year.

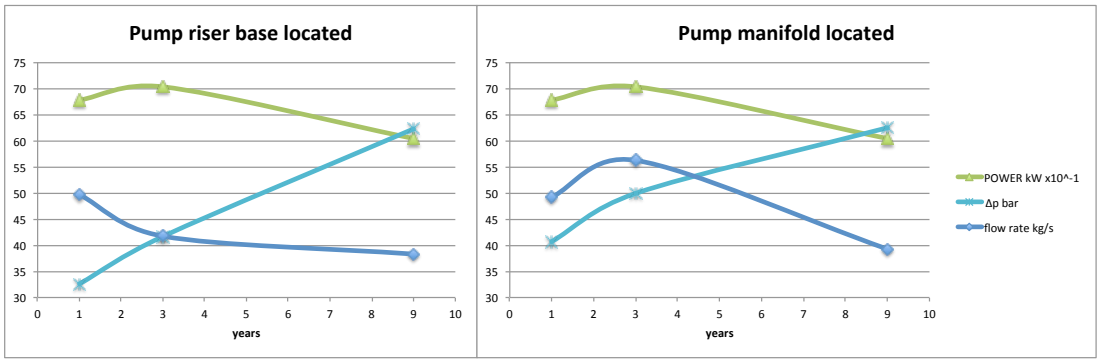

Chart 27: Pump power, differential pressure, flow rate for both pump locations.

Indeed, water phase increases the mixture density and OLGA pump model operates a constant head, therefore the pump produces more pressure boost increasing the inlet density ($\Delta p_{real} = H \times \rho_{avarage}$). Thus, the pump Δp has increased during the field life, while flow rate has sensibly decreased. The maximum power point is a compromise between the two trends.

For what concerns displacing the pump from riser base to the manifold, a shaft power reduction was expected. However, this was not observed during a first analysis, due to two different factors:

- OLGA pump model operates a constant head, therefore the pump produces more Δp increasing the inlet density ($\Delta p_{real} = H \times \rho_{avarage}$);

- When the pump is manifold located, the system produces more oil due to higher pump Δp and lower frictional losses across the pipeline.

Thus higher flow rates and Δp lead to higher pump requirements. The table below resumes the previous statement, showing the shaft power for each scenario, the real Δp and the specific work performed by the pump.

	Real Δp bar					
location	Riser			Manifold		
rated Δp	30	60	90	30	60	90
I year	19	33	42	23	41	56
III year	25	37	53	25	49	74
IX year	34	62	85	32	62	86

Tab.39: Effective differential pressure for both pump locations.

	Power kW					
location	Riser			Manifold		
rated Δp	30	60	90	30	60	90
I year	317	677	995	359	770	1404
III year	216	758	1086	279	903	1562
IX year	191	604	938	149	624	1404

Tab.40: Pump powers for both pump locations.(bold borders mean that one single pump is operating, while red cells underline that the pump is operating under slugging conditions).*

	Specific power kJ/kg					
location	Riser			Manifold		
rated Δp	30	60	90	30	60	90
I year	6,8	13,6	20,2	7,5	15,6	29,4
III year	6,7	13,5	21,9	6,2	17,0	24,3
IX year	9,8	15,8	23,8	12,5	13,6	20,2

Tab.41: Pump specific powers for both pump locations.(bold borders mean that one single pump is operating, while red cells underline that the pump is operating under slugging conditions).*

From these data would be naturally instinctive to prefer riser base as pump location. However, a further analysis has been performed forcing the pump to work under constant Δp with different inlet densities, as would occur if the pump was volumetric. For each producing year has been chosen an effective Δp, high enough to ensure flow stability and low enough to avoid wells from choking. The table below shows the pump operating conditions and performances in each of the three analyzed years.

year		I year		III year		IX year		
target Δp [bar]		30		50		62		
Location		Riser	Manifold	Riser	Manifold	Riser	Manifold	
Δp		29,85	30,18	50,05	49,92	62,25	62,47	bar
GT	in	49,1	52,3	50,8	56,2	38,3	39,3	kg/s
	out	49,1	52,3	50,8	56,2	38,5	39,4	
GVF	in	45,3	24,0	44,4	20,7	8,5	8,2	%
	out	28,9	13,0	18,5	6,3	1,2	1,2	
mixture density	in	479,9	642,4	508,8	707,9	882,9	884,3	kg/mc
	out	603,1	714,3	717,0	809,1	945,1	940,9	
Power		603,0	524,6	1027,0	933,0	604,0	623,5	kW
η_{vol}		72,0	67,1	67,9	63,5	60,9	62,0	%
N		1297	1115	1331	1196	1238	1272	rpm
η		47,7	46,0	43,1	43,3	42,0	42,8	%
Specific work		12,3	10,0	20,2	16,6	15,8	13,6	kJ/kg
increase[%] in specific work		22,3		21,9		15,6		%

Tab.42: Pump location comparison (shaft data) under same actual differential pressure.

The simulations outcomes are now in great agreement with previous expectations. Flow rate is higher when the pump is manifold located and the specific work lower. The last raw shows the percentage increase in specific work displacing the pump from manifold to riser base. Such parameter decreases with time, due to higher water fractions, thus lower inlet GVF differences between the two locations. Eventually, the energetic advantage of displacing the pump from riser base to manifold decreases with inlet GVF. In single phase liquid fields, no relative advantage can be appreciated due to pump displacing, while in gassy fields, pump location represents a key parameter for the system performance.

Pump efficiency has shown to be sensible to Δp, according to predictions; indeed, pump back-flow is pressure driven. A precious outcome is the positive effect that GVF has on the volumetric efficiency. Such behavior is due to two main factors:

- Lower mass density. Volumetric back-flow is mainly function of pressure difference and viscosity. Thus, lower overall mass density means lower mass-

$$\dot{m} = \rho \dot{Q}$$

backflow. The Martinelli-Lockhart correlation links frictional pressure losses in multiphase flow and volumetric flow rate. Such losses increases slightly with GVF.

Thus an increase of GVF could mean either a backflow reduction either growth, depending on the mixture properties behavior under different thermodynamic conditions. Indeed, if the viscosity growth effect overwhelms the density reduction and the Martinelli-Lockhart ones, pump performances decrease with GVF. For such reasons the use of empirical correlations for air-water mixtures cannot effectively predict the pump behavior with complex multiphase and multicomponent mixtures. The following table resumes the former statements, highlighting the relationship between pressure difference and efficiency.

	Efficiency %					
location	Riser			Manifold		
rated Δp	30	60	90	30	60	90
I year	49,8	47,4	45,7	47,0	43,4	39,2
III year	51,0	47,3	42,0	54,1	43,0	41,3
IX year	35,4	42,0	40,7	27.86	42,8	39,2

Tab.43: Pump locations efficiency comparison (bold borders mean that one single pump is operating, while red cells underline that the pump is operating under slugging conditions).

9.5.2. GL

GL shaft power requirements can be analyzed by indirect comparison. Indeed, the gas need to be compressed from the available pressure to 300 bar in order to be injected. Compressed gas is suctioned 90% from the HP separator at 20 bar and 10% from the LP one at atmospheric pressure. The following table reports the power requirements for each flow rate.

GL				
Gas flow rate	10	15	20	MMscf/d
Power	1420	2131	2841	kW

Tab.44: Gas compressors shaft powers in GL strategy.

9.5.3. MPP+GL

Coupling the multiphase pump with gas lift, the pump shaft power is expected to drop, although the gas compression work must be taken into account. The analysis has been performed only on the first producing year due to lack of stable flow conditions during the following ones and has been summarized in the table below.

	MPP+GL, location comparison						
Location	Riser			Manifold			
rated Δp	30	60	90	30	60	90	
effective Δp	18	30	39	22	39		bar
flow rate	45	46	47	48	48		kg/s
Power	312	642	957	353	710		kW
η_{vol}	75	74	75	69	64		%
N	1119	1375	1603	1012	1155		rpm
η	51	48	47	47	43		%
Specific Work	7	13	19	7	14		kJ/kg

Tab.45: Pump performances for both locations in MPP+GL strategy (I year)

Gas lift compression		
Gas flow rate	10	MMscf/d
Power	1420	kW

Tab.46: Gas compressors shaft power (MPP+GL strategy).

Same conclusions can be drawn as in the MPP scenario: indeed the pump displacement, from riser base to manifold, allows to increase oil recovery, by reducing back-pressure. Efficiency as well has shown to decrease with pump Δp and to increase with GVF, due to frictional losses rise (in the leakage paths) and fluid density reduction. Besides the pump power consumption, the gas compression must be taken into account, which is shown in table 46.

9.5.4. Shaft Power Analysis: Strategies comparison

The analysis has been performed by comparing the shaft specific work, the system requires to operate at nominal conditions. Specific work allows to estimate "pumping efficiency" under different flow rates. Indeed, any artificial lift method is performed in order to enhance the oil production and each scenario has a different flow rate. The following tables show the overall shaft specific work for each scenario (in MPP+GL pump and gas compressor shaft powers were summed up together).

	MPP: Specific work kJ/kg					
location	Riser			Manifold		
rated Δp	30	60	90	30	60	90
I year	7	14	20	7	16	29
III year	7	14	22	6	17	24
IX year	10	16	24	12	14	20

	GL: Specific work kJ/kg		
GL MMscf/d	10	15	20
I year	33	50	67
III year	101	88	118
IX year	33	75	100

	MPP+GL: Specific work kJ/kg					
location	Riser			Manifold		
rated Δp	30	60	90	30	60	90
I year	33	50	67	35	43	

Tab.47: Specific powers for each producing strategy.(bold borders mean that one single pump is operating, while red cells underline that the pump is operating under slugging conditions).*

First clashing result is the huge amount of energy required to lift up the fluid during the third and ninth year in GL strategy. This is due to lower production flow rate and steady gas injection one. GL appears to be the worst solution for prompting the production, from a shaft power analysis point of view. Indeed, power needs to be transmitted through the umbilical and is wasted within due to voltage losses.

Second unexpected outcome is substantial increase in specific shaft work when gas lift is coupled with the multiphase pump. Indeed, the system has a fixed discharge pressure (due to processing facility requirements) and gas injection decreases the pressure drop across the riser, thus all the subsea system operates at higher GVF. Increasing the GVF, the frictional losses as well as pump power surge.

All strategies share, as common feature, the specific work increase when artificial lift is further prompted. Indeed, increasing pump pressure boost or gas flow rate, system pressure decreases and GVF raises. Thus, a share of backpressure reduction is eaten by the frictional losses promotion. The following pictures show the frictional losses vs pump Δp for both pump locations. In the graphs are also reported the linearized trend lines, which highlight the friction losses increases due to a pump Δp promotion.

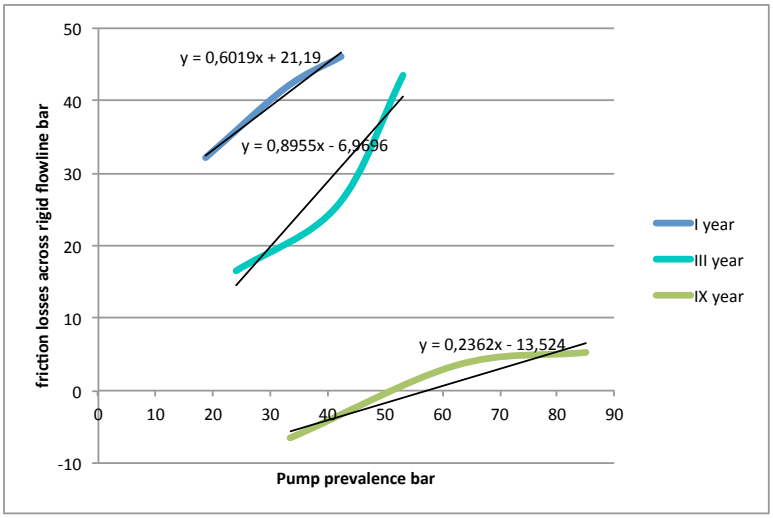

Chart 28: Frictional losses [bar] plotted against pump (riser base located) differential pressure.

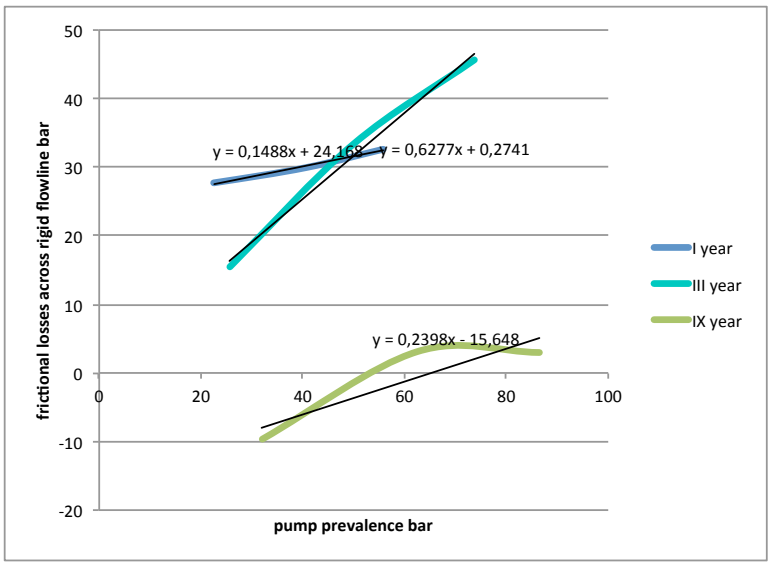

Chart 29: Frictional losses [bar] plotted against pump (manifold located) differential pressure.

When the pump is riser base located, 60% to 89% of additional Δp is converted into further frictional losses from the first to the third year. Then, GVF collapses and frictional losses drops as well. When the pump is manifold located, all the flow line is pressurized and "only" 14% to 63% of the pump Δp is converted into additional frictional losses.

In conclusion, multiphase pump deployment ensures the lowest shaft power consumption during all field life, especially when is manifold located. These results do not take into account electrical losses during power transmission. In the following sections an electrical power analysis is performed, finding out the best transmission solution for each production strategy. Then, comparisons are performed and conclusion drawn.

9.6. Electrical analysis

Manifold pump is farther than the riser one and farther more than the gas compression unit, which is located right on the FPSO. The previous analysis has shown that closer the boosting unit is to wells, lower is shaft power consumption. However power must be transmitted to the boosting unit and some is lost during this process.

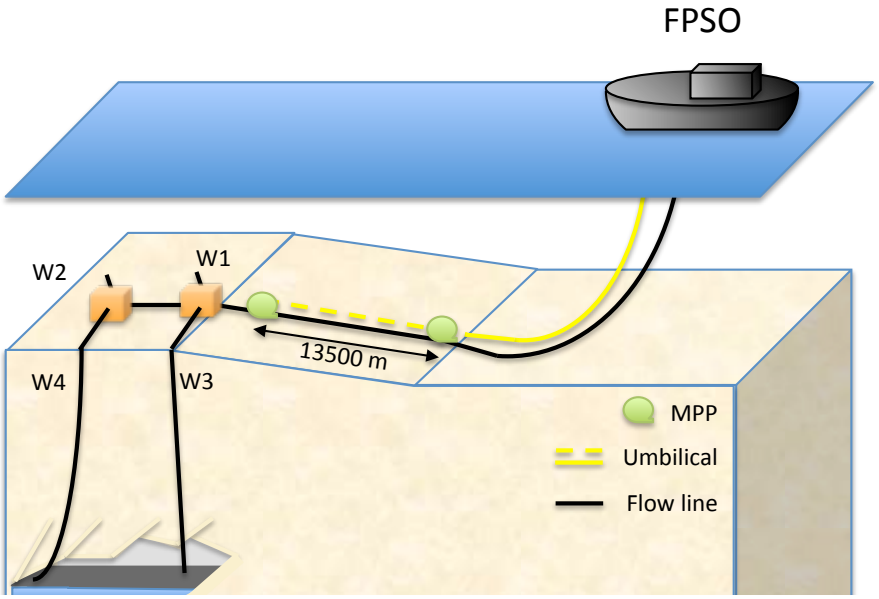

Fig.99: Pump displacement from riser base to manifold and further umbilical length.

9.6.1. Sensibility analysis to transmission parameters

There are different changeable parameters which strongly affect the power losses across the line. Therefore an earlier analysis must be performed to find and point out the electrical scheme which suites best each production strategy. Conductor diameter and arrival voltage strongly affect line losses, thus four different solutions have been studied for each pump location:

- Conductor cross section 120 mm^2 and 6 kV of arrival voltage;
- Conductor cross section 240 mm^2 and 6 kV of arrival voltage;
- Conductor cross section 120 mm^2 and step up to 11 kV of arrival voltage;
- Conductor cross section 240 mm^2 and step up to 11 kV of arrival voltage.

In the first two solutions, power is directly delivered at the pump voltage, while in the second ones, voltage is increased along the line by means of two transformers, which have an electrical efficiency of 96%. The subsea motor efficiency has been assumed equal to 90% and the gas compressor one equal to 95%; subsea pump power factor and the subsea frequency converter have

respectively been assumed equal to 0,85 and 95%. Transmission losses have been determined using power equations for a three-phase line shorter than 20 km (otherwise capacitor effects between the three conductors should have been considered):

$$\Delta P = i\Delta V$$

Where:

$$\Delta V = \sqrt{3}i\left(R\cos\varphi + Xsen\varphi\right)$$

$$R = \rho\frac{l}{S}$$

$$X = 2\pi f(4,606Log_{10}\frac{2D}{d} + 0,5)l \cdot 10^{-7}[\Omega]$$

R= electrical resistance,

φ = power factor

ρ = resistivity,

l = line length in m

S = cross sectional

D = conductor cables distance = d + 0,0656 [m]

d = conductor diameter [m]

f = frequency [Hz]

X = reactance [Ω]

The reactance calculation formula is determined by summing up together the magnetic fields of three wires with same electric current. The following table resumes the overall transmission efficiencies, for each solution and pump location.

		Electrical transmission efficiency								
year		I year			III year			IX year		
rated Δp [bar]		30	60	90	30	60	90	30	60	90
Riser	12,36mm 6kV	84,1	82,6	81,3	84,6	82,3	80,9	84,7	82,9	81,5
	17,48mm 6kV	84,5	83,4	82,4	84,8	83,1	82,1	84,9	83,6	82,6
	12,36mm 11kV	78,4	77,9	77,6	78,5	77,8	77,4	78,6	78,0	77,6
	17,48mm 11kV	78,5	78,2	77,9	78,6	78,1	77,8	78,6	78,2	77,9
Manifold	12,36mm 6kV	79,1	72,8	64,8	80,4	71,0	63,1	82,7	74,9	64,8
	17,48mm 6kV	80,7	75,9	69,4	81,7	74,4	68,0	83,4	77,5	69,4
	12,36mm 11kV	78,5	76,3	73,2	78,9	75,6	72,5	79,6	77,1	73,2
	17,48mm 11kV	77,4	75,8	73,5	77,7	75,3	73,0	78,2	76,4	73,5

Tab.48: Overall electrical transmission efficiencies for both pump locations and for each transmission strategy.

Transmission efficiency includes subsea motor, transformer, subsea converter and line voltage losses. It decreases when power surges, due to an electric current increase. Line losses depend on electric current by square relationship, thus when the pump shaft power is higher (during first years and higher pressure differences), transmission efficiency is lower. This behavior hinders and hampers further the manifold located pump, which already faces more electric losses due to longer tieback. Indeed, as seen in the previous chapter, the manifold located pump recovers more oil and requires higher shaft power. To such location, the power must be transmitted at higher voltage, in order to reduce the electric current, achieving two advantages: a stronger reduction in power losses across the line and a stabilization in transmission efficiency respect to shaft power. Indeed, when voltage is stepped up to 11 kV, line efficiency slightly depends on shaft power, due to higher voltages and lower current values. When the pump is riser base located, the optimal solution appeared to be without the voltage step up, which induces electrical losses within the transformers. Hence, two different electrical schemes have been chosen, depending on the pump location:

- Riser base: conductor cross section 120 mm^2 and 6 kV of arrival voltage;
- Manifold: conductor cross section 120 mm^2 and step up to 11 kV of arrival voltage.

The following tables show in detail power losses during transmission for the chosen conductor diameter and voltage. The first table concerns the riser base pump, while the second concerns the manifold one.

	I year			III year			IX year			
Δp_{rated}	30	60	90	30	60	90	30	60	90	bar
P_{shaft}	317	677	995	216	758	1086	191	604	938	kW
P_{motor}	352	752	1106	240	842	1207	212	671	1042	kW
P_{trasf}	371	792	1164	253	887	1270	223	706	1097	kW
V_a	6	6	6	6	6	6	6	6	6	kV
l	4000	4000	4000	4000	4000	4000	4000	4000	4000	m
A	120	120	120	120	120	120	120	120	120	mm^2
ΔV_{line}	99	211	310	67	236	338	59	188	292	Volt
ΔP_{line}	6	28	60	3	35	72	2	22	53	kW
η_{line}	0,98	0,97	0,95	0,99	0,96	0,95	0,99	0,97	0,95	-
$P_{line, in}$	377	820	1224	255	921	1342	226	729	1150	kW
η_{trasf}	1,00	1,00	1,00	1,00	1,00	1,00	1,00	1,00	1,00	-
P_{FPSO}	377	820	1224	255	921	1342	226	729	1150	KW
$\eta_{trasm\ el}$	0,84	0,83	0,81	0,85	0,82	0,81	0,85	0,83	0,82	-

Tab.49: Power losses during power transmission and pumping process (riser base).

	I year			III year			IX year			
Δp_{rated}	30	60	90	30	60	90	30	60	90	bar
P_{shaft}	359	770	1404	279	903	1562	149	624	1404	kW
P_{motor}	399	856	1560	309	1004	1736	166	693	1560	kW
P_{trasf}	437	938	1711	339	1100	1903	182	760	1711	kW
V_a	11	11	11	11	11	11	11	11	11	kV
l	17500	17500	17500	17500	17500	17500	17500	17500	17500	m
A	120	120	120	120	120	120	120	120	120	mm^2
ΔV_{line}	278	596	1086	215	699	1208	115	482	1086	Volt
ΔP_{line}	11	51	169	7	70	209	2	33	169	kW
η_{line}	0,98	0,95	0,91	0,98	0,94	0,90	0,99	0,96	0,91	-
$P_{line, in}$	448	989	1879	346	1170	2112	183	793	1879	kW
η_{trasf}	0,98	0,98	0,98	0,98	0,98	0,98	0,98	0,98	0,98	-
P_{FPSO}	458	1009	1918	353	1194	2155	187	809	1918	KW
$\eta_{trasm\ el}$	0,78	0,76	0,73	0,79	0,76	0,72	0,80	0,77	0,73	-

Tab.50: Power losses during power transmission and pumping process (manifold located pump).

Riser base location has higher transmission efficiencies, whereas the line efficiency is lower; indeed transformer losses, equal to 0,92, are liable for the efficiency difference during the transmission process between the two locations. The following chapter regards the energy analysis, or exergy analysis, for the considered production strategies.

9.6.2. Electrical power analysis

Using the method described in the previous paragraph, electrical powers, required to be produced by the FPSO power plant, have been calculated for the subsea pump and for the compression unit; furthermore, specific electric powers have been obtained by dividing power values by the produced fluid mass flow rate. The following tables illustrate the specific power values for each analyzed production strategy.

	MPP:Specific power@FPSO kJ/kg					
location	Riser			Manifold		
rated Δp	30	60	90	30	60	90
I year	8	17	25	10	20	40
III year	8	16	27	8	23	34
IX year	12	19	29	16	18	28

Tab.51: Specific electric powers for both pump locations.(bold borders mean that one single pump is operating, while red cells underline that the pump is operating under slugging conditions)..*

	GL:Specific power@FPSO kJ/kg		
GL MMscf/d	10	15	20
I year	35	52	70
III year	106	92	124
IX year	35	79	105

Tab.52: Specific electric powers for gas compression

	MPP+GL:Specific power@FPSO kJ/kg					
location	Riser			Manifold		
rated Δp	30	60	90	30	60	90
I year	42	49	57	41	50	#DIV/0!

Tab.53: Specific electric powers for both pump locations

Despite the favorable position and process efficiency, GL strategy appears to be the most expensive in terms of energy cost. The pump and gas injection coupling does not show any benefit rather than simple pump deployment. Indeed, this last strategy offers the lowest energy (exergy) consumption, as anticipated during the shaft power analysis. Concerning the position effect on the pump energetic performance, these data cannot be rightly assessed due to different working conditions. Indeed, the pump should be tested under constant differential pressure in order to gauge the real electric power consumption. Hence, datas from the shaft power analysis have been taken to determine the electric power requirements. The table below shows the calculation outcomes.

	I year		III year		IX year		
	Riser	Manifold	Riser	Manifold	Riser	Manifold	
effective Δp	30	30	50	50	62	62	bar
η overall	39,55	35,69	34,99	32,72	34,82	32,98	%
P FPSO	727	676	1265	1236	729	809	KW
Specific power	14,80	12,93	24,91	21,98	19,02	17,70	kJ/kg

Tab.54: Pump locations overall comparison: electrical powers, overall efficiencies and specific electric powers.

The table shows contrasting results, indeed the riser base pump has higher overall efficiencies, mainly due the location closeness to the processing facility; while the manifold located pump, despite the lower efficiency, has lower electric power requirements and lower specific power consumptions. This disagreement can be explained simply by the phase difference between the two locations: the gas compression is far more expensive rather than the liquid pumping, despite it is performed less efficiently. The diagram below illustrates the energy fluxes and losses during the first producing year.

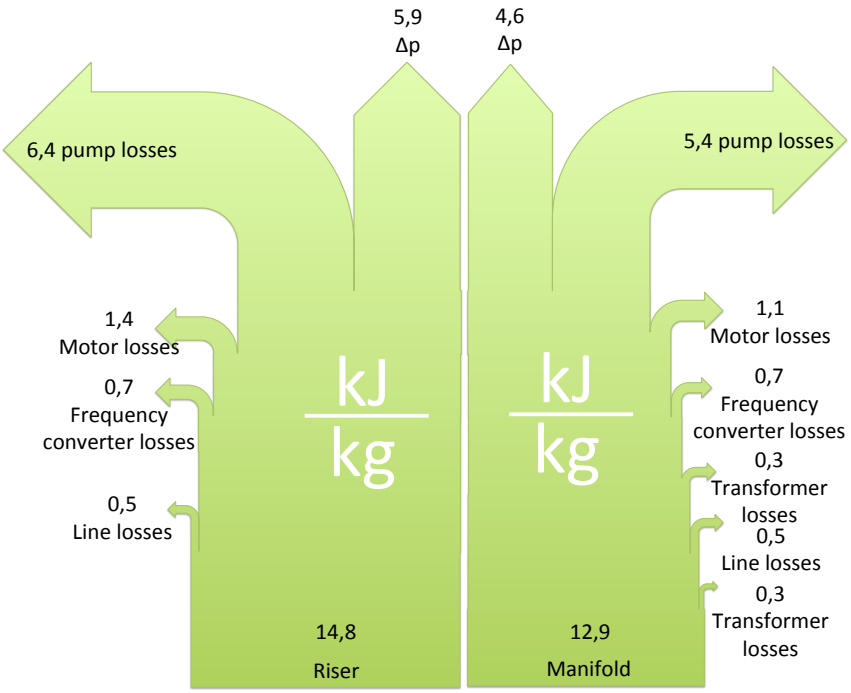

Fig.100: Energy losses comparison between riser base and manifold located pumps (I producing year, differential 30 actual bar.

The manifold located pump ensures the best energy performances, not due to higher efficiencies, but thanks to lower vapor fractions. In conclusion, the energy saving benefits of upstream pump locations increase with vapor content; indeed during the last producing year, when water content is maximum, such benefits fade away.

9.7. Restart Analysis

Once the system has been shut down, the system can be restarted afterwards the no touch time or after the preservation one. The second type of restart is quite challenging because the system typically is at seabed temperature and filled of diesel, which has much higher mixture density. The system is thus highly pressurized, due to greater geodetic pressure difference across the riser, and bottom hole pressure is definitely high. In such conditions, the system is unable to self flow, thus an artificial method is required. There are two main kinds of restart after preservation:

- Cold restart: huge amount of methanol is flushed in well tubings when valves open. Methanol inhibits hydrate formation even at very low temperatures.
- Warm restart: Before opening wellhead valves, hot diesel is loped from riser to service flowline, until the system reaches a temperature high enough to ensure a safe emergency shutdown. Shutdown simulations shown that riser base is the most threatened section, where 50°C has been chosen as conservative temperature, during a restart. Then one well at time is opened every four hours, beginning from the stronger to the weakers.

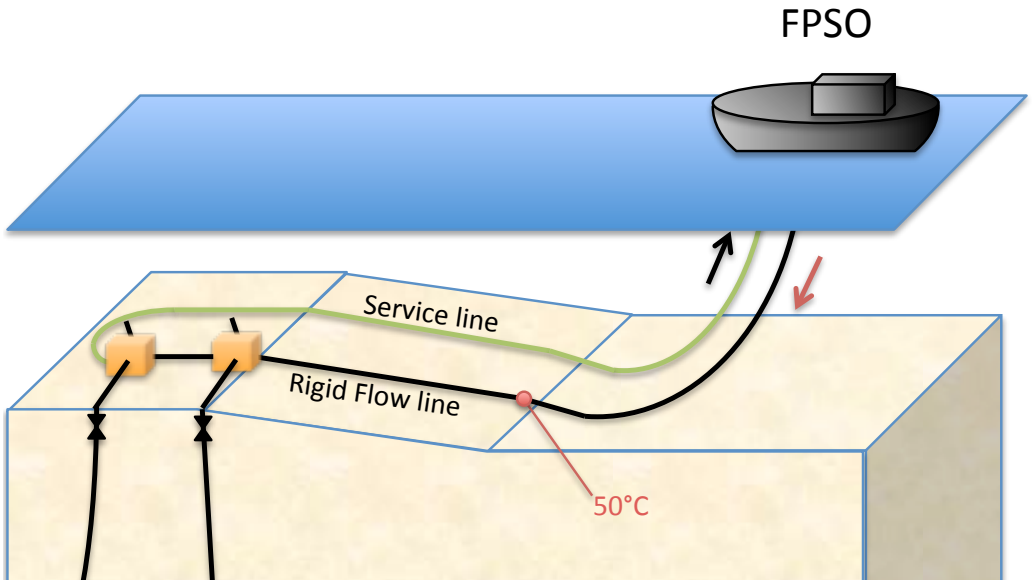

Fig.101: Hot diesel circulation path: from production riser to service riser.

The main challenge is faced by the multiphase pump, which has to convey a heavier fluid than the one it has been projected for. Therefore, effective pressure difference can be higher than rated one and shaft power could exceed the maximum one. Gas injection could effectively lighten the fluid column in the riser and ease the restart.

A restart can be considered successful when each well is allowed to produce; indeed, liquid can accumulate in the tubing blocking the well production. The best restart strategy is the one can restart the field in every situation and faster as possible. An important parameter to assess is the time which wellhead jumpers take to warm up to 50°C. Indeed, only the main flow line is flushed with warm diesel, while jumpers are heated since wellhead valves are opened and reservoir fluid is flowing through them. During the jumper warm-up time (JWUT), methanol must be injected in order to avoid hydrate formation till an emergency safe shutdown temperature is reached. This temperature ensures to provide an acceptable cool down time sufficiently long to allow operators to intervene in case of emergency shutdown.

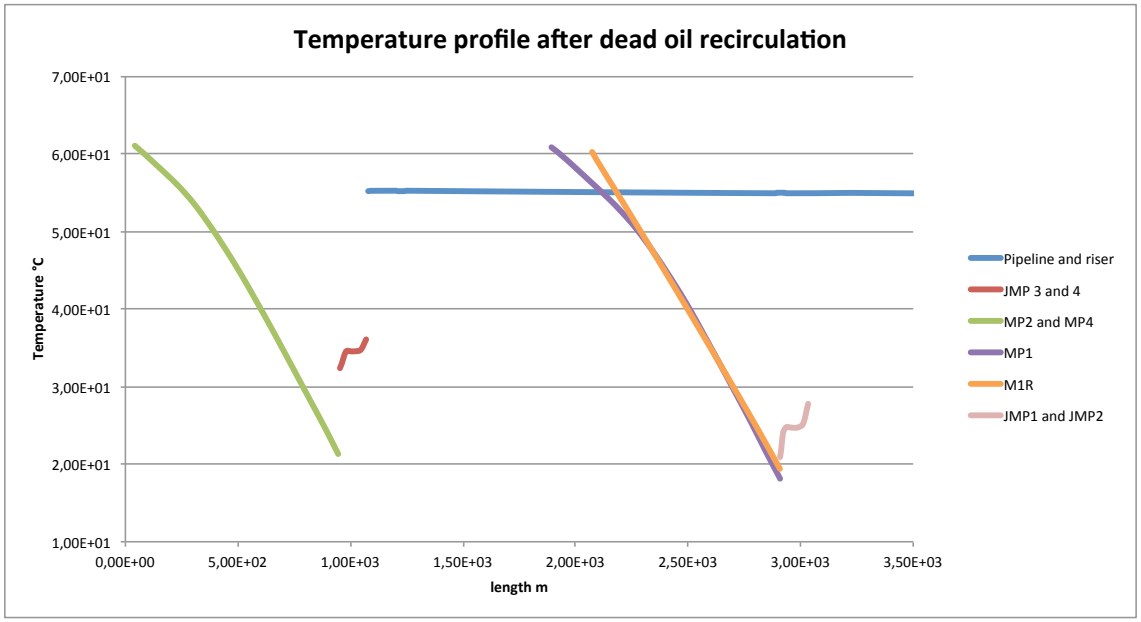

Chart 30: Temperature profile after the warm-up procedure.

9.7.1. MPP

The multiphase pump has effectively restarted the field during each analyzed year. Pump Δp has been set equal to 60 bar for both pump locations, which have shown to be both suitable for the task. Fortunately, the pump has not been excessively stressed during restarts (while pumping Diesel); the highest shaft power value was detected during the first year and equal to 855 kW. No appreciable differences were detected between the two pump locations. The following chart shows JWUTs for each well during the three analyzed years.

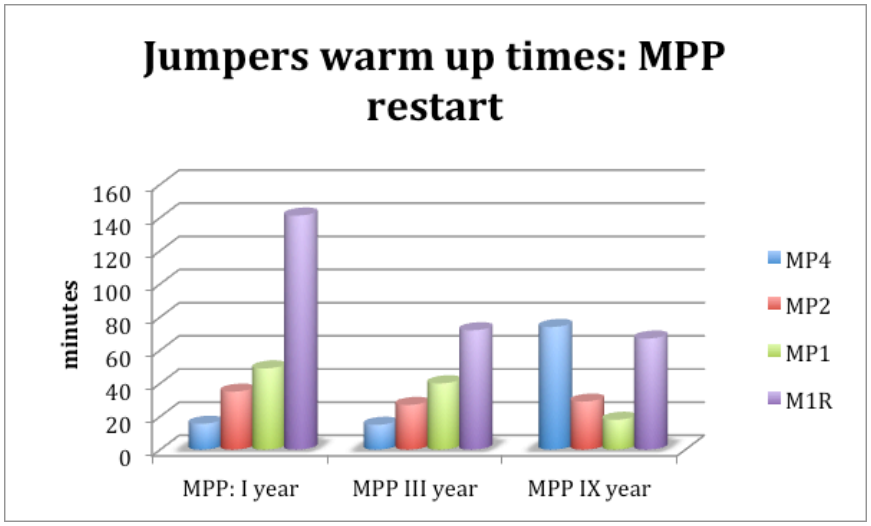

Chart 31: Wellhead jumpers warm-up times in MPP strategy.

As can be easily observed M1R well, which is the last to be restarted, is always struggling to reach the required temperature, because increasing the overall flowrate, frictional losses along the tieback surge. Thus, while the overall flow rate increases, the single well one decreases each time a well is restarted. As consequence of that, the last activated well is most critical one.

Regarding the shaft power concerns, no warning values were detected thanks to low rated pressure difference and tight flow rates.

9.7.2. GL

Gas injection flow rate has been set equal to 15 MMscf/d during restart run. The field was successfully activated during the first year, whereas in the third year the last well could not be activated due to the additional backpressure of a liquid column in the tubing; during the ninth year strong slugging has been detected. Injection flow rate was stepped up to even 20 MMscf/d of gas, but the system shown the same problems. The main reason, which underlies the gas lift inability to restart the field, is the injection point location. Indeed, the pipe geometry hampers the gas from flowing towards the processing facility and promotes it in the opposite direction.

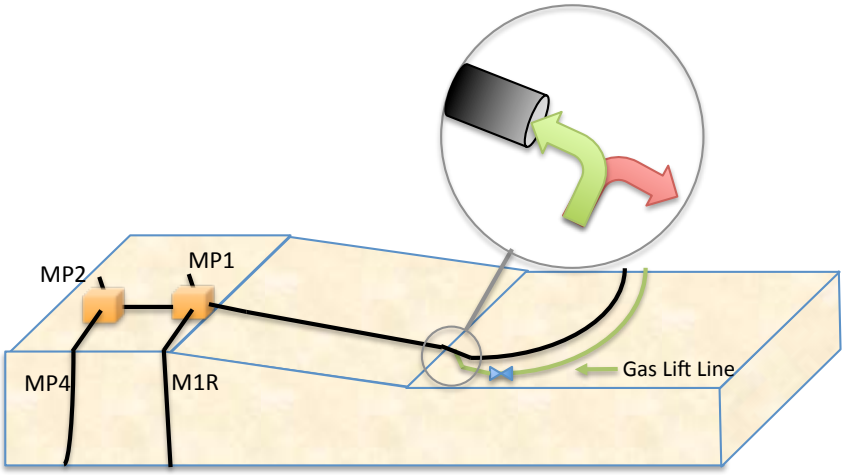

Fig. 102: Preferential gas path: the gas moves towards wells pushed by buoyancy forces.

Probably, the same gas flow rate would restart easily the field if performed bottomhole. The following chart reports the JWUTs, which denote strong instabilities during the well activation process.

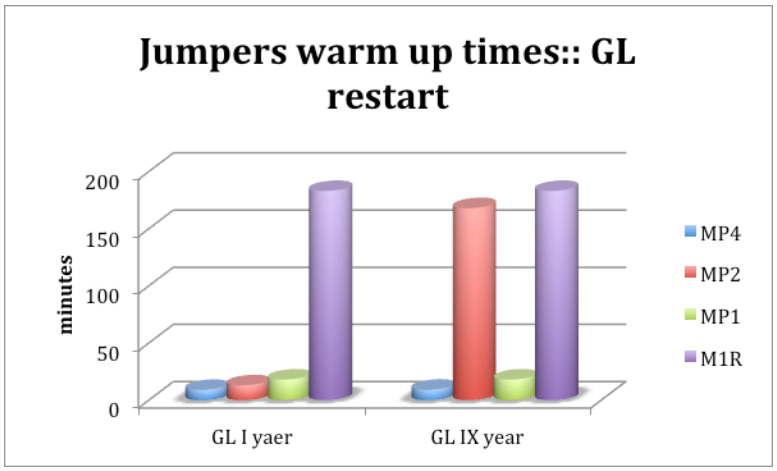

Chart 32: Wellhead jumpers warm-up times in GL strategy.

9.7.3. MPP+GL

Pump rated pressure difference has been set equal to 60 bar and, afterwards the conclusion on flow stability analysis performed at the beginning of this chapter, gas flow rate has been wisely decreased from 10 to 5 MMscf/d. Indeed, in former simulations has been observed strong slugging under nominal operating conditions during third and ninth years for both pump locations. Once decreased the flow rate, the field has been successfully restarted during all years for both pump locations. The following picture compares the JWUTs for both pump locations. Datas are divided by producing year and pump location in different columns, highlighting the sum of all JWUTs per restart.

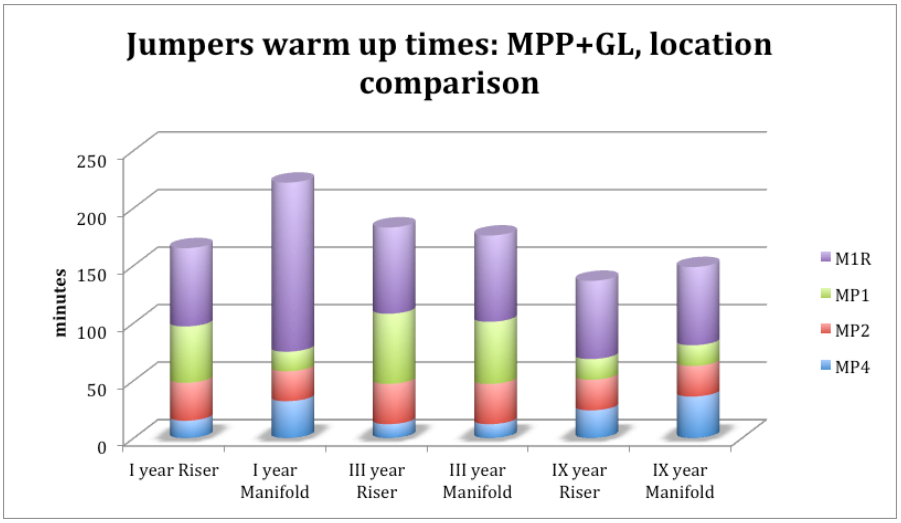

Chart 33: Wellhead jumpers warm-up times in MPP+GL strategy.

The results does not appoint any pump location as the best one. Indeed, beside the first year, the two location appear to have the same performances.

9.7.4. Restart analysis: strategies comparison

Pump deployment has proven to be essential to effectively restart the field during last years, when reservoir energy is lower. Pump location does not preferentially ease the field activation, as well as pump and gas injection coupling shown to provide some further advantages, as can be verified in the following chart, which has been built up simply summing together in columns the average JWUTs per year and production strategy. The pump and gas injection coupling has proved to be successful because the pump ensures fluid to flow in the right direction (not always happening without the pump) and the gas injection coupling allows to further reduce backpressure on wells without imposing high load to the pump (see paragraph Restart analysis).

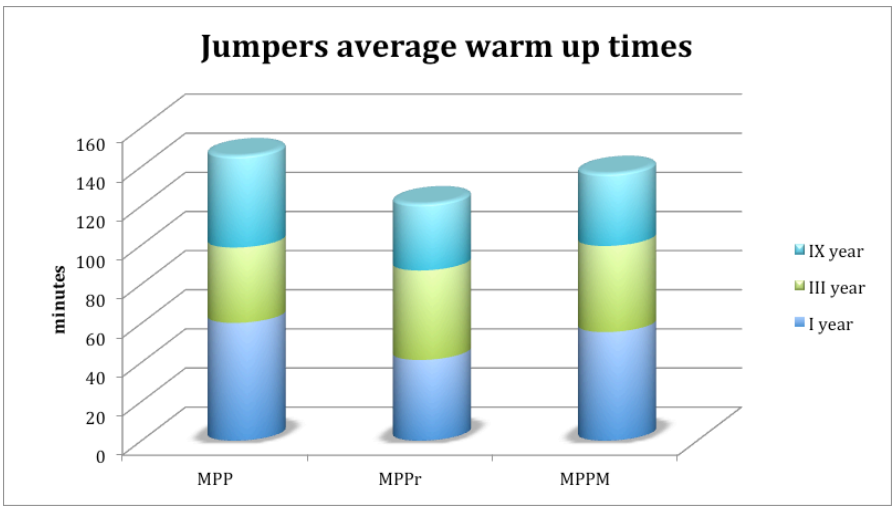

Chart 34: Strategy comparison: average wellhead jumpers warm-up times.

10. Conclusions

Subsea multiphase pumps benefits have been analyzed in this dissertation, throughout the assistance of simulation tools. To this purpose, the performances of an existing deepwater oilfield were simulated in OLGA with different production strategies:

- Self-flowing wells;
- Multiphase pump deployment;
- Riser base gas lift;
- Pump and gas lift contiguous operation.

Pump location effect analysis on system performances was also successfully carried out.

A model for pump performances prediction has been built up in HYSYS, based mainly on thermodynamic laws, assumptions and pump geometrical datas. The assumptions, such as different velocities for hydraulic and thermal transient processes and uniform multiphase flow in geometrical clearances, have shown to be acceptable simplifications for approaching the problem. The model, indeed, has been verified with manufacturer data for an air-water mixture and validated for the tested conditions; the maximum error was measured equal to 8,6% and standard deviation during non off-load operations (differential pressure higher than 0 bar) was 4,1%. Due to a lack of further experimental data the model has not been verified for the target hydrocarbon mixture. However, since the nature of the model and since its assumptions are not based on mixture properties, it is reasonable to rely on model predicted datas even for a hydrocarbon mixture.

System results analysis shown that multiphase pump deployment ensures the most efficient field exploitation, particularly:

- High oil production rates, thanks to strong backpressure reduction;
- Lowest energy consumption;
- Longest cool down times after a shutdown;
- Fast and reliable restart operations.

The main pump disadvantage is the reduced flexibility to changes in operating conditions. Indeed, when one or more wells are shut down, the flow rate decreases and slugging occurs. On the other hand, gas injection offers the

opposite advantage. Gas injection at riser base has shown to definitely ease the fluid deliverability and to allow stable operation during most of operational conditions. Main gas injection disadvantages have shown to be:

- Definitely lower riser base available cool down times due to high gas content and low gas injection temperatures;
- Unreliable and unpredictable restart operations;
- High power requirements for gas compression.

The coupling of the multiphase pump and gas lift have proved to be either effective either detrimental. Indeed, the pump Δp and gas flow rate must be opportunely chosen: excessive reduction in backpressure leads to valve choking. Further backpressure reductions are simply a waste of energy (both for pumping the fluid and compressing the injected gas) and can reduce the cool down time.

Thermal analysis has shown huge uncertainty in available cool down time determination, due to the low reliability on hydrate formation temperature prediction, which is further amplified by the exponential heat exchange mechanism. Thus appeared reasonable to use, for conservative purposes, the hydrate formation temperature obtained flashing the mixture at 1 bar; probably, this is not the real hydrate formation temperature, but 1°C of hydrate forming temperature uncertainty means more than one and a half hour of cool down time uncertainty.

Pump location analysis has proved that location advantages are strictly connected to system layout and specifications (geometry, mixture volatility etc.). Indeed, manifold located pump, which operates at definitely lower GVF, provides:

- Higher oil production;
- Lower power consumption.

If the produced fluid was completely liquid, riser base would be the most suitable pump position.

Both wellhead and riser base cool down times are not affected by pump location, although the manifold located pump keeps the pipeline at higher temperatures; Results show that pump position does not preferentially ease the restart.

	Flow rate in MMscf/d		I year
I year	Steady state		MPP 90 rated bar
	Turn down	I well	GL rate < 10 MMscf/d
		II well	GL rate < 15 MMscf/d
	Restart		MPP 60 rated bar + GL 5 MMsf/d
III year	Steady state		MPP 90 rated bar
	Turn down	I well	MPP 60 rated bar
		II well	GL rate < 15 MMscf/d
	Restart		MPP 60 rated bar + GL 5 MMsf/d
IX year	Steady state		MPP <90 rated bar
	Turn down	I well	MPP 60 rated bar
		II well	MPP <60 rated bar
	Restart		MPP 60 rated bar + GL 5 MMsf/d

Tab.55: Optimized production strategies for each operating condition.

For the analyzed system the best production strategy would be using a multiphase pump, manifold located, during most of the time. However, gas lift integration is suggested during turndown conditions and while restarting the field. In table 55 are reported the most suitable production strategies for each operating condition.

References

Andersen, K 1998, "Maximizing production from gravel packed wells at Gullfaks field by stimulation and installation of multiphase booster pumps."

Anon 2001, "SPE 71094Handling, Treatment and Transportation of Fluids Tailor-Made for Faja Crudes," pp. 1–8.

Anon 2003, "SPE 84062Two-Phase Helico Axial Turbines," pp. 1–8.

Bein, T & Hamilton, J 1982, "Computer Modelinq of an Oil Flooded Single Screw Air Compressor."

Beran, W 1994, "On the Threshold: Subsea Multiphase Pumping."

Bratu, C 2005, "Progressing Cavity Pump (PCP) Behavior in Multiphase Conditions."

Bratu, C 1995, "Two-phase pump transient behaviour."

Bratu, C & Petrole, du, IF 1997, "Rotodynamic Two-Phase Pump Performances ," pp. 1–13.

Bratu, C & Seince, L 2005, "New Progressing Cavity Pump (NPCP) for Multiphase and Viscous Liquid Production.."

Cao, F, Gao, T, Jiao, J, Pan, T & Xing, Z 2009, "Study of a screw rotor with different stocks and leads for a twin-screw multiphase pump," *Proceedings of the Institution of Mechanical Engineers, Part C: Journal of Mechanical Engineering Science*, vol. 223, no. 11, pp. 2637–2645.

Cao, F, Gao, T, Li, S, Xing, Z & Shu, P 2011, "Experimental analysis of pressure distribution in a twin screw compressor for multiphase duties," *Experimental Thermal and Fluid Science*, vol. 35, no. 1, pp. 219–225.

Chan, E 2009, "Wet-gas compression in twin-screw multiphase pumps."

Cornelis Kees Dorenbos, DM-LAJ 2001, "Sand Handling During Multiphase Operations With Twin-Screw Pumps," pp. 1–9.

Corteville, J, Ferschneider, G, Hoffmann, F & Valentin, E 1987, "Research on jet pumps for single and multiphase pumping of crudes."

Dagan, X, Zenan, X, Yongzhang, Y & Hamilton, J 1986, "The Computer Simulation of Oil--Flooded Refrigeration Twin-Screw Compressors."

Devegowda, D & Scott, S 2004, "An assessment of subsea production systems," *Journal of petroleum technology*, vol. 56, no. 8, Society of Petroleum Engineers, pp. 56–57.

E Loth, GTYTSEECTCABMROSTFYOABVW 2006, "MULTIPHASE FLOW HANDBOOK," pp. 1–158.

Egashira, K, Shoda, S, Tochikawa, T & Furukawa, A 1998, "Backflow in twin-screw-type multiphase pump," *Old Production & Facilities*, vol. 13, no. 1, Society of Petroleum Engineers, pp. 64–69.

Erwinsyah, P & Uphold, D 1999, "Multiphase Pumps for Minas Light Oil Steam Flood, Sumatra-Indonesia," *SPE Asia Pacific Oil and Gas Conference and ….*

Falcimaigne, J & Durando, P 1996, "Multiphase Pumping-Operation & Control."

Falcimaigne, J, Durando, P, Loupias, M & Vilagines, R 1994, "Multiphase Rotodynarnic Pumps Extend their Operating Capabilities."

Foucault, H, Charles, T, Fulton, J & JAFFREZIK, V 2005, "Coupling Complex Multiphase Pumps Surface Constraints to Reservoir Models for Optimising the Future Management Plan of a Mature North Sea Field."

Gi, P, Buvat, P, Bratu, C & Durando, P 1992, "Poseidon Multiphase Pump: Field Tests Results," *Offshore Technology Conference*.

Giuggioli, A 1995, "Innovative technologies improve the profitability of offshore heavy oil marginal fields."

Giuggioli, A, Villa, M, Ghetto, G & Colombi, P 1999, "Multiphase pumping for heavy oil: Results of a field test campaign."

Gonzalez, R 1996, "Two-Screw Multiphase Pump Behavior In Heavy Crude Oil."

Gonzalez, R & Guevara, E 1995, "Economic field development in Venezuela heavy oil fields using multiphase pumping technology."

Grimstad, H 2004, "Subsea Multiphase Boosting-Maturing technology Applied for Santos Ltd's Mutineer and Exeter field."

Guerrato, D, Nouri, JM, Stosic, N & Arcoumanis, C 2007, "Flow and pressure characteristics within a screw compressor," *Journal of Physics: Conference Series*, vol. 85, p. 012012.

Hua, G, Falcone, G, Teodoriu, C & Morrison, G 2011, "Comparison of Multiphase Pumping Technologies for Subsea and Downhole Applications."

J O A Baruzzi, EFCAJRFN 2001, "Production Forecast for a Subsea Multiphase Pumping System in the Marlim Field," pp. 1–10.

Jaggernauth, A, Brandt, JU & Muller-Link, D 1996, "Offshore Multiphase Pumping Technology-Identifying the Problems; Implementing the Solutions-Part 1."

Jens-Uwe Brandt, DM-LGR 2008, "Leakage is Management by a New Sealing System for Twin-Screw Multiphase Pumps," pp. 1–7.

Karassik, IJ, Messina, JP, Cooper, P, Heald, CC, Krutzsch, W, Hosangadi, A, Kittredge, C, Fraser, WH, Marscher, WD & Boyadjis, PA 2001, "Pump handbook," vol. 3, McGraw-Hill New York.

Klein, O 2007, "Erosioncorrosion Testing of Materials for the use as Screw Materials in Twin Screw Multiphase Pumps in the Oil and Gas Production Industry."

Leporcher, E & Taini, S 1995, "Multiphase pumping: The lessons of long-term field testing."

Leporcher, E, Delaytermoz, A, Renault, JF, Gerbier, A & Burger, O 2001, "Deployment of multiphase pumps on a north sea field."

M ller-Link, D, Brandt, J, Reichwage, M & Schr der, G 2002, "Wet Gas Compression-A Logical Step to Follow Multiphase Boosting."

Mali, P, Singh, R, De, S & Bhatta, M 1999, "Downhole ESP & Surface Multiphase Pump-Cost Effective Lift Technology for Isolated and Marginal Offshore Field Development."

Martin, A & Scott, S 2002, "Modeling Reservoir/Tubing/Pump Interaction Identifies Best Candidates for Multiphase Pumping."

Mueller-Link, D, Jaschke, A & Schroder, G 2005, "Multiphase Boosting in Oil and Gas Production."

Nakashima, CY, de Oliveira, S, Jr. & Caetano, EF 2006, "Heat transfer in a twin-screw multiphase pump: Thermal modeling and one application in the petroleum industry," *Energy*, vol. 31, no. 15, pp. 3415–3425.

Nakashima, CY, Oliveira, S, Jr & Caetano, E 2004, "Subsea multiphase pumping

system vs gas lift: an exergo-economic comparison," *Thermal Engineering*, vol. 3, pp. 1676–1790.

Nikhar, H 2009, "Flow assurance and multiphase pumping."

Pagnier, P, Noik, C, Maurel, P, Ricordeau, A & Volle, JL 2008, "Multiphase Loop Tests for Subsea Separation-Unit Development."

Perry, R 2012, "Subsea processing technologies are coming of age," *Offshore*.

Putra, E 2001, "Multiphase Pumps for Light Oil Steam Flood, from Design and Operation Perspectives," pp. 1–7.

Räbiger, K, Maksoud, T, Ward, J & Hausmann, G 2005, "Development of a finite volume model for the compressible gap flow inside a screw pump," Georg-Simon-Ohm-Fachhochsch.

Räbiger, K, Maksoud, T, Ward, J & Hausmann, G 2006, "Thermo-and fluid dynamic model of a multiphase screw pump, operating at very high gas volume fractions," Georg-Simon-Ohm-Fachhochsch.

Räbiger, K, Maksoud, TMA, Ward, J & Hausmann, G 2008, "Theoretical and experimental analysis of a multiphase screw pump, handling gas–liquid mixtures with very high gas volume fractions," *Experimental Thermal and Fluid Science*, vol. 32, no. 8, pp. 1694–1701.

Ruschel, A & Schlücker, E 2010, "Modelling flows for efficiency gains," *World Pumps*, vol. 2010, no. 5, Elsevier, pp. 29–31.

Saadawi, H 2007a, "An overview of multiphase pumping technology and its potential application for oil fields in the gulf region."

Saadawi, H 2007b, "Operating Multiphase Helicoaxial Pumps in Series To Develop a Satellite Oil Field in a Remote Desert Location."

Saadawi, H & Olama, S 2003, "Application of Multiphase Pumps in a Remote Oil Field Onshore Abu Dhabi," *Middle East Oil Show*.

Sangfors, B 1982, "Analytical modeling of helical screw machine for analysis and performance prediction."

Scott, S, Xu, J & Lenz, C 2006, "Subsea Multiphase Pressure Boosting and a New Approach for Speed Control Using a Hydrodynamic Variable Speed Drive."

Shippen, M & Scott, S 2002, "Multiphase pumping as an alternative to

conventional separation, pumping and compression."

Shrikant Dhodapkar, KJASH 2006, "MULTIPHASE FLOW HANDBOOK," pp. 1–101.

V A Pershukov, JDSAMC 2001, "Multiphase Pumps for 250,000 bbl/D Field Development," pp. 1–4.

Vetter, G, Wirth, W, Korner, H & Pregler, S 2000, "Multiphase Pumping with Twin-Screw Pumps-Understand and Model Hydrodynamics and Hydroabrasive Wear," pp. 153–170.

Villa, M, Ghetto, G, Paone, F, Giacchetta, G & Bevilacqua, M 1999, "Ejectors for boosting low-pressure oil wells," *Old Production & Facilities*, vol. 14, no. 4, Society of Petroleum Engineers, pp. 229–234.

Xu, J 2008, "Modeling of wet gas compression in twin-screw multiphase pump," TEXAS A&M UNIVERSITY.

Ringraziamenti

Anche se questo testo riporta la firma di un solo autore, non sarebbe stata possibile la sua stesura senza il prezioso contributo di tutti coloro che mi hanno aiutato durante questi nove mesi di lavoro.

Vorrei innanzitutto ringraziare il Prof. Lozza per la sua perenne disponibilità e per la piena fiducia che mi ha concesso. Devo ringraziare specialmente l'Ing. Michael Gassert, che mi ha dato la possibilità di lavorare all'interno del suo dipartimento, rendendo possibile la stesura della tesi. Oltre ad un ringraziamento formale, un Grazie di cuore spetta all'Ing. Magi, che è stato più di un maestro e che mi ha sempre aiutato quando ho avuto bisogno.

Grazie a Giovanna, Angelo, Mario, Nicolas e Franco per aver condiviso le loro conoscenze tecniche ogni volta che ho avuto bisogno, specialmente durante le pause pranzo. In particolare, devo una parola di sincera gratitudine a Nicolas e Franco per la loro perenne disponibilità e pazienza. Grazie al Prof. Colombo che, oltre ad avermi aiutato durante la fase di creazione del modello della pompa multifase, mi ha fatto tanto ridere con le sue brillanti battute.

Grazie a Gianraniero, Alfonso e Francesco per avermi ospitato tutte le volte che sono rimasto a Milano (e per le bellissime chiacchierate assieme). Grazie a quell' "ambientalista" di Tullio, che ha messo da parte le sue remore verso il petrolio e mi ha aiutato a formattare la bibliografia. Grazie a Vittorio e Donatella per l'aiuto, il supporto e l'affetto che mi hanno dato. Grazie a Cristiana per... Troppe cose. Grazie a mia madre e mio padre, perchè non basta solo dare un aiuto economico ai figli, bisogna guidarli: grazie per avermi guidato fin qui.